CHEMICAL REVIEWS

REVIEW

pubs.acs.org/CR

Organic Photocatalysts for the Oxidation of Pollutants and Model Compounds

M. Luisa Marin,[†] Lucas Santos-Juanes,[‡] Antonio Arques,[‡] Ana M. Amat,[‡] and Miguel A. Miranda*[,†]

[†]Instituto Universitario Mixto de Tecnología Química-Departamento de Química (UPV-CSIC), Avda. de los Naranjos s/n, E-46022, Valencia, Spain

[‡]Departamento de Ingeniería Textil y Papelera, Universidad Politécnica de Valencia, Campus de Alcoy, Plaza Ferrándiz y Carbonell s/n, E-03801 Alcoy, Spain

CONTENTS

1. INTRODUCTION

Water constitutes a key resource for life on Earth; as a consequence, development of civilizations throughout history has been directly related to the availability of sufficient sources of water with the required quality.[1] Despite the abundance of this resource, its actual availability is limited by the following facts: (a) ca. 97% is found as seawater and 2/3 of the rest is immobilized in poles and glaciers, (b) neither is water homogeneously disseminated nor are all the lands equally populated, and c) human activities have resulted in the generation of increasing amounts of wastewaters, which do not meet the required standards of quality to be reused and may cause pollution of the aqueous systems where they are discharged. Therefore, water scarcity constitutes an increasing concern, whose solution is a major challenge.[2]

An opportunity to increase water availability is decontamination and reuse of wastewaters. Much work has been recently devoted to this issue, and in developed areas, most household and urban effluents are processed in conventional sewage treatment plants. They generally consist of a physicochemical pretreatment followed by a biological step and, eventually, a tertiary treatment to ensure disinfection and decontamination.[3] However, further scientific and technical work is still required because a number of chemicals are not amenable to bioremediation, owing to their reluctance to conventional treatments or even to their toxicity to the biological systems.[4]

Chemical oxidation constitutes an alternative to bioprocesses for degradation of toxic or nonbiodegradable species.[5−7] Ozonation,[8,9] wet oxidation,[10] hydrogen peroxide-based methods,[11] and electrochemical[12,13] or photochemical oxidation have been used for this purpose. In particular, the applicability of photochemical processes for decontamination of water and air has received considerable attention over the last few decades. Some reviews and monographs have been devoted to report general advances in this field,[14,15] and others have dealt with the use of this type of methods to remove specific pollutants such as methyl *tert*-butyl ether,[16] chlorophenols,[17] dyes,[18] or pesticides.[19] A variety of radiation sources with different wavelength ranges have been used: (a) VUV-radiation, with $\lambda < 200$ nm, to decompose pollutants by direct photolysis or to generate oxidizing species such as hydroxyl radical (·OH) or ozone from water or oxygen,[20] (b) UV−C (commonly with $\lambda = 254$ nm, produced by low pressure mercury lamps), which is also able to photolyze a number of compounds, thus enhancing the effect of ozone or hydrogen peroxide by formation of ·OH,[14,21] and (c) UVB−UVA−visible, which usually requires the presence of a photocatalyst and corresponds to the fraction of the solar spectrum reaching the Earth's surface.

In this context, photocatalysis is an interesting approach for photochemical detoxification. According to the IUPAC,[22] a photocatalyst is a substance that is able to produce, by absorption of light quanta, chemical transformations of the reaction participants, repeatedly coming with them into the intermediate chemical interactions and regenerating its chemical composition after each cycle of such interactions. Thus, the photocatalyst must be efficient in substoichiometric amounts. Accordingly, photocatalysis is defined as a "change in the rate of a chemical reaction or its initiation under the action of ultraviolet, visible, or infrared radiation in the presence of a substance—the photocatalyst—that absorbs light and is involved in the chemical transformation of the reaction partners". The

Received: February 15, 2011
Published: October 31, 2011

dx.doi.org/10.1021/cr2000543 | *Chem. Rev.* 2012, 112, 1710–1750

term photocatalyst is closely related to photosensitizer, which is defined as an agent that absorbs light and subsequently initiates a photochemical or photophysical alteration in the system, with the agent not being consumed therewith. In the case of chemical alteration, the photosensitizer is usually identical to a photocatalyst. Photocatalysis can be considered as one of the emerging green processes, which has been employed for different purposes such as hydrogen production, organic synthesis, and water or air decontamination.[23−25] In particular, photocatalysts employed in pollution remediation are able to generate highly oxidizing species upon excitation, which are able to react with the contaminant molecules. Most of these processes can benefit from the additional economical and ecological advantages associated with the use of freely available, natural sunlight.[26] This topic is gaining momentum, as indicated by a rather conservative estimation of ca. 1500 papers on photocatalysis per year, 50% of them evaluating the possibility of using sunlight. Specific information on the use of sunlight for wastewater detoxification can be found in a series of review articles summarizing recent advances in the field.[26−30]

Photocatalysts employed for air and water decontamination can be divided into two groups: (a) semiconductors, such as metal oxides and sulfides, and (b) organic compounds and metal−organic complexes with strong absorption bands in the UVA−visible range, capable of participating in photocatalytic processes.

Semiconductors probably constitute the most widely used heterogeneous photocatalysts. Much work has been devoted to elucidate their mechanism of action; detailed information on this

Chart 1. Structures of Photocatalysts

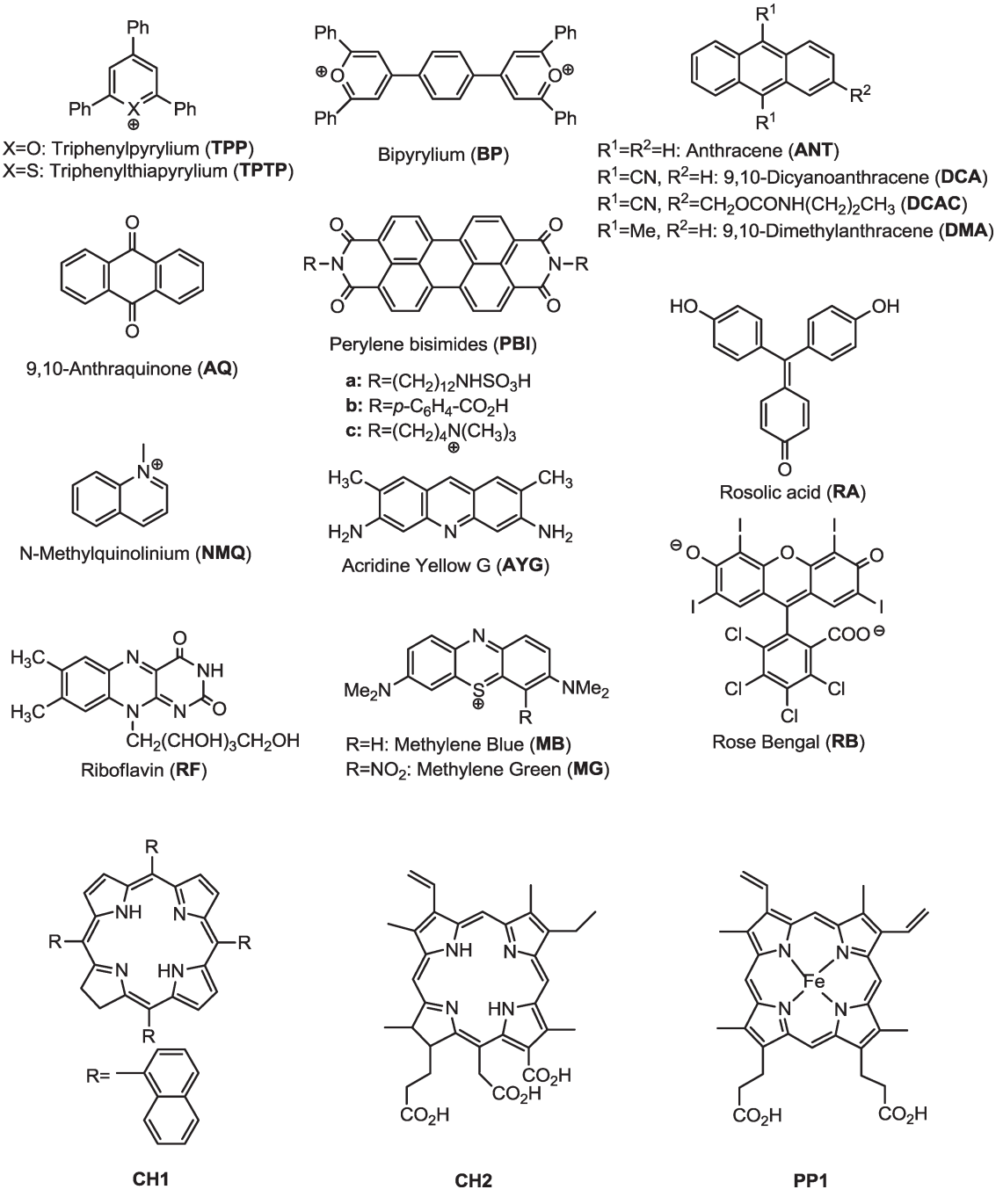

dx.doi.org/10.1021/cr2000543 |Chem. Rev. 2012, 112, 1710–1750

Chart 1. Continued

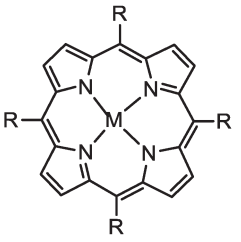

PP2

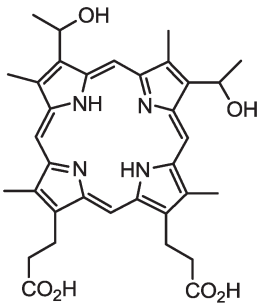

PP3

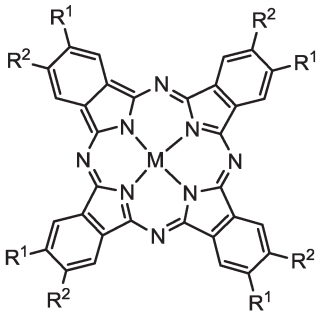

PC1

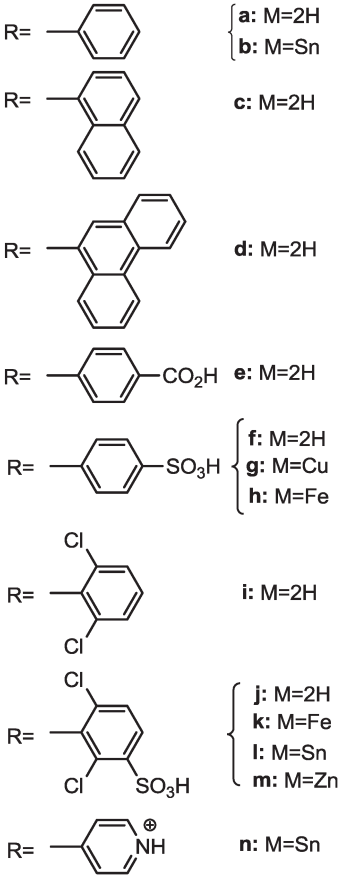

a: M=2H
b: M=Sn
c: M=2H
d: M=2H
e: M=2H
f: M=2H
g: M=Cu
h: M=Fe
i: M=2H
j: M=2H
k: M=Fe
l: M=Sn
m: M=Zn
n: M=Sn

a: $R^1=R^2=H$; M=Cu
b: $R^1=R^2=H$; M=Fe
c: $R^1=R^2=H$; M=Mn
d: $R^1=R^2=H$; M=Zn
e: $R^1=SO_3Na$, $R^2=H$; M=2H
f: $R^1=SO_3Na$, $R^2=H$; M=Al(III)OH
g: $R^1=SO_3Na$, $R^2=H$; M=Al(III)Cl
h: $R^1=SO_3Na$, $R^2=H$; M=Co(II)
i: $R^1=SO_3Na$, $R^2=H$; M=Fe(II)
j: $R^1=SO_3Na$, $R^2=H$; M=Ga
k: $R^1=SO_3Na$, $R^2=H$; M=Pd(II)
l: $R^1=SO_3Na$, $R^2=H$; M=Zn(II)
m: $R^1=COOH$, $R^2=H$; M=Co(II)
n: $R^1=COOH$, $R^2=H$; M=Zn(II)
o: $R^1=R^2=COOH$; M=Al
p: $R^1=R^2=COOH$; M=Zn
q: $R^1= H_2CS-C(=\overset{\oplus}{N}(CH_3)_2)-NH(CH_3)_2$, $R^2=H$; M=Cu

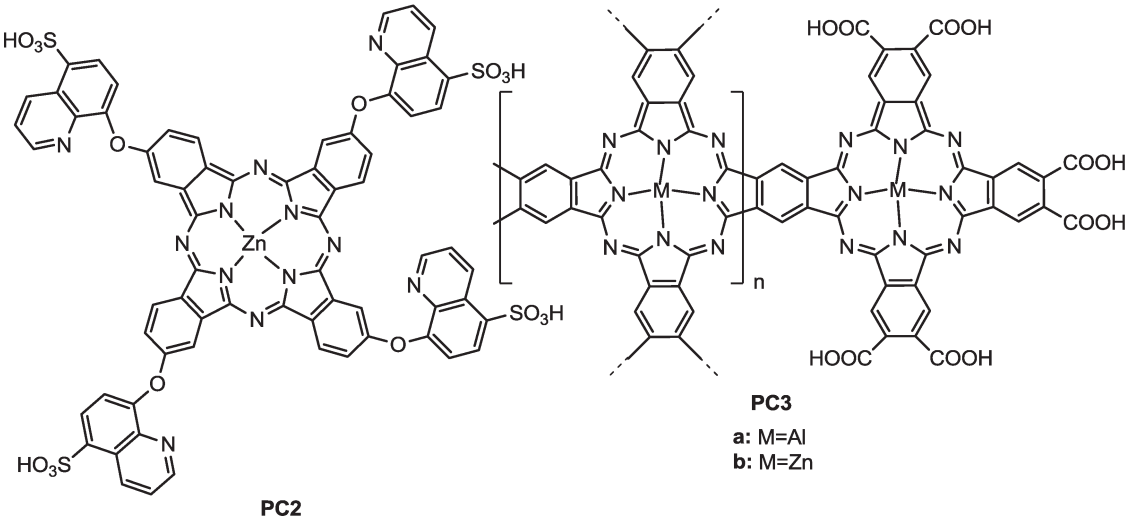

PC2

PC3

a: M=Al
b: M=Zn

dx.doi.org/10.1021/cr2000543 |*Chem. Rev.* 2012, 112, 1710–1750

issue is available elsewhere.[31−33] Briefly, electrons are promoted from the valence band to the conduction band upon irradiation, thus generating a high-energy electron and a corresponding oxidizing hole (h^+) in the valence band; these species can react directly with the pollutant, or give rise to secondary oxidizing species, such as hydroxyl radical. Although different materials have been tested, in most cases titanium dioxide is the photocatalyst of choice. The role of this solid was established in 1972 by Fujishima and Honda,[34] and the principle was first employed for decontamination by Carey et al. in 1976.[35] Since then, a wide range of pollutants and wastes have been successfully treated by TiO_2-driven photoprocesses, such as dyes,[18,36] volatile organic compounds,[37] chlorophenols,[17] or pesticides;[38] furthermore, a specific review has appeared on the fundamentals of TiO_2 solar photocatalysis and solar photoreactors.[39] Current efforts in the field are being devoted to optimize the efficiency of these processes,[40] mainly by enhancing sunlight absorption (only λ < 380−400 nm can be used, which accounts for <10% of the photons reaching the Earth's surface) and retarding recombination of electrons and holes.

The use of photoactive organic compounds as photocatalysts constitutes a possible alternative,[25] in particular when visible light is used.[41] In fact, it is well established that dissolved organics may play a key role in self-cleaning of rivers, lakes, and seas, photogenerating highly reactive species upon sunlight irradiation.[42]

Different organic compounds, such as dyes, porphyrins, and phthalocyanines, as well as transition metal complexes, participate in photochemical electron transfer[43] and energy-transfer[44] processes. Hence, they have been employed as photocatalysts for a variety of purposes, such as formation of C−C bonds in organic synthesis,[23] photopolymerization,[45] photodynamic therapy,[46,47] or construction of solar cells.[48]

Organic photocatalysts have been used for the remediation of water and air, mostly in the past decade. However, a comprehensive review paper on this issue is still missing, so the existing information has not been sufficiently organized and systematically presented. To provide a critical impulse for the development of the field, we aim to review the use of organic photocatalysts for the oxidation of pollutants and model compounds, with special emphasis on the involved concepts and mechanistic aspects.

The Fenton process, discovered at the end of the 19th century,[49] is based on the use of a mixture of iron salts and hydrogen peroxide. Although the reaction occurs in the dark, it is remarkably enhanced under UV−visible irradiation (λ < 550 nm). However, this can be hardly considered as a photocatalytic method, as only iron is catalytic, while hydrogen peroxide plays a sacrificial role. The mechanism of the process is very complex and still remains incompletely elucidated; it is widely accepted that hydroxyl radical plays a major role as oxidizing agent, although involvement of other species, such as high-valence iron, has not been ruled out. Detailed information on this issue can be found in a review paper.[50] In addition to iron, other transition metals photocatalyze the generation of •OH, and hence variations have been proposed (Fenton-like and photo-Fenton-like processes);[51] use of persulfate instead of H_2O_2, addition of oxalate or other iron-complexing agents, and heterogeneization by iron immobilization have been investigated.[26] Scientific and technical aspects of the use of photo-Fenton methodologies for wastewater treatment have been widely covered.[27,50]

Hybrid materials containing organic dyes or metal complexes, such as bipyridyl ruthenium deposited onto titania, are not included in this paper. Although they have certainly been employed for wastewater remediation, they are generally considered as modifications of TiO_2 to achieve absorption of visible light.

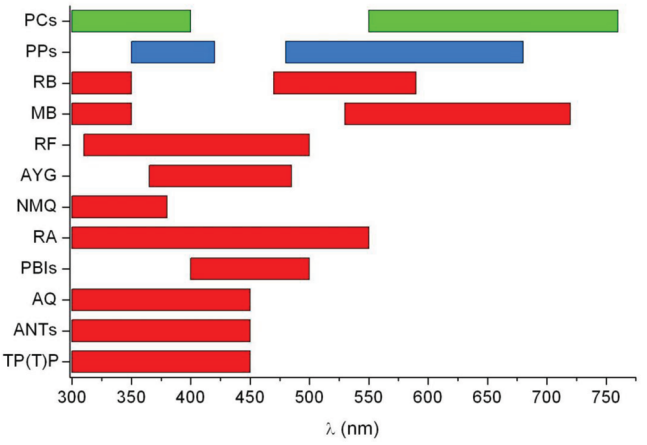

Figure 1. Typical absorption ranges of the organic photocatalysts in the UVB−UVA−vis range.

This issue has been conveniently addressed in several review papers on TiO_2 photocatalysis.[26,33,41] The use of organic photocatalysts for the elimination of pathogenic species (i.e., disinfection of drinking water, closely related to photodynamic antimicrobial chemotherapy) also falls beyond the scope of the present review.[52−61] We will not cover the elimination of pollutants (e.g., sulfides) from gaseous effluents.[62−66]

2. ORGANIC PHOTOCATALYSTS: STRUCTURES AND PROPERTIES

Chemical structures of the organic photocatalysts that have been used in the photodegradation of pollutants and model compounds are shown in Chart 1. They display a marked diversity, encompassing from aromatic to heteroaromatic rings, porphyrins, or phthalocyanines. For a systematic treatment, photocatalysts have been grouped into the following families: pyrylium salts, aromatics, heteroaromatics, chlorins, porphyrins, and phthalocyanines.

The first requirement for a photocatalyst to be applicable is light absorption in the UV−visible range. Figure 1 illustrates the most significant absorption bands for the photocatalysts mentioned above. For the sake of clarity, the following color codes are used: red for pyryliums, aromatics, heteroaromatics, and chlorins;[43,67−83] blue for porphyrins;[84−90] and green for phthalocyanines.[91−98]

The characteristic singlet excited-state properties of photocatalysts are listed in Table 1,[72,74,82,83,88,99−135] including the emission wavelength (λ_{em}), singlet state energy (E_S), fluorescence quantum yield (Φ_F), and lifetime of the singlet excited state (τ_S). When different values are reported (due, for instance, to the use of different solvents or experimental conditions), several data points are included.

Likewise, Table 2 collects the most characteristic triplet excited-state properties of photocatalysts.[44,74,78,80,88,99,101,103,104,109,117,119,120,122,127,128,130,135−150] They include intersystem crossing quantum yield (Φ_{ISC}), triplet−triplet absorption wavelength (λ_{T-T}), triplet state energy (E_T), lifetime of the triplet excited state (τ_T), and singlet oxygen quantum yield (Φ_Δ).

3. POLLUTANTS AND MODEL COMPOUNDS

Chemical structures of the pollutants and model compounds that have been treated with organic photocatalysts are shown in

dx.doi.org/10.1021/cr2000543 |Chem. Rev. 2012, 112, 1710–1750

Table 1. Characterization of Singlet Excited States

photocatalyst[ref]	λ_{em}/nm	E_S/(kJ mol^{-1})	Φ_F	τ_S/ns
TPP[99]	465	276	0.47	4.4
TPTP[99−101]	465	276	0.06	4.4
ANT[102,103]	390	318	0.3	5.3
	418			
	437			
	468			
DCA[103−107]	440	284	0.9	13[105]
	465			15.3[104]
	490			
DMA[103,108]	407	300	0.93	14.0
	430			
	457			
AQ[103,106,109−112]	430	263[a]		7.0
	455	284[b]		
PBIa[83]	536[a]	247[a]	0.064[a]	4
	572[a]	242[b]	0.003[b]	
	548[b]			
	584[b]			
PBIb[72]	470[b]	228[a]	0.87[a]	8.1[a]
	506[b]	257[b]	0.86[b]	15.0[b]
NMQ[104,113−117]	402	341	0.85	20
				13
AYG[74,103,118−120]	495	252	0.47	5.1
RF[103,121−123]	515-	263	0.12[103]	2.3[103]
	520		0.26[b]	5[122]
			0.47[a]	5.75[123]
MB[103,124−126]	674	180	0.04	0.38[b]
RB[127−129]	573	214	0.08	0.4
CH1[130]		183	0.36	
CH2[82,131]	661		0.19	
	667[131]			
PP2a[132]	650	184	0.10	12.4
	709			
PP2c[130]		184	0.16	
PP2d[130]		183	0.13	
PP2f[88,103]	641	188	0.054[88]	10.4
	697		0.16[103]	
PP2i[130]		181	0.005	
PP2j[88]	643	187	0.0013	
	704			
PP2l[88]	624	197	0.0015	
	649			
PP2m[88]	612	196	0.0035	
	658			
PC1a[133,135]	678	177	0.09	
PC1d[103,133−135]	679	175[103]	0.30[103]	4.1[133]
	708	177[135]	0.18[134]	3.8[135]
	742			
PC1e[135]	702	179	0.62	9.8
PC1f[131]	684		0.51	
PC1g[135]	675	175		5.3
PC1l[134,135]	685	176	0.12[134]	2.9
	710		0.32[135]	
	748			

[a] Organic solvent. [b] Aqueous medium.

Chart 2. They can be grouped into the following families: sulfur derivatives (S), phenols (P), aromatic aldehydes and acids (A), carbamates (C), heteroaromatics (H), and miscellaneous (M).

Table 3 provides a matrix showing the photocatalysts used for the oxidation of pollutants, together with the corresponding references.[63,67,68,72,74,80,83,88,90,94,95,97,98,102,104−107,109,110,116,121,123,124,129,130,141−144,146−148,150−219]

4. REACTION MECHANISMS

One of the main advantages of organic photocatalysts is associated with the possibility of designing a mechanistically based treatment for each particular pollutant. This is because of the diversity of the involved reaction pathways. Basically, relevant information can be obtained by means of two types of studies: (a) detection of short-lived excited states or reactive intermediates by time-resolved techniques (emission, transient absorption spectroscopy, etc.) or (b) steady-state photolysis (assessed by a variety of endpoints) and identification of the photoproducts obtained at different oxidation stages. These two aspects are dealt with below in separate sections.

4.1. Experimental Mechanistic Evidence

In this context, Scheme 1 represents most of the possible mechanistic pathways that can take place in a photocatalytic process. Thus, the reaction starts when a photocatalyst (represented by **P**) absorbs light of the appropriate wavelength and reaches the first singlet excited state ^{1}**P***. From this state different processes can occur: ^{1}**P*** can react directly with the pollutant or model compound (represented by **Q**) by an electron transfer reaction,[220] to give the oxidized form of the pollutant ($\mathbf{Q}^{\bullet+}$) and the reduced form of the photocatalyst ($\mathbf{PM}^{\bullet-}$), **pathway i**. In addition, ^{1}**P*** can undergo intersystem crossing to the triplet excited state ^{3}**P***. In principle, the reaction of either ^{1}**P*** or ^{3}**P*** with water could give rise to hydroxyl radical $\mathbf{OH}^{\bullet}$, together with the radical anion of the photocatalyst, as shown in **pathways ii** and **iii**.[163,164,188] In the triplet manifold, ^{3}**P*** can participate in an electron transfer reaction[220] yielding $\mathbf{Q}^{\bullet+}$ and $\mathbf{P}^{\bullet-}$, **pathway iv**, but it can also react with O_2 by an energy transfer process, giving singlet oxygen ($^1\mathbf{O_2}$), **pathway v**.

Furthermore, a complex between the ground state of the photocatalyst and the pollutant can be formed. This complex (**P---Q**) may absorb light, with the result of charge separation leading to $\mathbf{Q}^{\bullet+}$ and $\mathbf{P}^{\bullet-}$, **pathway vi**. A further mechanistic alternative involves generation of superoxide radical anion $\mathbf{O_2}^{\bullet-}$ by reaction of the semireduced photocatalyst $\mathbf{P}^{\bullet-}$ with molecular oxygen (**pathway vii**).

The final oxidation products can be obtained by reaction of the pollutant radical cation $\mathbf{Q}^{\bullet+}$ with molecular oxygen or superoxide radical anion; moreover, the pollutant, **Q**, can react in its ground state with the active oxygen species, $\mathbf{OH}^{\bullet}$ or $^1\mathbf{O_2}$.

In general, detection of transient species derived from the photocatalyst, such as excited states or reactive intermediates, by time-resolved spectroscopic methods provides a powerful tool for the study of fast reaction kinetics. The decay of these species (usually in the microsecond or nanosecond time scale) is strongly influenced by the presence of pollutants, acting as quenchers. A plot of the reciprocal lifetime versus quencher concentration gives the so-called Stern−Volmer linear relationships, whose slopes afford the reaction rate constants. Related information can be obtained from steady-state experiments, for instance, by plotting the relative emission intensity versus quencher concentration. The Stern−Volmer constants are typically given in M^{-1} units; they can be

dx.doi.org/10.1021/cr2000543 |*Chem. Rev.* 2012, 112, 1710–1750

Table 2. Characterization of Triplet Excited States

photocatalyst[ref]	Φ_{ISC}	λ_{T-T} /nm	E_T/kJ mol^{-1}	τ_T/μs	Φ_Δ
TPP[99,136]	0.53	450	222	6.3	
TPTP[99,101,137]	0.94	460	218	4.4	
ANT[103,138]	0.70	432	178	670	0.7
DCA[103,138]	0.02[138]−0.23[103]	440	175	100	2[a]
DMA[103,138]	0.02	435	168		1[a]
AQ[103,109,139]	0.90	390	261	0.11	0.62
NMQ[104,117,138]			255		0.86
AYG[74,103,119,120]	0.45	550	220[103]	12.8	
			242[119]		
RF[78,122,140−142]	0.38−0.7	640−720	200	10−120	0.49−0.59
MB[103,143]	0.52	420	138	450	0.52
RB[80,127,128,144]	0.76−0.98	620	171	100−150	0.76−0.9
CH1[130]	0.55			0.35[b]	0.55
PP2a[130,135]	0.73[130]		138[135]	0.35[130b]	0.67
	0.82[135]			1389[135]	
PP2c[130]	0.86			0.48[b]	0.86
PP2d[130]	0.87			0.57[b]	0.72
PP2f[103,145]	0.78	790		420	0.7
PP2i[130]	1			0.64[b]	0.98
PP2j[88]	0.88	460		397	0.73
PP2k[150]	1	460		378	1
PP2l[88]	0.83	460		432	0.51
PP2m[88]	0.92	460		368	0.51
PC1a[44]	0.7		109	0.035	0
PC1d[103,135,145,146]	0.65	480	109	245	0.53
PC1e[44,135,145,147]	0.22−0.25			170	0.14−0.17
PC1f[145,147]	0.33			500	0.34
PC1g[135,148]		490	116	290[148]	0.34
				500[135]	
PC1h[147,149]				0.065	0
PC1j[145]	0.36				0.38
PC1l[44,135,148]	0.56		108	245[44]	0.45
				165[148]	

[a] Calculated at infinite oxygen concentration. [b] Under oxygen.

converted into reaction rate constants (as M^{-1} s^{-1}) by taking into account the initial lifetime of the unquenched species.

The processes outlined in Scheme 1 are usually very fast, as they occur during the lifetime of short-lived species. Therefore, competition between the different reaction pathways is subjected to kinetic control. For this reason, it is of paramount importance to obtain reaction rate constants, as these are the key parameters that determine the nature of the predominating mechanistic routes.

Experimental evidence will be reviewed, and some typical examples will be discussed in detail. ^{1}**P*** can react by electron transfer (**pathway i**, Scheme 1).[74,83,102,104,105,107,109,110,116,141,144,148,156,161,176,185,186,191,202,207,212,213] Some of them illustrate the use of a triphenylpyrylium salt (**TPP**) as the photocatalyst and different aromatic derivatives such as acids **A5a**−**d**,[191] **A3c**−**h**,[186] and **A2**, phenol **P1h**,[185] or 2,4-dimethylaniline (**M3f**)[212,213] as pollutants. Involvement of the singlet excited state of acridine yellow G (**AYG**) in the photooxidation of ferulic acid (**A5d**) has also been reported.[74] Further evidence has been obtained in the photodegradation of sulfur compounds **S1c** or **S1i**−**m** by **TPP** or 9,10-dicyanoanthracene (**DCA**),[109,161] disulfide **S2b** by **DCA**,[105] or **S1c** and **S1f** by **DCAC**.[107]

In the case of triadimenol (**TDM**), a photoelectron transfer mechanism has been inferred, because photodegradation occurs only in the presence of photocatalysts known as electron acceptors (**DCA**/**TPP**) but not in the presence of rose bengal (**RB**) ($^1O_2$ generator).[207] With other photocatalysts, such as anthraquinone (**AQ**), the nature of the obtained photoproducts and the favorable thermodynamics, based on the reduction potential of the excited photosensitizer, support the electron transfer mechanism in the photodegradation of **M1** and carbamates **C1a** and **C1c**.[110]

Further examples involving different photocatalysts include quenching of riboflavin (**RF**) singlet excited state with high rate constants (in the order of 10^9 M^{-1} s^{-1}) by several pollutants and model compounds, like phenol and heterocyclic derivatives. Thus, values of 5.9, 2.4, 2.9, and 2.4 × 10^9 M^{-1} s^{-1} have been obtained for hydroxypyridines **H1a** and **H2b**, hydroxyquinoline **H3b**, and pyrimidine **H5c**, respectively, from the corresponding Stern−Volmer plots.[144,202] In the case of chorophenols, the relative reactivity is **P1e** > **P1k** > **P1o**.[176] Fluorescence quenching by bisphenol derivatives

dx.doi.org/10.1021/cr2000543 |*Chem. Rev.* 2012, 112, 1710–1750

Chart 2. Structures of Pollutants and Model Compounds

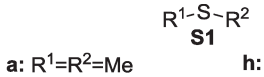

S1

a: $R^1=R^2=Me$
b: $R^1=R^2=Et$
c: $R^1=R^2=(CH_2)_3CH_3$
d: $R^1=R^2=(CH_2)_4$
e: $R^1=R^2=(CH_2)_5$
f: $R^1=R^2=Ph$
g: $R^1=R^2=CH_2CH_2Cl$
h: $R^1=Me$, $R^2=Ph$
i: $R^1=Et$, $R^2=C_{12}H_{25}$
j: $R^1=Et$, $R^2=CH_2Ph$
k: $R^1=Et$, $R^2=(CH_2)_2Ph$
l: $R^1=Et$, $R^2=CMe_2Ph$
m: $R^1=Et$, $R^2=CHPh_2$
n: $R^1=CH_2Ph$, $R^2=CH_2CH=CH_2$
o: $R^1=H$, $R^2=CH_2CH_2OH$

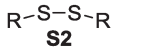

S2

a: R=Me
b: $R=(CH_2)_3CH_3$
c: R=Ph

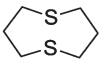

S3

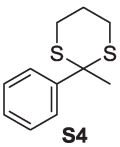

S4

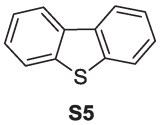

S5

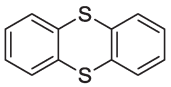

S6

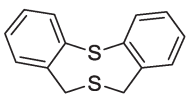

S7

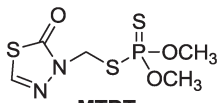

MTDT

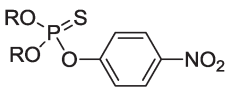

PTM: R=Me
PTE: R= Et

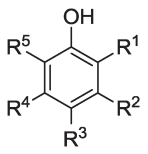

P1

a: $R^1=R^2=R^3=R^4=R^5=H$
b: $R^1=OH$, $R^2=R^3=R^4=R^5=H$
c: $R^3=OH$, $R^1=R^2=R^4=R^5=H$
d: $R^3=OCH_3$, $R^1=R^2=R^4=R^5=H$
e: $R^1=Cl$, $R^2=R^3=R^4=R^5=H$
f: $R^2=Cl$, $R^1=R^3=R^4=R^5=H$
g: $R^3=Cl$, $R^1=R^2=R^4=R^5=H$
h: $R^3=CH_2CH_2OH$, $R^1=R^2=R^4=R^5=H$
i: $R^3=Ph$, $R^1=R^2=R^4=R^5=H$
j: $R^3=NO_2$, $R^1=R^2=R^4=R^5=H$
k: $R^1=R^3=Cl$, $R^2=R^4=R^5=H$
l: $R^1=R^5=Me$, $R^2=R^3=R^4=H$
m: $R^1=R^5=C(CH_3)_3$, $R^2=R^3=R^4=H$
n: $R^1=R^3=R^4=Cl$, $R^2=R^5=H$
o: $R^1=R^3=R^5=Cl$, $R^2=R^4=H$
p: $R^1=R^2=R^3=R^4=R^5=Cl$

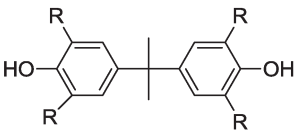

P2

a: R=H
b: R=Br
c: R=Me

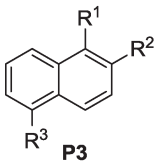

P3

a: $R^1=OH$, $R^2=R^3=H$
b: $R^2=OH$, $R^1=R^3=H$
c: $R^1=R^3=OH$, $R^2=H$
d: $R^1=N=NC_6H_4SO_3H$, $R^2=OH$, $R^3=H$

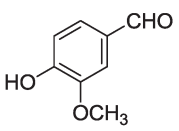

A1

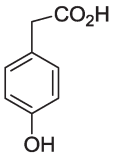

A2

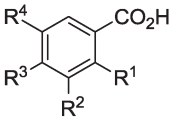

A3

a: $R^1=R^2=R^3=R^4=H$
b: $R^1=SH$, $R^2=R^3=R^4=H$
c: $R^3=OH$, $R^1=R^2=R^4=H$
d: $R^2=R^3=OH$, $R^1=R^4=H$
e: $R^2=OCH_3$, $R^3=OH$, $R^1=R^4=H$
f: $R^2=R^3=OCH_3$, $R^1=R^4=H$
g: $R^2=R^3=R^4=OH$, $R^1=H$
h: $R^2=R^4=OCH_3$, $R^3=OH$, $R^1=H$

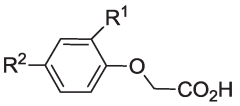

A4

a: $R^1=H$, $R^2=Cl$
b: $R^1=R^2=Cl$

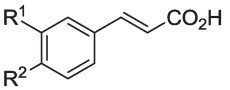

A5

a: $R^1=R^2=H$
b: $R^2=OH$, $R^1=H$
c: $R^1=R^2=OH$
d: $R^1=OCH_3$, $R^2=OH$

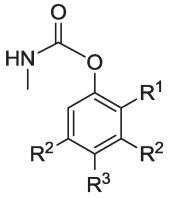

C1

a: $R^1=CH_2SCH_2CH_3$, $R^2=R^3=H$
b: $R^1=OCH(CH_3)_2$, $R^2=R^3=H$
c: $R^1=H$, $R^2=Me$, $R^3=SCH_3$

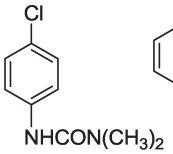

C2

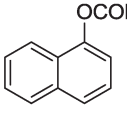

CBR

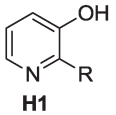

H1

a: R=H
b: R=Me
c: $R=NH_2$
d: R=Br
e: R=Cl
f: $R=CO_2H$
g: $R=CONH_2$
h: R=OH

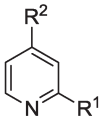

H2

a: $R^1=OH$, $R^2=H$
b: $R^2=OH$, $R^1=H$
c: $R^1=R^2=OH$

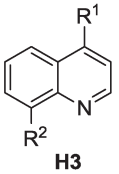

H3

a: $R^1=OH$, $R^2=H$
b: $R^2=OH$, $R^1=H$

dx.doi.org/10.1021/cr2000543 |*Chem. Rev.* 2012, 112, 1710–1750

Chart 2. Continued

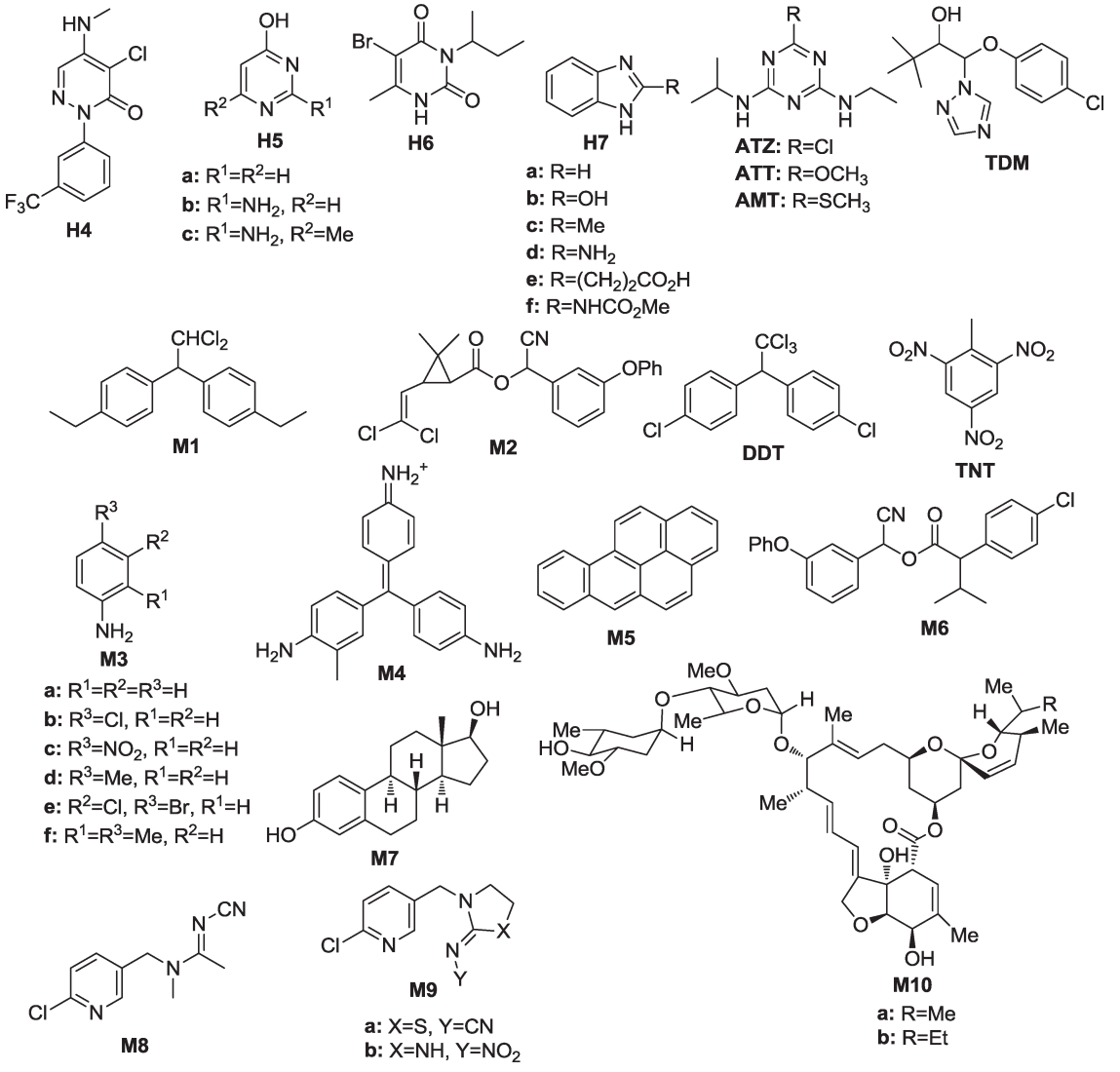

P2a−**c** has been assessed by steady-state and time-resolved techniques. A positive curvature in the Stern−Volmer plot obtained in the steady-state experiments indicates a dark association between the bisphenols and ground-state riboflavin; by contrast, a linear plot is obtained for the time-resolved data, affording dynamic quenching constants of 5.32, 2.93, and 5.99 × 10^9 M^{-1} s^{-1}.[141] As regards heterogeneous photoreactions, oxidation of parathion-ethyl (**PTE**) photosensitized by an anthracene (**ANT**)-substituted dextran involves a photoinduced electron transfer process. Energy transfer from the **ANT** singlet excited state (3.31 eV) to **PTE** (4.53 eV) is unfavorable; nevertheless, the photosensitizer excited state is quenched efficiently (k_q = 4.1 × 10^9 M^{-1} s^{-1}).[102] Likewise, fluorescence of perylene bisimide **PBIa** is quenched by increasing concentrations of cinnamic acid (**A5a**) with a rate constant above the diffusion limit (8.7 × 10^{11} M^{-1} s^{-1}).[83]

Participation of ^{1}**P*** in an electron transfer mechanism is also supported by the static quenching of **TPP** fluorescence by benzoic acids **A3c**−**h** and by the parallel shortening of its singlet state lifetime. The corresponding Stern−Volmer plots have been obtained (Figure 2); the rate constants calculated therefrom are in the range 1.5 × 10^{10} to 6.6 × 10^{10} M^{-1} s^{-1}.[186]

The good correlation obtained within a family of pollutants, such as cinnamic acids **A5a**−**d**, between the kinetic values (3.6 × 10^9−1.0 × 10^{11} M^{-1} s^{-1}) and the calculated thermodynamic parameters constitutes additional evidence for the involvement of an electron transfer process (Figure 3).[191]

Photoinduced electron transfer involving the singlet excited state of phthalocyanines **PC1g** and **PC1l** has been postulated in the photodegradation of phenols **P1a**, **P1b**, and **P1g**.[148] An absorption maximum at 590 nm appearing immediately after the laser pulse indicates formation of the **PC** anions. Furthermore, the triplet state of phthalocyanines **PC1g** and **PC1l** (λ_{max} = 490 nm) is not significantly affected by the presence of these phenol derivatives.

Further insight into mechanistic **pathway i** has been obtained by laser flash photolysis (LFP) detection of the generated species. Thus, reaction of the singlet excited state of *N*-methylquinolinium (^{1}**NMQ***) with sulfides **S1c** and **S1h** occurs with rate constants of 1.8 and 2.4 × 10^{10} M^{-1} s^{-1}, respectively.[104] Analysis of the signals obtained by LFP in the presence of **S1h** reveals formation of three transient species (Figure 4). The absorption band with maximum at 520 nm is attributed to the pollutant radical cation (**PhSMe**)$^{\cdot+}$; the

dx.doi.org/10.1021/cr2000543 |*Chem. Rev.* 2012, 112, 1710–1750

Table 3. Photocatalysts Used for the Oxidation of Specific Pollutants

	photocatalysts				
pollutants	pyryliums	aromatics	heteroaromatics	chlorins and porphyrins	phthalocyanines
CN^-					PC1a[152]
Na_2S					PC1d[146]
					PC1e[147]
					PC1f[147]
					PC1h[147]
					PC1l[147,155]
					PC1m[146,155]
					PC1n[146,155]
					PC1o[155]
					PC1p[155]
					PC3a[155]
					PC3b[155]
$Na_2S_2O_3$					PC1d[146]
					PC1h[95]
					PC1l[95,155]
					PC1m[95,146,155]
					PC1n[146,155]
					PC1o[155]
					PC1p[155]
					PC2[95]
					PC3a[155]
					PC3b[155]
NDMA[a]				PP2b[90]	
				PP2n[90]	
DCANa[b]				PP2b[90]	
				PP2n[90]	
S1a		ANT[106]			
		DCA[63,106,107]			
		AQ[63,106]			
S1b	TPP[156,157]	DCA[156]	NMQ[156]		
	TPTP[157]				
S1c	TPP[109]	ANT[109]	NMQ[104]		
		DCA[104,105,107,109]	RB[109]		
		DCAC[107]			
		AQ[109]			
S1d			MB[158]		
S1e			MB[158]		
S1f	TPP[107,156,157,159]	DCA[107,156]	NMQ[156]		
	TPTP[157,159]	DCAC[107]	MB[158]		
S1g	TPP[160]				PC1b[160]
					PC1c[160]
S1h	TPP[157]	DCA[104]	NMQ[104]		PC1g[153]
	TPTP[157]				PC1k[153]
S1i	TPP[161]	DCA[161]			
S1j	TPP[157,161]	DCA[161]			
	TPTP[157]				
S1k	TPP[161]	DCA[161]			
S1l	TPP[161]	DCA[161]			
S1m	TPP[161]	DCA[161]			
S1n					PC1g[153]
					PC1k[153]
S1o					PC1h[95]
					PC1l[95]
					PC1m[95]
					PC1n[95]
					PC2[95]
S2a		DCA[63]			
		AQ[63]			
S2b		ANT[109]			
		DCA[105]			
S2c	TPP[159]				
	TPTP[159]				
S3	TPP[116]		NMQ[116]		
			MB[116]		
S4	TPP[159]				
	TPTP[159]				

dx.doi.org/10.1021/cr2000543 |*Chem. Rev.* 2012, 112, 1710–1750

Table 3. Continued

	photocatalysts				
pollutants	pyryliums	aromatics	heteroaromatics	chlorins and porphyrins	phthalocyanines
S5	TPP[159]				
	TPTP[159]				
S6	TPP[159]				
	TPTP[159]				
S7	TPP[116]		NMQ[116]		
			MB[116]		
MTDT	TPP[162]		AYG[162]		
	TPTP[162]				
PTM	TPP[163,164]				
PTE		ANT[102]			
P1a	TPP[68,165,166]		PBIc[167]	PP2e[167]	PC1f[167,172]
	TPTP[165,166]		RB[167−169]	PP2f[172]	PC1g[148,171,172]
	BP[68]		RF[123,170]		PC1j[167]
			MB[167]		PC1l[148,167]
P1b	TPP[173]	DCA[173]	RB[173]	PP2k[174]	PC1g[148]
					PC1l[148]
P1c			RB[124]		
			MB[124]		
P1d			RB[168]		
			RF[123]		
P1e			RB[80,143,167,168,175]	CH2[143]	PC1f[167]
			RF[176]		
			MB[143]		
P1f			RB[167,168]		PC1f[167]
P1g			RB[167,168]	PP2b[90]	PC1f[167]
			RF[123]	PP2j[88]	PC1g[94,148,171]
				PP2k[150]	PC1k[177]
				PP2l[88]	PC1l[94,148]
				PP2m[88]	PC1o[94]
				PP2n[90]	PC1p[94]
P1h	TPP[173,185]	DCA[173]	RB[173]		
P1i			RF[123]		
P1j		ANT[102]	RB[168]		PC1g[171]
			RF[123]		PC1l[154]
					PC1p[154]
P1k	TPP[218]		RB[168]		PC1g[171]
			RF[170,176]		PC1k[177]
P1l				PP2j[88]	
				PP2l[88]	
				PP2m[88]	
P1m			RB[124]		
			MB[124]		
P1n			RB[178]		PC1g[179]
			MB[178]		
P1o			RB[168]		PC1g[171]
			RF[170,176]		PC1k[98,177,180]
P1p			RB[168]		PC1g[179]
			RF[170]		
P2a			RB[141]		PC3a[97]
			RF[141]		PC3b[97]
P2b			RB[141,181]		
			RF[141]		
			MB[181]		
P2c			RB[141]		
			RF[141]		
P3a			RB[124,182]		
			RF[170]		
			MB[124,182]		
P3b			RB[182]		
			MB[182]		
P3c				CH1[130]	
				PP2a[130]	
				PP2c[130]	
				PP2d[130]	
				PP2f[183]	
				PP2i[130]	

dx.doi.org/10.1021/cr2000543 |Chem. Rev. 2012, 112, 1710–1750

Table 3. Continued

	photocatalysts				
pollutants	pyryliums	aromatics	heteroaromatics	chlorins and porphyrins	phthalocyanines
P3d				PP2b[90]	
				PP2n[90]	
A1			MB[184]		
A2	TPP[185]				
A3a	TPP[186]		MB[186]		
A3b					PC1g[153]
					PC1k[153]
A3c	TPP[173,186]	DCA[173]	RB[173]		
			MB[186]		
A3d	TPP[186]		MB[186]		
A3e	TPP[173,186]	DCA[173]	RB[173]		
			MB[186]		
A3f	TPP[186]		MB[186]		
A3g	TPP[186]		RF[187]		
			MB[186]		
A3h	TPP[186]		MB[186]		
A4a	TPP[188]				
A4b			PBIb[72]	PP2b[90]	
				PP2n[90]	
A5a	TPP[189−191]		PBIa[83]		
			MB[191]		
A5b	TPP[173,189−191,193]	DCA[173]	RB[173]	PP2k[174]	
			MB[191,193]		
A5c	TPP[173,189−192]	DCA[173]	RB[173]	PP2k[174]	
	TPTP[192]		MB[191]		
A5d	TPP[67,189−192,194,195]	RA[67]	AYG[67,74]		PC1q[67]
	TPTP[67,192]		MB[67,191]		
C1a		AQ[110]			
C1b	TPP[196]				
C1c		AQ[110]			
C2			RF[197]		
CBR	TPP[67,162]		AYG[162]		
	TPTP[67,162]				
H1a		DMA[199]	RB[144,198−200]		
			RF[144,200]		
H1b			RB[144,198]		
H1c			RB[144,198]		
H1d			RB[144,198]		
H1e			RB[144,198]		
H1f			RB[144,198]		
H1g			RB[144,198]		
H1h			RB[144]		
H2a		DMA[199]	RB[144,199]		
H2b		DMA[199]	RB[144,199,200]		
			RF[144,200]		
H2c			RB[144]		
H3a		DMA[199]	RB[144,199]		
			RF[144]		
H3b		DMA[199]	RB[144,199]		
			RF[144]		
H4			RB[142]		
			RF[142]		
H5a		DMA[199]	RB[144,199,201]		
H5b			RB[144,201]		
H5c			RB[144,201]		
			RF[144,202]		
H6			PBIb[72]		
H7a			RB[121]		
			RF[121]		
H7b			RB[121]		
			RF[121]		
H7c			RB[121]		
			RF[121]		
H7d			RB[121]		
			RF[121]		
H7e			RB[121]		
			RF[121]		

Table 3. Continued

	photocatalysts				
pollutants	pyryliums	aromatics	heteroaromatics	chlorins and porphyrins	phthalocyanines
H7f			**RB**[121]		
			RF[121]		
ATZ			**RF**[203,204]	**PP1**[205]	**PC1i**[205]
				PP2f[206]	
				PP2j[206]	
ATT			**RF**[204]		
AMT			**RF**[204]	**PP2f**[206]	
				PP2j[206]	
TDM	**TPP**[207]	**DCA**[207]	**RB**[207]		
M1		**AQ**[110]			
M2			**RB**[208]		
			RF[208]		
			MB[208]		
TNT			**RF**[209]	**PP2f**[210]	
				PP2g[210]	
				PP2h[210]	
DDT			**MG**[211]		
M3a	**TPP**[165,166]		**RF**[170]		
	TPTP[165,166]				
M3b			**RF**[170]		
M3c			**RF**[170]		
M3d			**RF**[170]		
M3e			**RF**[170]		
M3f	**TPP**[212,213]				
M4				**PP3**[151]	
M5			**RF**[214,215]		
M6	**TPP**[216]				
M7			**RB**[217]		
			RF[217]		
M8			**RB**[129]		
M9a			**RB**[129]		
M9b			**RB**[129]		
M10a			**RB**[219]		
			RF[219]		
M10b			**RB**[219]		
			RF[219]		

[a] Nitrosodimethylamine. [b] Sodium dichloroacetate.

reduced form of the photocatalyst **NMQ**$^{\bullet}$, with maximum at 550 nm, and the dimeric form of the radical cation $(\mathbf{PhSMe})_2^{\bullet+}$, peaking at 780 nm, are also involved (Scheme 2).[104]

Similar results are obtained from the LFP of **NMQ** in the presence of sulfide **S1b** that results in a broad band with maximum at 525 nm, due to the overlap of the radical **NMQ**$^{\bullet}$ absorption (λ_{max} = 550 nm) and the sulfide radical cation dimer $(\mathbf{S1b})_2^{\bullet+}$ (λ_{max} = 485 nm).[156] In the case of Ph_2S (**S1f**), the transient absorption spectrum contains the **NMQ**$^{\bullet}$ band (550 nm) and the $\mathbf{S1f}^{\bullet+}$ trace centered at 740 nm.

Photooxygenation of sulfides such as **S3** and **S7** is mechanistically complex and strongly dependent on the photocatalyst used. In fact, in the presence of **NMQ** or **TPP**, the reactions display the characteristics of electron transfer photooxygenations. Thus, both photocatalysts are quenched by **S3** and **S7** at a diffusion rate constant, and the LFP experiments reveal the presence of **NMQ**$^{\bullet}$ or **TPP**$^{\bullet}$, together with the sulfide radical cations.[116] In addition, Rehm−Weller calculations indicate that electron transfer is indeed exergonic. However, the diverging photoproduct patterns suggest the possibility of different photooxygenation pathways. Hence, a new mechanism has been proposed involving addition of oxygen to **TPP**$^{\bullet}$ with formation of two peroxy radicals. These intermediates react with sulfide radical cations, forming two persulfoxides that subsequently decompose affording thiadioxirane.[116]

Only a few reports have appeared on the involvement of **OH**$^{\bullet}$ (**pathways ii** and **iii**) in the oxidation with organic photocatalysts;[163,164,188,221] one of them deals with the photodegradation of 4-chlorophenoxyacetic acid (**A4a**)[188] or methylparathion (**PTM**)[163,164] by **TPP** encapsulated in zeolite Y. Photodegradation of **PTM** leads to paraoxon and 4-nitrophenol. An electron transfer mechanism from the singlet excited state of **TPP** (E_{ox} = −2.5 V vs SCE)[43] can be safely ruled out due to the high E_{ox} of **PTM** (2.6 V vs SCE). However, the involvement of hydroxyl radical has been inferred from the following experiments: (a) generation of **OH**$^{\bullet}$ in the photolysis of **TPP** encapsulated within zeolite Y in the presence of methyl viologen gives rise to an absorption band centered at 470 nm that corresponds to the **OH**$^{\bullet}$ adduct of methyl viologen; (b) irradiation of heterogeneous **TPP** in the presence of 5,5-dimethyl-1-pyrroline-*N*-oxide generates an EPR signal at g = 1.997, attributable to the formed **OH**$^{\bullet}$ adduct; (c) formation of hydrogen peroxide and suppression of the photoreaction in $CDCl_3$ provides a further piece of evidence for the involvement of hydroxyl radical. Moreover, irradiation of a model compound, benzhydrol, in the presence of **TPP** in zeolite Y gives only benzophenone.

In fact, the reactivity of **OH**$^{\bullet}$ radical with different pollutants has been quantitatively determined by competition experiments, looking at the decrease of the typical transient absorption of the stilbene adduct at 390 nm. Figure 5 shows the formation and

dx.doi.org/10.1021/cr2000543 |*Chem. Rev.* 2012, 112, 1710–1750

Scheme 1. Alternative Mechanistic Pathways

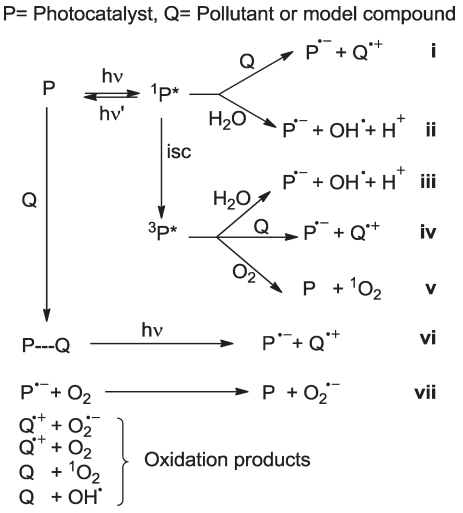

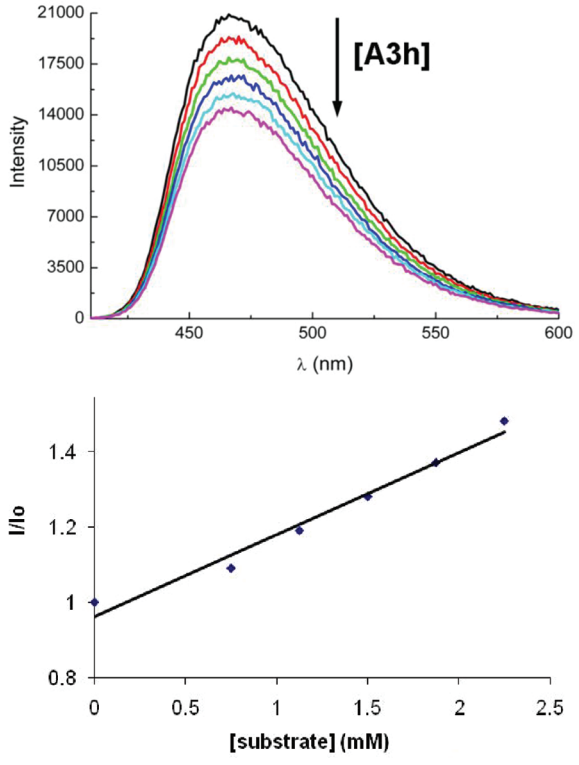

Figure 2. (Top) Quenching of the **TPP** fluorescence by the phenolic pollutant **A3h** at several concentrations (up to 2.5 × 10^{-3} M) in acidic aqueous medium. (Bottom) Stern−Volmer relationship between the emission intensity and the concentration of **A3h**. Adapted with permission from ref 186. Copyright 2001 Elsevier BV.

decay of this band in the presence of increasing concentrations of methidation (**MTDT**). Comparison of the Stern−Volmer slope (Figure 5, bottom) with that of a standard (naphthalene) yields a rate constant of 7.1 × 10^9 M^{-1} s^{-1} for **MTDT** in acetonitrile, close to the diffusion limit.[221]

Electron transfer from photocatalyst triplet states to pollutants, **pathway iv**, also occurs.[67,88,121,141,142,150,192,200,202,217] For

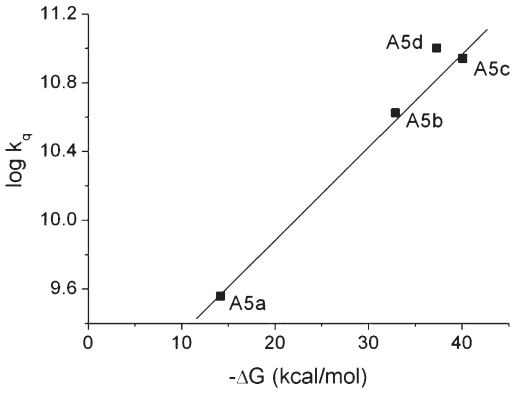

Figure 3. Semilogarithmic plot of k_q versus ΔG associated with photoinduced electron transfer from phenolic pollutants (**A5a**, **A5b**, **A5c**, and **A5d**) to the singlet excited state of **TPP**. Adapted with permission from ref 191. Copyright 2000 Elsevier BV.

instance, triplet riboflavin, ^{3}**RF***, is quenched by benzimidazoles **H7a**, **H7b**, **H7d**, **H7f**, and 17β-estradiol (**M7**) efficiently; the lifetime of the broad absorption at 600−700 nm (^{3}**RF***) is shortened in the presence of pollutants, with concomitant production of a new band at 530 nm, due to **RF**$^{\bullet-}$.[121,217] Even more, the transient spectrum of **RF** in the absence of pollutants shows a broad absorption with maximum absorbance at 600−700 nm assigned to ^{3}**RF***; in the presence of pollutants, the ^{3}**RF*** lifetime is shortened with concomitant production of a new band centered at 530 nm, due to **RF**$^{\bullet-}$. Disappearance of the ^{3}**RF*** signal has been monitored at 670 nm in the presence of increasing concentrations of pyridine **H2b**, norflurazon (**H4**), and pyrimidine **H5c**.[142,200,202] From the Stern−Volmer plots the calculated quenching rate constants are 1.2, 5.9, and 2.7 × 10^7 M^{-1} s^{-1}, respectively. Again the shape of the transient spectrum with maximum at 530 nm recorded in the presence of **H2b**, due to **RF**$^{\bullet-}$, further confirms the electron transfer process (Figure 6).

The interaction of ^{3}**RF*** with bisphenols **P2a−c** has also been studied by LFP; the bimolecular rate constants range between 1.4 and 2.1 × 10^9 M^{-1} s^{-1}. In the presence of **P2a−c**, the signal ascribed to the triplet excited state is replaced by a long-lived absorption due to the semiquinone radical **RFH**$^{\bullet}$ arising from protonation of **RF**$^{\bullet-}$.[141]

In other examples, **TPP** and triphenylthiapyrylium (**TPTP**) are very efficient photocatalysts for degradation of cafeic (**A5c**) and ferulic acids (**A5d**).[67,192] In fact, both photocatalysts are quenched by **A5c−d** in CH_3CN with rate constants near diffusion control (k_q ca. 1 × 10^{10} M^{-1} s^{-1}). Moreover, the fluorescence of ^{1}**TPTP*** is efficiently quenched, in water, with a constant of 2.8 × 10^8 M^{-1} s^{-1}. However, since the intersystem crossing quantum yield is ca. 0.94 for **TPTP**, involvement of the excited triplet state seems more likely. Actually, LFP experiments show a transient with broad maximum between 450 and 700 nm, attributed to the T_1-T_n absorption of **TPP** (Figure 7, top) or **TPTP** (Figure 8, top). Upon addition of increasing concentrations of **A5c** and **A5d**, a faster decay of the triplet is observed than in the case of **TPP**, concomitant with the appearance of a new band with maximum at 550 nm, assigned to the pyranyl radical (Figure 7, bottom).

Likewise, the triplet lifetime of **TPTP** progressively decreases upon addition of increasing concentrations of **A5c** or **A5d** (Figure 8, bottom). Quenching constants determined for deactivation of

dx.doi.org/10.1021/cr2000543 |*Chem. Rev.* 2012, 112, 1710–1750

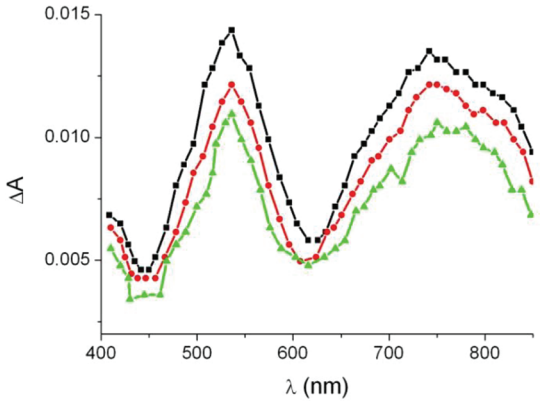

Figure 4. Time-resolved absorption spectra obtained upon LFP (λ_{exc} = 355 nm) of **NMQ** (3.5×10^{-3} M) and the sulfide **S1h** (1×10^{-3} M) in deaerated CH_3CN. Adapted with permission from ref 104. Copyright 2003 American Chemical Society.

triplet excited **TPP** and **TPTP** by **A5c** and **A5d** are shown in Table 4.

Thermodynamic calculations using the Rehm−Weller equation indicate that in the four cases photoinduced electron transfer is feasible from both excited states. Nevertheless, under the reaction conditions employed, quenching of the singlet state is <5%, while intersystem crossing represents >50% in the case of **TPP** and up to 90% for **TPTP**. Taking into account the appearance of the pyranyl radical for **TPP**, concomitantly with triplet decay, photodegradation of **A5c**−**d** is mainly mediated by the triplet state of the photocatalysts.

Further examples of photocatalysts acting through an electron transfer mechanism from the triplet excited state (**pathway iv**, Scheme 1) are provided by porphyrins. For instance, upon excitation of porphyrin **PP2k** at 355 nm, a transient absorption with maximum at 460 nm (see Figure 9) has been ascribed to the triplet state. Its decay has been monitored in the presence of increasing concentrations of 4-chlorophenol (**P1g**); from the Stern−Volmer plot, a quenching rate constant of 1.68×10^6 M^{-1} s^{-1} has been determined.[150] Additional experiments indicate that triplet quenching of different porphyrins by **P1g** is strongly dependent on the nature of the central metal. Thus, for the free base porphyrin (**PP2j**) $k_q < 10^6$ M^{-1} s^{-1}, whereas for **PP2l** and **PP2m** the values are 2.2 and 1.9×10^7 M^{-1} s^{-1}, respectively.[88]

Participation of $^1O_2$, **pathway v**,[94,97,106,116,121,124,129,130,144,147,150,153,154,158,161,168,172,178,181−184,198,199,201,217,222,223] in the methylene blue (**MB**) photocatalyzed degradation of sulfide **S1d**,[158] phenols **P1c**[124] and **P1n**,[178] naphthol **P3a**,[124] or benzaldehyde **A1**,[184] has been inferred from experiments performed in the presence of typical singlet oxygen quenchers (NaN_3 or DABCO). Likewise, retarded photodegradation of 1,5-dihydroxynaphthalene (**P3c**) by **PP2f** in the presence of NaN_3 suggests the involvement of $^1O_2$ in the process.[183] In the photooxidation of **S1a** or **S1i**−**m** sensitized by 9, 10-dicyanoanthracene (**DCA**) or anthraquinone (**AQ**), participation of singlet oxygen has been postulated based on comparison of the photoproducts obtained with different photosensitizers.[106,161] Several phthalocyanines have been employed in the photodegradation of sulfides and phenol derivatives. The reaction mechanism depends on the nature of the coordinated metal ion. In the case of phthalocyanines **PC1e**, **PC1f**, and **PC1l**, participation of $^1O_2$ in the oxidation of Na_2S has been assumed from the experiments performed in the presence of sodium azide, whereas for **PC1h** an electron transfer mechanism where Co(II) is reduced to Co(I) seems to be supported by the appearance of additional absorption bands.[147] Phthalocyanines **PC1g** and **PC1k** have also been employed for the photooxidation of methyl phenyl sulfide (**S1h**), 2-propenyl sulfide (**S1n**), and 2-mercaptobenzoic acid (**A3b**), which is initiated by singlet oxygen as revealed by the effect produced by sodium azide (singlet oxygen quencher) and benzoquinone (superoxide scavenger).[153] Photodegradation of **P1g** in the presence of different photocatalysts, such as **PC1g**, **PC1l**, **PC1o**, and **PC1p**, proceeds through a $^1O_2$ mechanism; however, direct interaction between the singlet excited

Scheme 2. Postulated Mechanism for the Photooxidation of S1h by NMQ (Adapted with Permission from Ref 104; Copyright 2003 American Chemical Society)

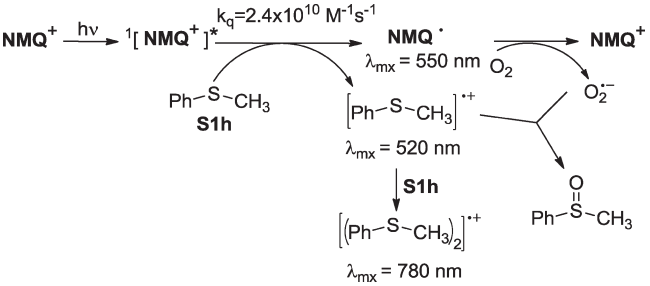

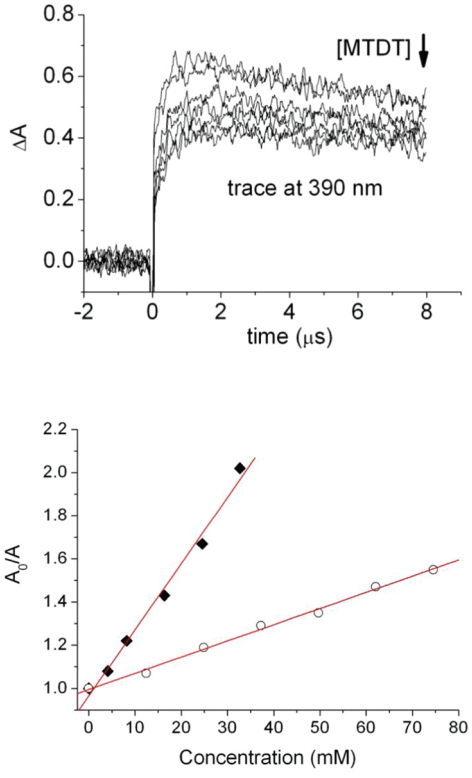

Figure 5. (Top) Kinetic traces due to stilbene-**OH**$^{\cdot}$ upon addition of increasing concentrations of **MTDT** (1×10^{-3} to 3.5×10^{-2} M) in deaerated acetonitrile. (Bottom) Stern−Volmer plots for **MTDT** (♦) and naphthalene (○) (standard) versus pollutant concentration. Adapted with permission from ref 221. Copyright 2011 Elsevier BV.

dx.doi.org/10.1021/cr2000543 |*Chem. Rev.* 2012, 112, 1710–1750

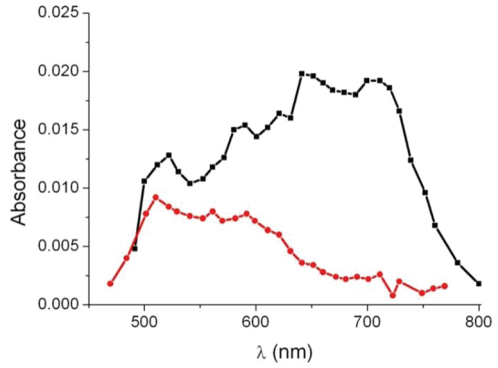

Figure 6. Transient absorption spectra of **RF** (1×10^{-5} M) in argon-saturated aqueous solution in the absence (black) and in the presence (red) of **H2b** (8×10^{-3} M). Adapted with permission from ref 200. Copyright 2001 Elsevier BV.

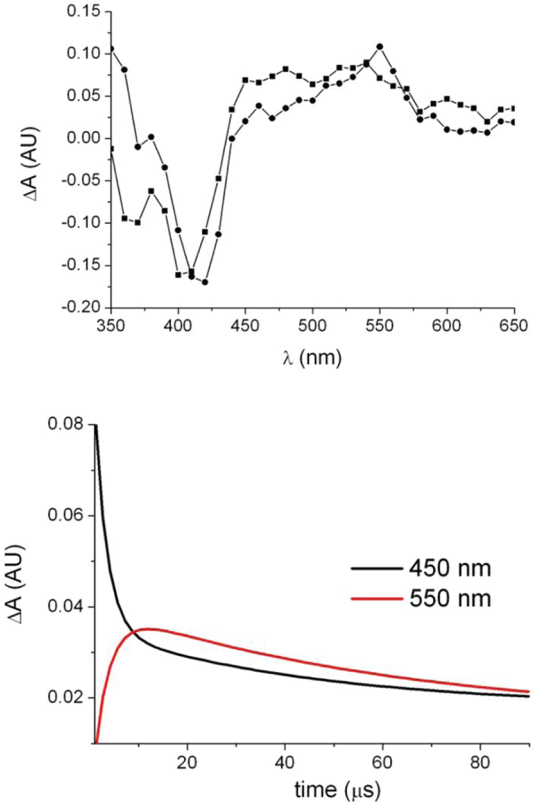

Figure 7. (Top) Transient absorption spectra obtained upon LFP (λ_{exc} = 355 nm) of **TPP** (7×10^{-5} M) in deaerated CH_3CN, in the absence (■) and in the presence (●) of the phenolic pollutant **A5d** (4.7×10^{-4} M). (Bottom) Decay and growth traces monitored at 450 (^{3}**TPP***) and 550 (**TPP**$^{\bullet}$) nm, respectively, in the presence of **A5c** (3.5×10^{-5} M). Adapted from ref 192 by permission of The Royal Society of Chemistry (RSC) for the European Society for Photobiology, the European Photochemistry Association, and the RSC.

state of the photosensitizers and **P1g** is also possible. Experiments at different concentrations and in the presence of NaN_3 show that the relative contribution of both mechanisms is concentration dependent.[94] When a mixture of sulfonated Zn phthalocyanines is used, the photooxidation of **P1g** follows mainly a ^{1}**O$_2$** mechanism, as indicated by the use of 9,10-dimethylanthracene (**DMA**) as a

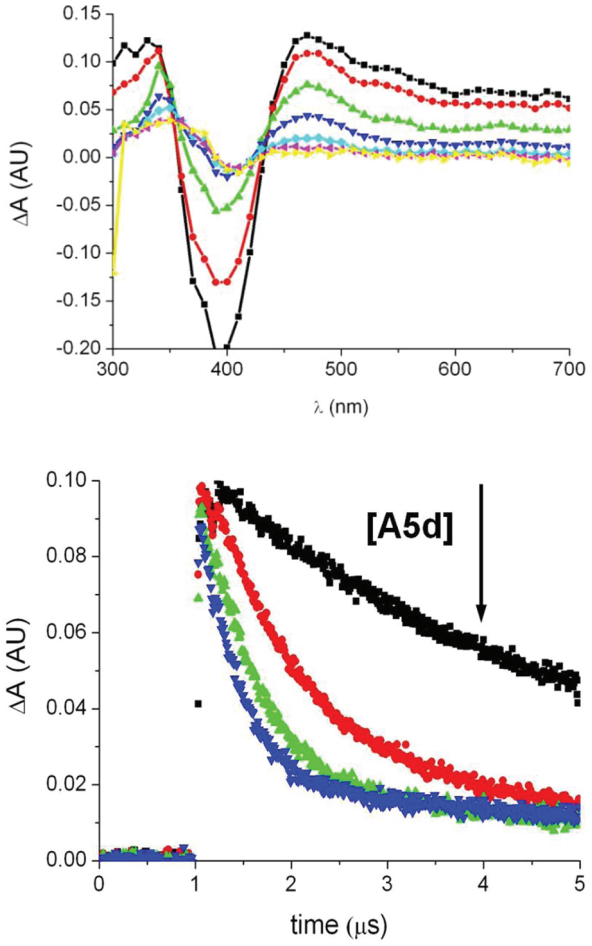

Figure 8. (Top) Transient absorption spectra obtained upon LFP (λ_{exc} = 355 nm) of **TPTP** (7×10^{-5} M) in deaerated CH_3CN at different times after the laser pulse. (Bottom) Decay of ^{3}**TPTP*** obtained upon LFP at 355 nm, monitored at 490 nm, upon addition of increasing concentrations of **A5d** (0–1.7×10^{-4} M). Adapted with permission from ref 67. Copyright 2007 Elsevier BV.

Table 4. TPP/TPTP Triplet-State Quenching Constants by the Model Pollutants A5c and A5d

photocatalyst	model pollutant	^3k_q (M^{-1} s^{-1})
TPP	**A5c**	1.3×10^{10}
TPTP	**A5c**	4.9×10^{9}
TPP	**A5d**	9.7×10^{8}
TPTP	**A5d**	8.9×10^{9}

quencher.[222] Involvement of singlet oxygen in the photodegradation of other phenol derivatives, such as **P1j**, in the presence of **PC1l**, **PC1p**, or a mixture of sulfonated Zn phthalocyanines, has also been confirmed using NaN_3.[154] In the heterogeneus photodegradation of phenol (**P1a**) using porphyrin **PP2f** or phthalocyanines **PC1f–g**, participation of ^{1}**O$_2$** (as well as **O$_2$**$^{\bullet-}$) has been proposed based on the effects observed in the presence of additives.[172]

Stronger evidence for the generation of ^{1}**O$_2$** has been provided by different spectroscopic techniques. For instance, in the case of **PC3b**,[97] electron paramagnetic resonance (EPR) evidence has been obtained using 2,2,6,6-tetramethylpiperidine (TEMP) as singlet oxygen probe. Thus, Figure 10 shows that visible light

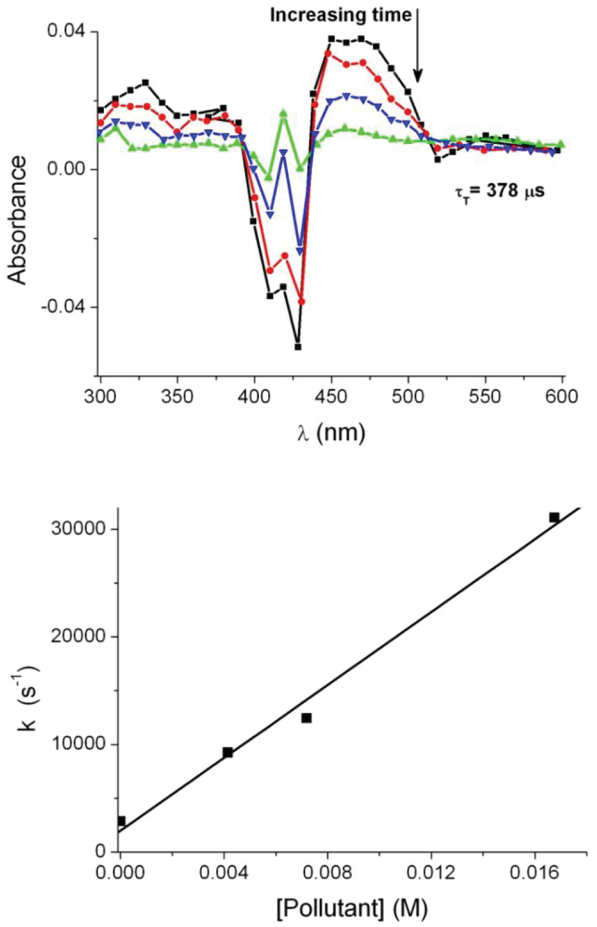

Figure 9. (Top) Transient absorption spectra of **PP2k** (6.2×10^{-4} M) obtained after laser flash excitation at 355 nm in deaerated water at different times after the laser pulse. (Bottom) Kinetic plot of the reciprocal triplet lifetime versus chlorophenol **P1g** concentration. Adapted from ref 150 by permission of The Royal Society of Chemistry (RSC) for the European Society for Photobiology, the European Photochemistry Association, and the RSC.

irradiation of **PC3b** in aerated medium gives rise to a 1:1:1 triplet signal, characteristic for the reaction of $^1O_2$ with TEMP.[97] In a control experiment, no signal is observed in the absence of photocatalyst or in the dark.

For direct detection of $^1O_2$, time-resolved near-infrared emission at 1270 nm is necessary. Thus, when rose bengal (**RB**) is excited at 532 nm, the phosphorescence emission of $^1O_2$ at 1270 nm can be recorded in the absence and in the presence of pyridine **H1b**, in neutral and alkaline media (Figure 11).[198] The Stern−Volmer plots provide a higher quenching rate constant in alkaline medium, as the conjugate base is more easily oxidizable.

Other pollutants, like phenols **P1e**, **P1f**, **P1g**, **P1j**, **P1k**, **P1o**, and **P1p**; 17β-estradiol (**M7**); and neonicotinoids (**M8** and **M9a**−**b**) can be oxidized by $^1O_2$, generated by irradiation of **RB**.[129,168,217] Correlation between the determined quenching constants and the oxidation potentials reveals a quantitative structure−activity relationship.[168]

A number of heteroaromatic pollutants also react with $^1O_2$. Thus, rate constants for quenching of singlet oxygen by **H1a**−**h**, **H2a**−**c**, **H3a**−**b**, and **H5a**−**c** have been determined by time-resolved phosphorescence.[144,199,201] In the case of **H7a**−**f**, the value obtained is ca. 10^6 M^{-1} s^{-1}.[121] In a further example,

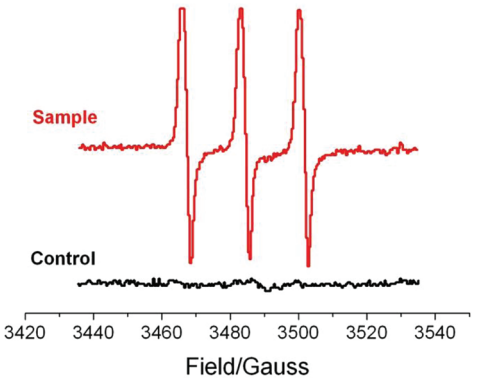

Figure 10. EPR spectra obtained after irradiation of a solution of TEMP (10^{-2} M) in the presence of **PC3b** (red trace). In the absence of **PC3b** or in the dark (control black trace), only the baseline is recorded. Adapted with permission from ref 97. Copyright 2005 Elsevier BV.

involvement of $^1O_2$ in the photooxidation of bisphenol **P2b** using either **RB** or **MB** as photocatalysts has been proven by phosphorescence quenching with k_q in the range 10^4−10^5 M^{-1} s^{-1}, depending on the aggregation. The radicals resulting from reaction of **P2b** with $^1O_2$ are detected by EPR.[181]

Photooxygenation of sulfides such as **S3** and **S7** in the presence of **MB** follows a typical singlet oxygen pathway, which is supported by the following pieces of evidence: (i) quenching of the 1270 nm emission of $^1O_2$; (ii) suppression of product formation in the presence of 1,4-diazabicyclo[2.2.2]octane (DABCO); (iii) isotope effect consistent with a persulfoxide intermediate; and (iv) lack of reactivity of the sulfur directly attached to the two phenyl rings, in accordance with the behavior of Ph_2S under singlet oxygenation conditions.[116]

Porphyrin photocatalysts are known to generate $^1O_2$. This species, obtained by irradiation of **PP2k** ($\Phi_\Delta \approx 1$), reacts with *p*-chlorophenol (**P1g**) with $k_q = 6.0 \times 10^6$ M^{-1} s^{-1}. Therefore, although this phenolic pollutant is able to quench the porphyrin triplet state with $^3k_q = 1.7 \times 10^6$ M^{-1} s^{-1}, its main photodegradation pathway involves reaction with singlet oxygen.[150]

By following the 1270 nm emission decay at different 1,5-dihydroxynaphthalene (**P3c**) concentrations, a plot of the pseudo-first-order rate constant versus pollutant concentration is obtained. From the slope of the linear plots, a quenching rate constant value of 6.5×10^6 M^{-1} s^{-1} is determined (Figure 12).[130] Quenching constants for other naphthalene derivatives such as **P3a**−**b** have also been calculated from time-resolved phosphorescence experiments.[182]

As regards heterogeneous media, after excitation at 355 nm of phthalocyanines **PC1b** or **PC1c** immobilized in zeolites, the characteristic singlet oxygen luminiscence is monitored at 1270 nm.[223] Concerning photoinduced electron transfer from a ground-state complex (**pathway vi** of the general mechanistic scheme), it operates in the photodegradation of methidathion (**MTDT**) and carbaryl (**CBR**) by using 2,4,6-triphenylpyrylium (**TPP**) and 2,4,6-triphenylthiapyrylium (**TPTP**) as photocatalysts (Scheme 3).[162]

The fluorescence of **TP(T)P** decreases in the presence of the pollutants, with quenching constants higher than the diffusion-controlled rate (Figure 13). However, singlet lifetimes of **TPP** and **TPTP** are not affected by the presence of **MTDT** nor **CBR**, indicating that the quenching is not dynamic and pointing to a

dx.doi.org/10.1021/cr2000543 |*Chem. Rev.* 2012, 112, 1710–1750

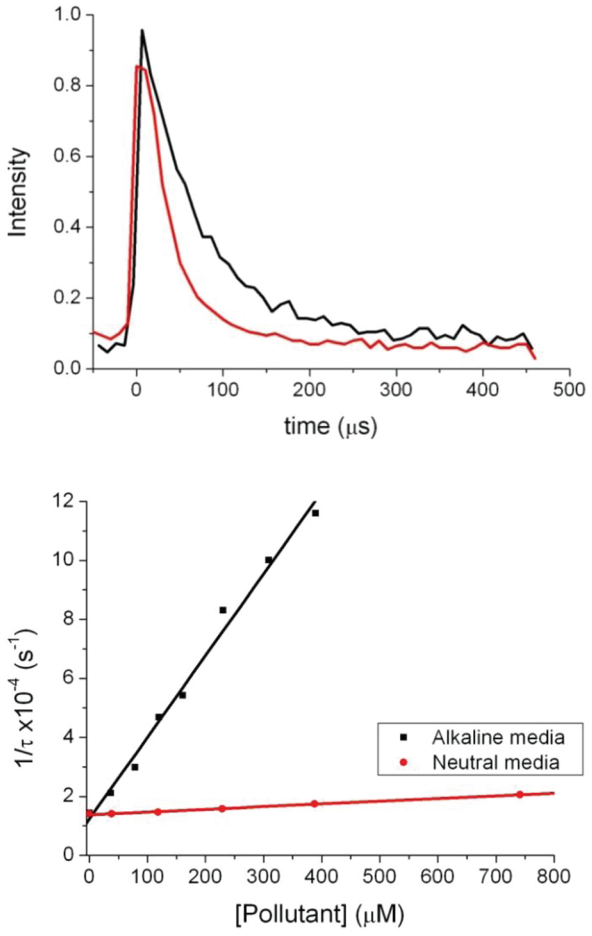

Figure 11. (Top) Decay of $^1O_2$ emission in alkaline CH_3CN/D_2O (4:1) recorded in the absence (black trace) and in the presence (red trace) of **H1b** (1.2×10^{-4} M) using **RB** as sensitizer and 532 nm as excitation wavelength. (Bottom) Stern−Volmer plot for quenching of $^1O_2$ by increasing concentrations of **H1b**, in alkaline (black) and neutral (red) media. Adapted from ref 198. Copyright 1999.

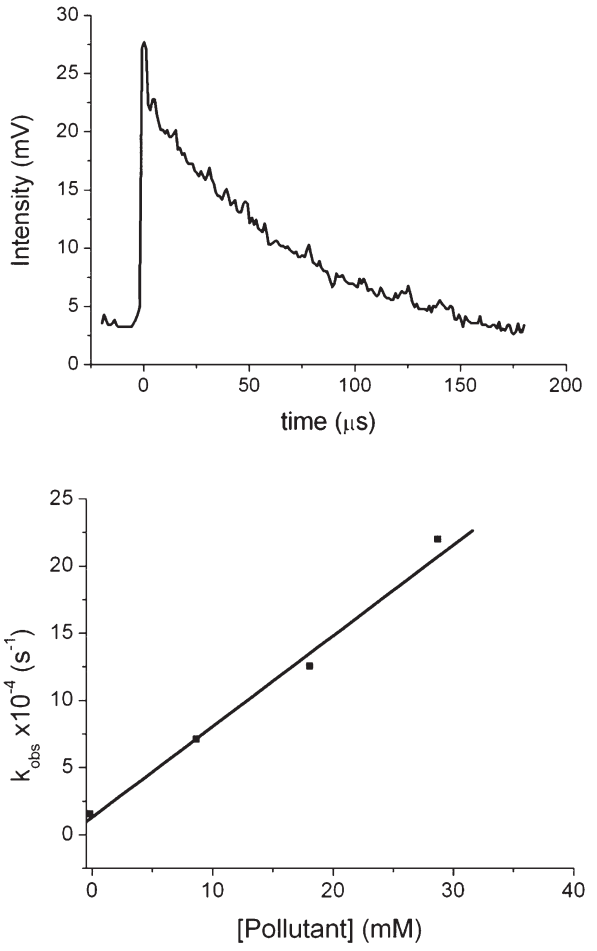

Figure 12. (Top) Typical kinetic trace of $^1O_2$ emission monitored at 1270 nm, obtained after laser flash excitation (λ_{exc} = 355 nm) of 2-acetonaphthone in aerated solutions (CH_3CN/CH_2Cl_2, 1:1). (Bottom) Stern−Volmer plot for the quenching of $^1O_2$ by **P3c**, obtained from time-resolved phosphorescence experiments. Adapted from ref 130 by permission of The Royal Society of Chemistry.

nonemissive ground-state complex as the species responsible for the reduced emission.

Laser flash photolysis experiments show a less efficient formation of the triplet state of the photocatalysts upon addition of the pollutants (without a clear effect on the triplet lifetime), together with an instantaneous increase in the signal due to the pyranyl radical (Figure 14). From these experimental results an excited ground state complex has been postulated as the key active species responsible for photoinduced electron transfer.

Participation of $O_2^{\bullet-}$, **pathway vii**,[107,109,123,151,187,206] has been postulated in the photodegradation of phenol derivatives **P1a**, **P1d**, **P1g**, **P1i**, and **P1j** with **RF**, where quenching of the triplet state occurs with concomitant appearance of the $RF^{\bullet-}$ transient. A good correlation between the ^3k_q value and the phenol oxidation potentials is also found.[123] Superoxide anion is formed by electron transfer from $RF^{\bullet-}$ to molecular oxygen regenerating the **RF** ground state. In this case, $^1O_2$ is quenched by **P1a**, **P1d**, **P1g**, **P1i**, and **P1j** in a physical fashion, without giving rise to oxidized photoproducts.

Photocatalytic degradation of **A3g** in the presence of **RF** involves participation of $^1O_2$, $O_2^{\bullet-}$, and H_2O_2 because the presence of superoxide dismutase, sodium azide, or catalase causes a delay in oxygen uptake.[187] Involvement of $^1O_2$ is monitored by fluorescence, laser flash photolysis, and time-resolved phosphorescence experiments.

In a number of examples, like photodegradation of **S1c** by **DCA** or **DCAC**, formation of $O_2^{\bullet-}$ from $P^{\bullet-}$ after an initial photoelectron transfer process is supported by the nature of the obtained photoproducts.[107,109] Photodegradation of **M4** by porphyrin **PP3** also occurs through an $O_2^{\bullet-}$ mechanism, as indicated by the effect of benzoquinone as a superoxide scavenger and DABCO as singlet oxygen quencher.[151]

Finally, $O_2^{\bullet-}$ is also involved in the photodegradation of atrazine (**ATZ**) by **PP2f** and **PP2j**, as suggested by the following observations: (a) no quenching of the triplet state by **ATZ** is noticed, (b) the presence of a singlet oxygen quencher does not produce any effect on the photodegradation, and (c) the triplet state of the porphyrins is efficiently quenched by O_2.[206]

4.2. Photodegradation and Identification of Photoproducts

Photooxidation of pollutants using organic photocatalysts rarely leads to complete mineralization, or to total elimination. Instead, highly oxidized and/or fragmented compounds are obtained, which may be less toxic and more suitable for subsequent biological treatment. Therefore, the terms

dx.doi.org/10.1021/cr2000543 |*Chem. Rev.* 2012, 112, 1710–1750

Scheme 3. Proposed Mechanism for the Photodegradation of CBR by TPP and TPTP (Adapted from Ref 162; Copyright 2009)

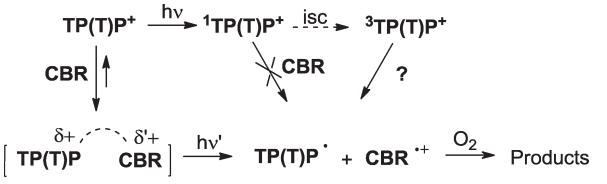

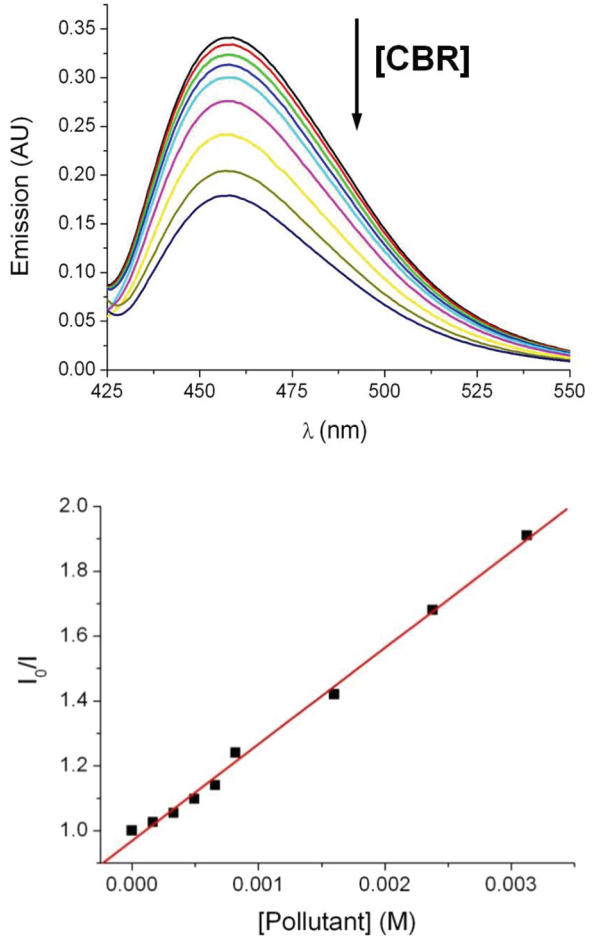

Figure 13. (Top) Quenching of **TPTP** fluorescence (λ_{exc} = 420 nm) upon addition of increasing concentrations of **CBR** (0−3.12 × 10^{-3} M). (Bottom) Stern−Volmer plot for the quenching of **TPTP** fluorescence by **CBR**. Adapted with permission from ref 162. Copyright 2009 Elsevier BV.

photooxidation and photodegradation will be used in this section when discussing the disappearance of pollutants as a result of photocatalytic reactions, rather than removal or elimination.

Different analytical procedures have been developed to evaluate the efficiency of photocatalytic processes. In some cases, classical methods such as titrations have been used; for instance, $AgNO_3$ has found application to follow disappearance of cyanide by means of copper phthalocyanine (**PC1a**) supported onto zeolite X.[152] Nonetheless, in most cases instrumental analytical

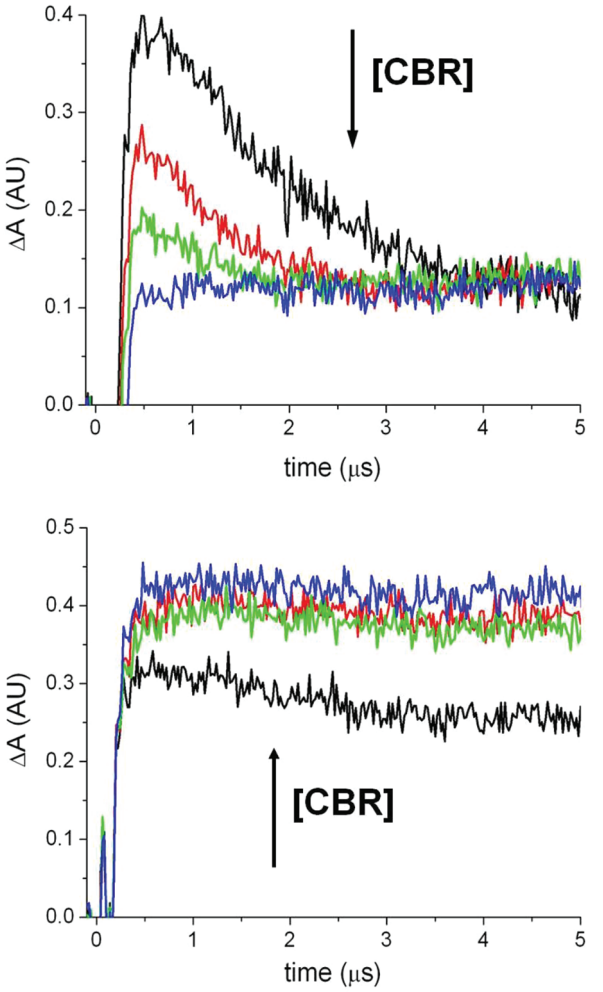

Figure 14. (Top) ^{3}**TPP*** trace obtained upon laser flash excitation (λ = 355 nm) recorded at 470 nm in the presence of increasing concentrations of **CBR** (0−3.3 × 10^{-4} M). (Bottom) Trace due to **TPP**$^{\bullet}$ recorded at 550 nm upon addition of increasing amounts of **CBR** (0−3.3 × 10^{-4} M). Adapted with permission from ref 162. Copyright 2009 Elsevier BV.

techniques are needed to assess photodegradation of the pollutant.

Changes in the UV−visible spectrum have been employed to monitor modifications in the composition of samples during irradiation.[72,154,176,183] This is a convenient procedure for studying photodegradation of different pollutants by means of riboflavin (**RF**) or rose bengal (**RB**).[142,144,176,182,198,199,201]

An interesting example is the photodegradation of 1,5-dihydroxynaphthalene (**P3c**) using a porphyrin (**PP2f**) as photocatalyst and an iodine tungsten lamp as the irradiation source.[183] The decreasing absorption in the region 275−350 nm, together with the increase at λ < 275 nm (see Figure 15), is attributed to photooxidation of the pollutant, with formation of 5-hydroxy-1,4-naphthoquinone as major photoproduct (confirmed by mass spectrometry and elemental analysis).

Absorbance changes have also been monitored at a selected wavelength, to obtain kinetic data[130,151,183] or to compare results under different experimental conditions. For instance,[183] the concentration of 1,5-dihydroxynaphthalene has been determined from

dx.doi.org/10.1021/cr2000543 |*Chem. Rev.* 2012, 112, 1710–1750

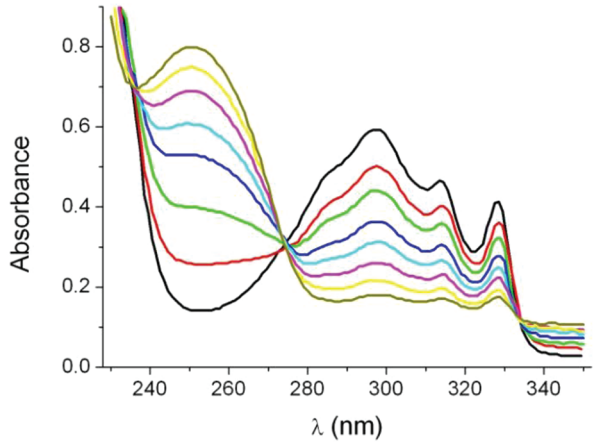

Figure 15. UV spectra obtained between 0 and 28 min during **PP2f** (2×10^{-4} M) catalyzed photodegradation of the naphthalene derivative **P3c** (2×10^{-4} M) at pH 3.8. Adapted with permission from ref 183. Copyright 2008 Elsevier BV.

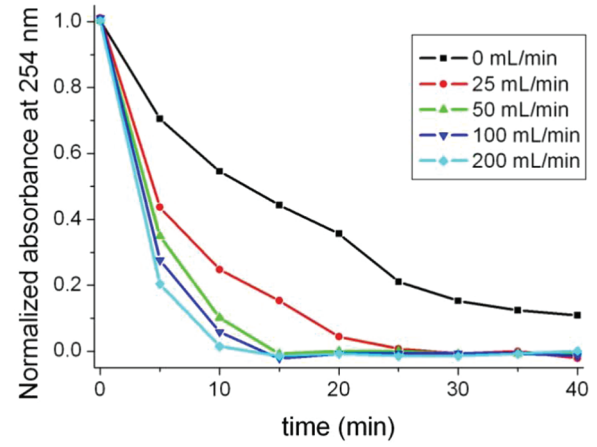

Figure 16. Oxidation of bisphenol A (**P2a**) 10^{-3} M in water at pH = 12 photocatalyzed by **PC3b** under different flow rates of air (0−200 mL min^{-1}) using visible light. Reaction monitored by HPLC using a C18 column and UV−vis detection (λ = 254 nm). Adapted with permission from ref 97. Copyright 2005 Elsevier BV.

its absorption at 329 nm; with this information, the effects of initial photocatalyst concentration and pH have been established.

Nevertheless, to avoid interferences due to the presence of other species absorbing at the monitoring wavelength, chromatographic analysis is often necessary. In this context, high-performance liquid chromatography (HPLC) coupled with UV−visible detection is by far the most widely employed method to follow photooxidation of pollutants.[67,68,74,80,88,90,97,102,143,148,150,153,156,157,161,162,165,166,168,170,171,173,175,177,179,180,185,186,188−197,203,205,206,209,210,212,213,222] As an example, the effect of air flow rate on the photodegradation of bisphenol A (**P2a**) in the presence of a polynuclear zinc phthalocyanine (**PC3b**)[97] is shown in Figure 16.

Likewise, the performance of different photocatalysts has been compared by HPLC. Photooxidation of a phenolic compound, namely, ferulic acid (**A5d**), has been studied using a solar simulator in the presence of six different photocatalysts: 2,4,6-triphenylpyrylium (**TPP**), 2,4,6-triphenylthiapyrylium (**TPTP**), acridine yellow G (**AYG**), methylene blue (**MB**), alcian blue

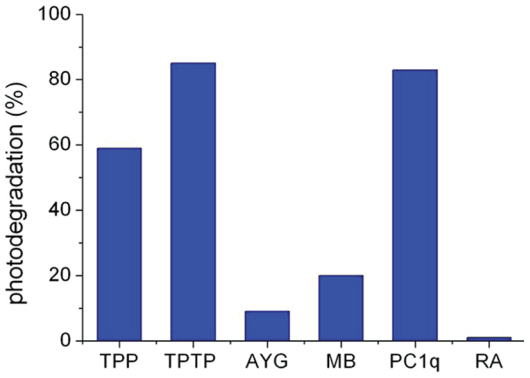

Figure 17. Degradation of aqueous solutions of ferulic acid **A5d** (10^{-3} M) using six different photocatalysts (10 mg L^{-1}) upon irradiation with a solar simulator. Adapted from ref 67. Copyright 2007.

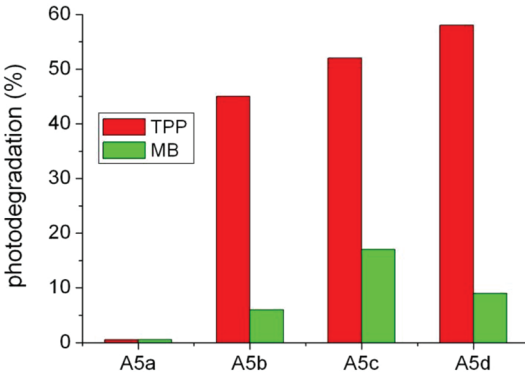

Figure 18. Solar photodegradation of four phenolic acids (10^{-3} M aqueous solutions) catalyzed by **TPP** (red bars) and **MB** (green bars). Data obtained after 6 h irradiation. Adapted from ref 191. Copyright 2000.

(**PC1q**), and rosolic acid (**RA**).[67,192] Results indicate that, after 3 h of treatment, ca. 80% photodegradation of the pesticide is achieved by **TPTP** and **AYG**, ~60% of the pollutant is photooxidized by **TPP**, and the other photocatalysts are less efficient (see Figure 17).

A similar methodology has been employed to compare the ability of two photocatalysts (**TPP** and **MB**) to oxidize a series of phenolic acids, namely, cinnamic acid (**A5a**), *p*-coumaric acid (**A5b**), caffeic acid (**A5c**), and ferulic acid (**A5d**).[191] Figure 18 shows that, in all cases, the electron transfer mechanism (**TPP**) is more efficient than singlet oxygen generation (**MB**). As regards the substrate, the order of reactivity observed in the **TPP**-catalyzed reaction is as follows: **A5d** > **A5c** > **A5b** > **A5a**. This has been attributed to the different substitution of the aromatic ring: two activating hydroxy and/or methoxy groups in **A5c** and **A5d**, only one hydroxy group in **A5b**, and none in the case of **A5a**.[186]

The reactivity of photocatalysts (**TPP**, **TPTP**, and **AYG**) toward various families of pesticides belonging to a variety of families has been evaluated.[162] Methidathion (**MTDT**) undergoes photodegradation faster than carbaryl (**CRB**); **TPTP** and **TPP** are more efficient than **AYG** (Figure 19).

Alternative chromatographic methods have also been employed: gas chromatography (GC) has been used for volatile compounds,[63,109,156,158,159,161,166,184,208] whereas ionic chromatography has been mainly employed to determine ions released during the reaction.[63] Both GC and HPLC have been coupled

dx.doi.org/10.1021/cr2000543 |*Chem. Rev.* 2012, 112, 1710–1750

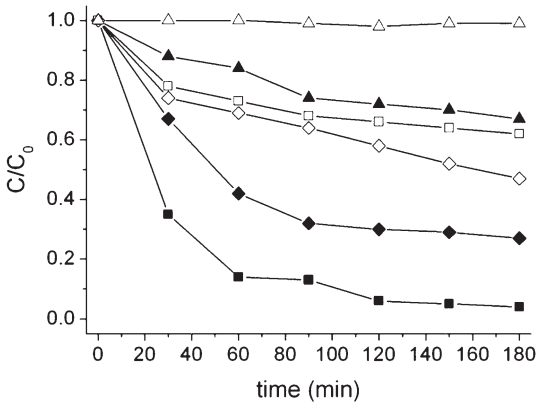

Figure 19. Plot of the relative concentration of **MTDT** and **CBR** (C/C_0, where C_0 = 50 mg L^{-1}) versus irradiation time in the presence of three different photocatalysts (10 mg L^{-1}): **TPP** (♦), **TPTP** (■), and **AYG** (▲). Filled symbols correspond to **MTDT**, and empty symbols correspond to **CBR**. Adapted with permission from ref 162. Copyright 2009 Elsevier BV.

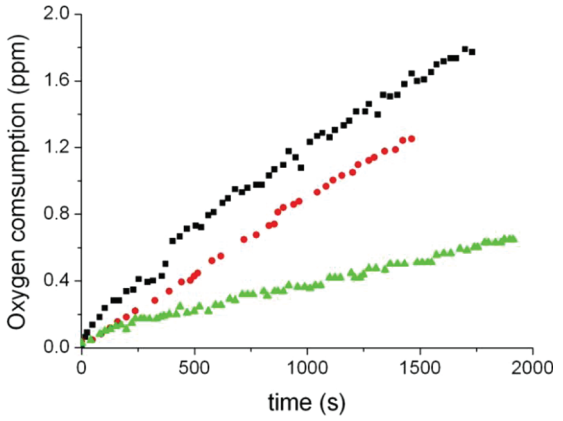

Figure 20. Oxygen consumption measured upon visible light (440 nm) irradiation of methanol/water solutions containing **RF** (2×10^{-2} M) and three phenols (1×10^{-1} M): **P1a** (●), **P1i** (■), and **P1j** (▲). Adapted with permission from ref 123. Copyright 2004 Elsevier BV.

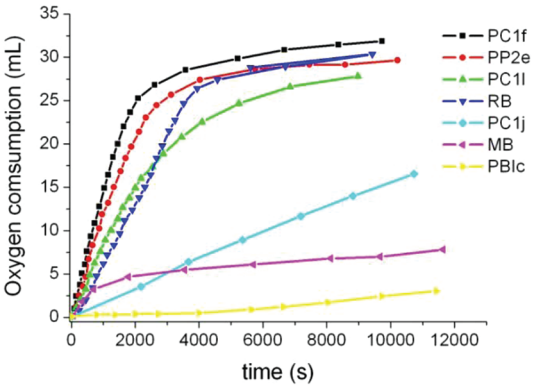

Figure 21. Oxygen uptake rate measured upon irradiation of aqueous solutions (pH = 13) containing phenol (**P1a**, 7.16×10^{-3} M) and seven different photocatalysts (5×10^{-6} M). Adapted with permission from ref 167. Copyright 1997 Elsevier BV.

with mass spectrometry detectors (GC-MS)[83,104,105,107,109,110,116,124,160,162,169,173,178,182,203,204,207,211] or (HPLC-MS);[141,154,164] however, these hyphenated techniques have been mainly employed to detect byproduct or to elucidate the reaction mechanism, an issue that will be addressed later in this section. In a number of cases, ^{1}H NMR[105,116,173,207,211] and ^{13}C NMR[105,173,211] have been used for a more reliable identification of byproduct.

Oxygen consumption (measured by means of a specific oxygen electrode) has been taken as an indicator to determine the reaction kinetics, especially for processes involving singlet oxygen as the reactive species.[95,121,141,146,147,155,182,198,200−202] An example is shown in Figure 20, where photooxidation of three phenolic compounds, phenol (**P1a**), *p*-phenylphenol (**P1i**), and *p*-nitrophenol (**P1j**), by visible light (ca. 440 nm) is catalyzed by riboflavin (**RF**).[123] In the absence of substrate or in the dark, no oxygen is consumed; by contrast, when solutions containing **RF** and the substrate are irradiated, phenols with lower oxidation potentials take up oxygen at higher rates. Photophysical measurements suggest that the reaction occurs by formation of a complex between ground-state phenol and singlet oxygen, followed by electron transfer.

A similar methodology has been used to compare the efficiency of a series of seven organic photocatalysts, namely, three phthalocyanines (**PC1f**, **PC1j**, and **PC1l**), a metal-free porphyrin (**PP2e**), a perylene bisimide (**PBIc**), rose bengal (**RB**), and methylene blue (**MB**), to achieve oxidation of phenol (**P1a**) (see Figure 21).[167] The low activity of **PC1j** and **PBIc** has been attributed to their tendency to aggregate in aqueous solution, whereas in the case of **MB**, the main drawback is associated with its low photostability. Among the photocatalysts showing better performance, limitations arise from a relatively low singlet oxygen quantum yield (**PC1f**) or from lack of stability (**PP2e** and **RB**). Experiments carried out in the presence of detergent, at different pH values, confirm the influence of aggregation and stability on the reaction rate.[224]

In some cases, the effect of operational conditions on the photochemical process has been studied using statistics and, in particular, response surface methodologies. An example can be found in Figure 22, where the effect of photocatalyst (**TPP**) and substrate concentration (xylidin, **M3f**) on the photooxidation is illustrated by means of an experimental design methodology based on Doehlert matrixes.[212] Figure 22 shows that higher percentages of photodegradation are achieved at lower substrate concentrations and in the presence of higher amounts of **TPP**.

In addition to monitoring photodegradation by chromatographic methods, in a limited number of cases the photoproducts have been identified by comparison with standards and/or by NMR. However, further effort is required to investigate the nature of the reaction products obtained by treatment of pollutants with organic photocatalysts, to elucidate the involved mechanism.

For example, different photocatalysts have been used in the photooxidation of a wide variety of model sulfides. Thus, sulfides **S1a**, **S1c**, and **S1e** are converted into the corresponding sulfoxides, sulfones, and disulfides by photocatalytic treatment with **DCA**, **AQ**, or **MB**.[63,104−107,109,158] Under similar conditions, disulfides (**S2a**−**b**) give thiosulfonates and sulfonic acids as the major photoproducts.[105,109] Interestingly, photooxidation of sulfur-containing compounds may depend on the nature of the photocatalyst and also on the presence or absence of O_2.[156,157,161] Thus, irradiation of **S1j** in the presence of **DCA** or **TPP** gives rise to the sulfoxide as the main photoproduct. It is formed either by reaction with $^1\mathbf{O_2}$ (generated from **DCA**) or by

electron transfer quenching of the **DCA**/**TPP** excited states, followed by reaction of the resulting radical ions with O_2. Alternatively, deprotonation of the sulfide radical cation can give rise to radical coupling products or, after oxygen trapping, to benzaldehyde (Scheme 4).[161]

One of the most studied families of pollutants or model compounds as targets for organic photocatalysis are phenols and their derivatives. Thus, **P1a** is oxidized to *p*-benzoquinone using porphyrin **PP2f**[172] or different phthalocyanines such as **PC1f**, **PC1g**, or **PC1l**.[148,167,172] The same product is obtained when **P1g** is photooxidized with porphyrins **PP2j**−**m**[88,150] or phthalocyanines **PC1g**, **PC1l**, or **PC1o**−**p**[94,148] or when quinol (**P1c**) is treated with **RB** or **MB**.[124] Catechol (**P1b**) and tyrosol (**P1h**) give dimers as the major photodegradation products with **RB** as photocatalyst.[173] Photodegradation of **P1j** with **PC1l** or **PC1p** gives 4-nitrocatechol and hydroquinone,[154] whereas 2,6-dimethylphenol (**P1l**) is transformed into 2,6-dimethylbenzoquinone using porphyrins **PP2j**, **PP2l**, or **PP2m**.[88] Chlorinated phenols such as 2,4,5-trichlorophenol (**P1n**) or pentachlorophenol (**P1p**) give 2,5-dichloro-1,4-benzoquinone and 2,3,5,6-tetrachloro-1,4-benzoquinone, respectively, by photocatalytic treatment with **RB**, **MB**, or **PC1g**.[178,179] Rose bengal mediates photodegradation of 2-chlorophenol (**P1e**) to pyrocatechol, 2-chloro-1,4-benzoquinone, 2-chlorohydroquinone, and maleic acid.[80] Naphthalene derivatives, such as 1-naphthol (**P3a**), afford 1,4-naphthoquinone as the major photoproduct when irradiated in the presence of **MB** or **RB**,[124,182] whereas in the case of **P3b**, phthalic acid and a dimer (2,2′-dihydroxy-1,1′-binaphthyl) are formed.[182] Dihydroxynaphthalenes like **P3c** undergo photodegradation by means of **PP2f** or **PP2i**, leading to 5-hydroxy-1,4-naphthoquinone as the major photoproduct.[130,183]

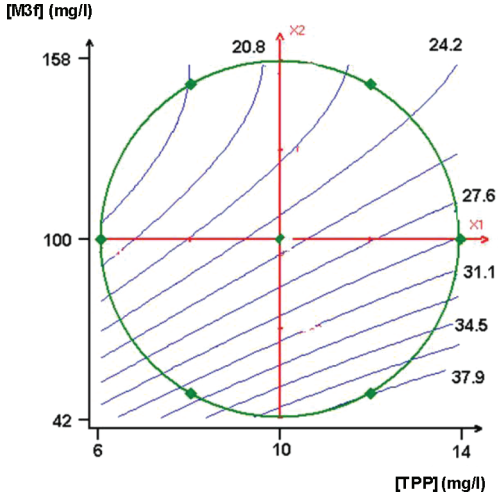

Figure 22. Response surface obtained for the percent of xylidine (**M3f**) photodegradation in aqueous solution (pH = 3) after 60 min of irradiation at different concentrations of catalyst and substrate, using a Doehlert matrix. Adapted from ref 212. Copyright 2004.

Oxidative degradation of bisphenol derivatives (**P2a**−**c**) has been achieved using **RB**, **RF**, **MB**, or **PC3a**−**b** as photocatalysts.[97,141,181] For example, in the case of **P2a** the photoreaction leads to *p*-isopropenylphenol, *p*-isopropylphenol, hydroquinone, and phenol, in a first stage. Further oxidation gives oxalic and maleic acids and, ultimately, carbon dioxide (Scheme 5).

Likewise, photochemical treatment of **P1h** or **A2** with **TPP** proceeds through initial oxidation of the benzylic position, to give in both cases *p*-hydroxybenzaldehyde.[185] Under similar conditions, *p*-coumaric acid (**A5b**) gives also *p*-hydroxybenzaldehyde, together with *p*-hydroxybenzoic acid, protocathechuic aldehyde, and maleic and oxalic acids.[193] Under **RB** photocatalysis, heteroaromatic compounds, for instance, **H1a**, are converted into maleimide, succinimide, 2,3-dihydroxypyridine, and maleic, fumaric, and oxalic acids.[144,198] By contrast, isomerization rather than oxidation occurs with *E*-cinnamic acid (**A5a**) in the presence of perylene bisimide **PBIa**, giving the *Z* isomer as major photoproduct.[83]

The dichlorinated pesticide **M1** as well as carbamates **C1a** and **C1c** have been treated with **AQ** as photocatalyst.[110] Thus, **M1** leads mainly to 1,1-dichloro-2,2-bis(4-acetylphenyl)ethane, whereas **C1a** yields 2-hydroxybenzaldehyde and 3-methylbenzo-[*e*][1,3]oxazine-2,4-dione, and **C1c** gives rise to 3,5-dimethyl-4-methylsulfinylphenol and 3,5-dimethyl-4-methylthiophenol. On the other hand, carbamate **C1b** affords *o*-dihydroxybenzene as the major photoproduct when photodegraded with **TPP** in heterogeneous media.[196]

In particular, photooxidation of **PTE** by anthracene (**ANT**) on a polymeric support yields paraoxon ethyl and 4-nitrophenol as the primary products[102] (Scheme 6). Likewise, irradiation of

Scheme 4. Mechanistic Pathways in the Photooxidation of Sulfide S1j Sensitized by DCA and TPP (Adapted with Permission from Ref 161. Copyright 2008 Wiley-VCH Verlag GmbH & Co. KGaA)

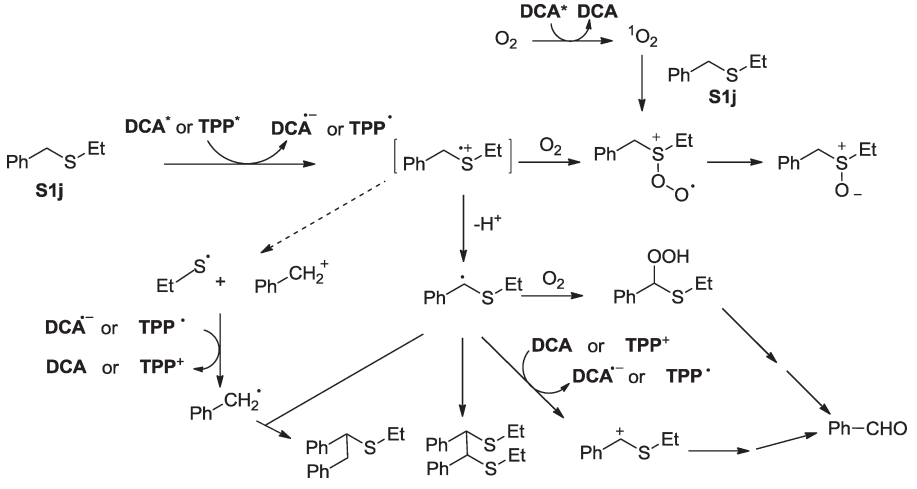

PTM in the presence of heterogeneous **TPP** results in formation of methyl paraoxon and 4-nitrophenol.[163,164]

Photochemical decomposition of **TDM** in the presence of **DCA** or **TPP** results in oxidation of the hydroxyl group or in fragmentation (Scheme 7).[207]

ATZ and the related compounds **ATT** and **AMT** are photodegraded by **RF**,[203,204] porphyrins **PP2f** or **PP2j**,[206] and phthalocyanine **PC1i**.[205] Oxidation or cleavage of the lateral chains gives rise to a mixture of photoproducts (Scheme 8).

Further examples are the photodegradation of **TNT** by **PP2f**, **PP2g**, or **PP2h**, to give trinitrobenzoic acid and trinitrobenzene;[210] the dehalogenation of **DDT** using **MG** as photocatalyst;[211] the oxidation of **M5** with **RF**, leading to 1,6-benzo[*a*]pyrenedione, 3,6-benzo[*a*]pyrenedione, and 6,12-benzo[*a*]pyrenedione;[214,215] the photodecarboxylation of **M6** in the presence of supported **TPP**;[216] the oxygenation of the aromatic ring of **M7** in the presence of **RB**;[217] or the singlet oxygenation of the neonicotinoid insecticides **M8** and **M9a**–**b**, affording 6-chloronicotinic acid.[129]

5. PHOTOCATALYTIC APPLICATIONS

5.1. Organic Photocatalysis in Heterogeneous Media

5.1.1. Preparation and Characterization of Supported Organic Photocatalysts. After establishing the feasibility of using organic dyes as photocatalysts, hetereogeneization of the systems seems a logical step forward; solid photocatalysts can be easily removed after the reaction, making it possible to operate in a continuous mode and thus to recycle the photocatalyst for further use. For this purpose, some strategies have been used to support catalysts onto different materials.

By far, 2,4,6-triphenylpyrylium (**TPP**) and 2,4,6-triphenylthiapyrylium (**TPTP**) hosted onto different inorganic supports are the most widely employed solid photocatalysts for elimination of model pollutants from aqueous solution. In some cases silica gel[157,195] or naturally occurring silicates, such as sepiolites, have been used;[194] in addition, **TPP** has been hosted onto carbon nanotubes[225] or mesoporous titanium dioxide.[226] Nonetheless, in most cases, zeolites have been employed as supports following different experimental procedures for incorporation of **TP(T)P**.

Thus, **TPP** has been included within extralarge pore zeolitic aluminosilicates, such as MCM-41. These materials provide an adequate balance between moderate cage effect and facilitation of molecular traffic through the mesopores.[227] As the diameter of the channels (2 nm) allows diffusion of **TPP**, a simple ion-exchange procedure can be employed to incorporate this organic cation (Figure 23).

Easily available Y-zeolite has also been employed as host for (thia)pyrylium cations. The dimensions of this material are compatible with the presence of large organic cations (0.95 nm × 1.2 nm) inside its supercages (1.3 nm diameter), yet the connecting channels are too small for free diffusion (0.74 nm). Hence, more complex processes have been developed to synthesize the desired hybrid materials, for instance, the "ship in a bottle" methodology. This procedure has been followed to synthesize different photocatalysts inside the cages of the zeolites from their immediate precursors, which are small enough to diffuse through the channels.[228] In the case of **TPP**, chalcone and acetophenone are mixed with acid Y-zeolite (HY) as illustrated in Figure 24; the Brönsted acid sites of the zeolite play a catalytic role.[229] The presence of **TPP** in the new material, as well as the absence of its precursors after thorough washing, can be checked by Fourier transform infrared (FT-IR), UV-diffuse reflectance,

Scheme 5. Oxidative Degradation of Bisphenol A (Adapted with Permission from Ref 97. Copyright 2005 Elsevier BV)

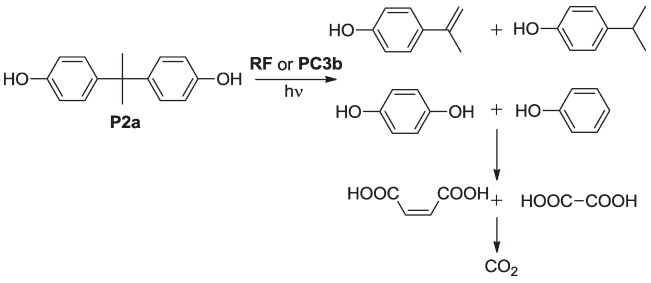

Scheme 6. Photocatalytic Oxidation of PTE (Adapted with Permission from Ref 102. Copyright 2005 Elsevier BV)

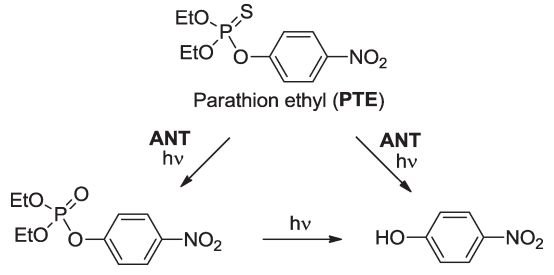

Scheme 8. Photocatalyzed Reactions of Triazine Derivatives (Adapted with Permission from Ref 203. Copyright 2002 Elsevier BV)

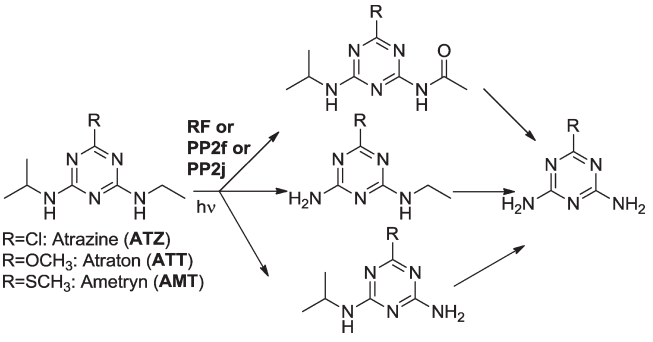

Scheme 7. Photodegradation of TDM in the Presence of DCA or TPP (Adapted from Ref 207; Copyright 2003)

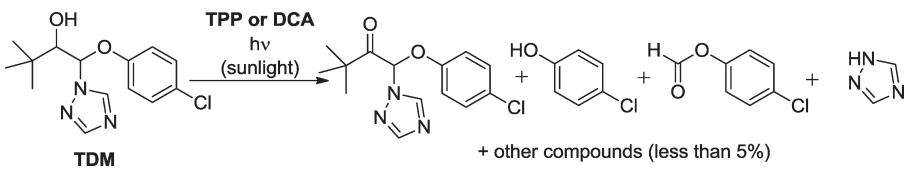

dx.doi.org/10.1021/cr2000543 |*Chem. Rev.* 2012, 112, 1710–1750

and temperature-programmed desorption (TPD) analysis. There are some reports of photocatalytic applications for the oxidation of hazardous chemicals, using **TPP**-loaded Y-zeolite prepared by this procedure.[188,216] Likewise, introduction of **TPTP**[159]and bipyrylium (**BP**)[68] inside Y-zeolite is achieved by an analogous strategy. It is interesting that, in the case of **BP**, the photocatalyst seems to occupy two neighboring supercages.

More recently, the "camel through the eye of a needle" approach has been proposed as an alternative to imprison **TPP** inside the Y-zeolite supercages. It is formally an ion-exchange process in aqueous medium, although it actually follows a more complex mechanism, summarized in Figure 25: (a) hydrolytic opening of the pyrylium ion to give a linear diketone, (b) diffusion of this diketone through the channel to reach the supercage, and (c) recyclization to **TPP** upon heating.[213]

This mechanism is supported by the IR spectrum of the final product, which shows the characteristic bands of **TPP**. In addition, a sample submitted to partial dehydration shows the presence of the diketone together with residual **TPP** (see Figure 26).

This methodology allows for a better control of zeolite loading, which can be tuned in the range 3−15% (w/w).[189] Modifications of the above procedure make use of 1,3,5-triphenylpent-2-en-1,5-dione as starting reagent; it is incorporated into the zeolite by stirring in an organic solvent, followed by filtration and final dehydration. This approach has been extended to host **TPP** in Y and β zeolite,[218] MCM-41, mesoporous TiO_2-SiO_2, and SiO_2.[230] Supercritical CO_2 at 60 °C can be used instead of the organic solvent for impregnation of Y-zeolite with 1,3,5-triphenylpent-2-en-1,5-dione; at higher temperature, cyclization of the diketone occurs inside the zeolite supercages to give **TPP**.[231] The resulting material has been characterized by X-ray diffraction, FT-IR, UV diffuse reflectance, and N_2 adsorption at 77 K.

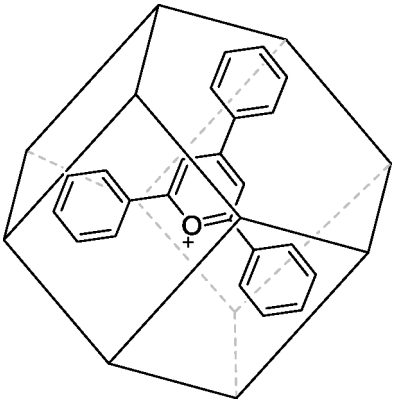

Figure 23. Incorporation of **TPP** inside the channels of mesoporous MCM-41. Adapted with permission from ref 227. Copyright 1994 American Chemical Society.

The "ship in a bottle" procedure has also been used with Y zeolites to host Fe(II), Mn(II), Co(II), Cu(II), Zn(II), and Ni(II) phthalocyanines. First, ion exchange is employed to load Na zeolite with the desired metal, and then *o*-phthalonitrile is added to synthesize "in situ" the organic moiety.[230] More simple is the introduction of methylene blue (**MB**) inside the cavities of Y zeolites, which can be achieved by direct ion exchange.[158]

A series of papers have appeared dealing with the use of silica gel to support different photocatalysts,[62−66,105−107,172] to remove gas-phase as well as dissolved pollutants. A very simple procedure has been described to host 9,10-dicyanoanthracene (**DCA**) and anthraquinone (**AQ**) onto large-particle silica gel, in which the support is added to a solution of the catalyst and then filtered and dried.[106] For obtaining porous silica monoliths containing **DCA**, tetramethyl-*ortho*-silicate is used as starting material, and the synthesis is carried out "in situ" in a solution containing **DCA**. Characterization of the material is achieved by N_2 adsorption at 77 K and diffuse reflectance UV. Alternatively, **DCA** is first grafted onto triethoxysilyl precursor to synthesize silica particles afterward.[107,232,233] Other photocatalysts that have been supported onto silica include ketones,[230] condensed aromatics,[231] tin porphyrins,[90] and the above-mentioned pyrylium salts.[157,195]

In a related application, formation of a silane gel from its precursors in the presence of photocatalysts has been employed to immobilize rose bengal (**RB**) and methylene blue (**MB**).[143,175] Supported photocatalysts have also been prepared from alumina, which has been used for different phthalocyanines.[146] Likewise, bentonite has found application as host for phthalocyanines and **MB**,[98,124,171,234] whereas Mg−Al layered double hydroxides have been used to host metal phthalocyanines[180] as well as 4-benzoylbenzoate.[235,236]

Biodegradable organic polymers, such as starch, dextran, chitosan, or hydroxyethylcellulose, can be used to support organic photocatalysts for wastewater treatment.[102,237−242] This constitutes a novel application of polymer-based photosensitizers, which were introduced originally for photo-oxidations.[243] For instance, an anthracene (**ANT**)-substituted dextran has been prepared by etherification with 9-chloromethylanthracene. The obtained

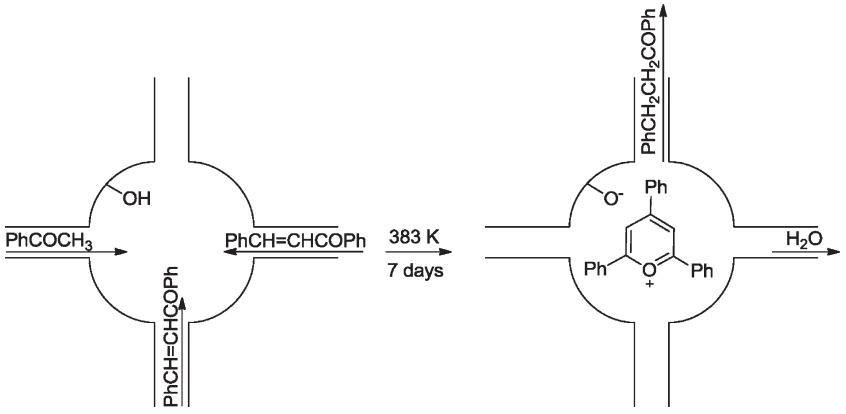

Figure 24. Loading of Y-zeolite with **TPP** following a "ship in a bottle" synthesis using acetophenone and chalcone as precursors. Adapted with permission from ref 229. Copyright 1994 American Chemical Society.

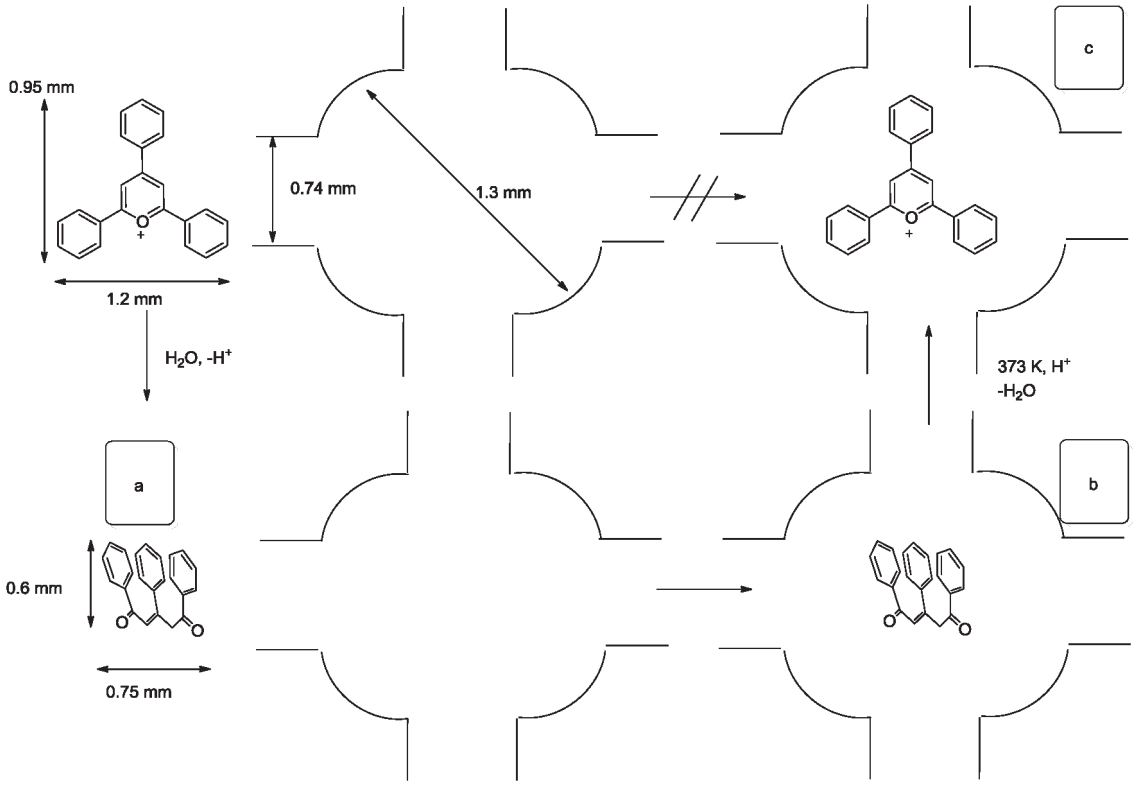

Figure 25. Mechanism of formal ion exchange to introduce **TPP** inside the Y-zeolite: (a) hydrolytic ring-opening leading to a linear diketone, (b) diffusion through the channel, and (c) thermal recyclization inside the supercage. Adapted with permission from ref 213. Copyright 2003 Wiley-VCH Verlag GmbH & Co. KGaA.

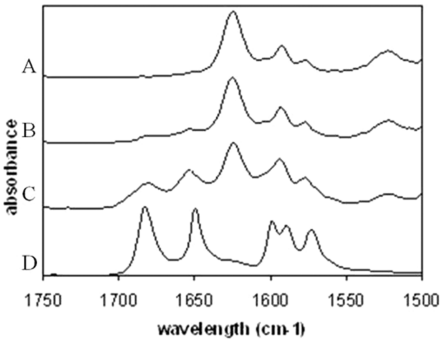

Figure 26. Infrared spectra of (A) **TPP** in KBr, (B) **TPP** hosted in Y-zeolite (dry product), (C) **TPP** hosted in Y-zeolite (wet product), and (D) 1,3,5-triphenylpent-2-en-1,5-dione. Adapted with permission from ref 213. Copyright 2003 Wiley-VCH Verlag GmbH & Co. KGaA.

polymer has been characterized by ^{1}H NMR, FT-IR, emission, and UV−vis absorption spectroscopy, as well as by gel permeation chromatography (GPC).[238] A modified chitosan has been obtained by functionalization with 1-naphthylacetic acid.[241] In this case, dynamic light scattering and atomic force microscopy have been used, in addition to spectroscopic methods and GPC, for characterization of the polymer.

Resins are alternative supports for photocatalysts. In particular, porphyrin **PP1** has been supported onto Amberlite, which is an ion-exchange resin.[205] Amberlite as support for photosensitizers has been used for other applications.[244] Different ion exchangers (Amberlite, Dowex) have been used to support a series of phthalocyanines and porphyrins to check their photostability and performance using phenol as model compound.[172] Finally polymeric ion exchangers have been attached to **RB**.[169,245] In all cases the procedure is simple, basically stirring the ion exchanger and the photocatalyst in an appropriate medium.

5.1.2. Photocatalysts Stability and Reuse. One of the major problems associated with the use of organic photocatalysts is their limited stability, as they can suffer photobleaching or solvolytic attack in the reaction medium. An example of this problem is the case of **TPP** in aqueous solutions.[195] This observation is explained by hydrolytic ring-opening of the heterocycle, outlined in Scheme 9.

Pseudo-first-order rate constants have been determined for bleaching of **TPP** at different pH values, both under irradiation (solar simulator) and in the dark. Data in Figure 27 indicate that **TPP** is moderately stable only at pH < 3 (useless for practical applications) and that degradation is accelerated under irradiation.[195]

As a consequence of the limited **TPP** stability, its efficiency decreases along the course of the reaction. By contrast, when this organic cation is supported onto silica gel plates, complete elimination of ferulic acid (**A5d**) is achieved without any significant loss of efficiency after 6 h of reaction.

Interestingly, upon incorporation of **TPP** inside the supercages of Y zeolite, the hybrid material does not show any changes in the intensity of the characteristic UV−vis **TPP** bands when it is stirred in water;[163] actually the encapsulated cation is indefinitely stable even at neutral pH. This stabilization has been attributed to geometrical constraints imposed by the rigid zeolite framework that make attack by reactive species to the encaged pyrylium ring more difficult.[218] Conversely, some hydrolysis occurs within MCM-41 zeolite or onto silica gel, where the steric confinement is less marked.[246]

dx.doi.org/10.1021/cr2000543 |*Chem. Rev.* 2012, 112, 1710–1750

Scheme 9. Hydrolytic Opening of the Pyrylium Ring to Give a Nonactive Diketone (Adapted with Permission from Ref 195. Copyright 2002 Elsevier BV)

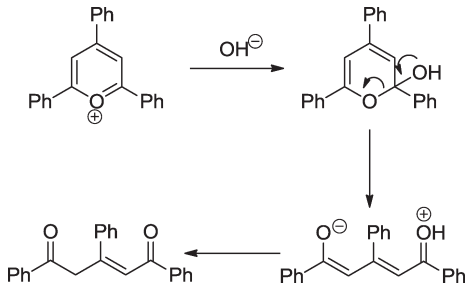

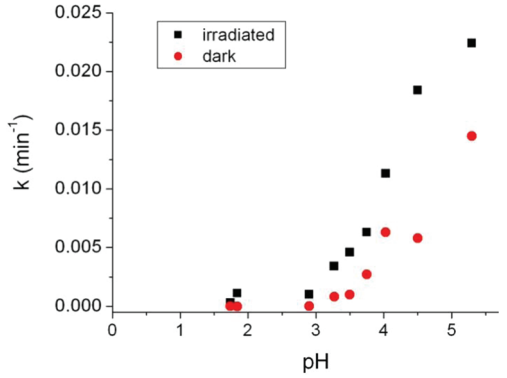

Figure 27. Pseudo-first-order rate constants for **TPP** degradation in aqueous medium (10 mg L^{-1}) at different pH values. Adapted with permission from ref 195. Copyright 2002 Elsevier BV.

Nonetheless, heterogeneization does not always guarantee an enhanced stability of the photocatalyst. For instance, irradiation of anthracene substituted dextran results in an important photodegradation,[102] as indicated by the strong inhibition of fluorescence with time. This has been attributed to oxidation of the anthracene moiety, to give a nonemitting anthraquinone derivative. In a similar process with naphthalene-modified hydroxyethylcellulose, not only is the photocatalyst is oxidized but degradation of the polymer is also observed.[240]

An additional advantage of heterogeneization is the possibility of recycling the photocatalysts for further use. Thus, **TPP** supported onto Y zeolite has been employed for abatement of xylidine (**M3f**) in aqueous solution (Figure 28).

After elimination of the pollutant, an extra amount of **M3f** is added for a new photocatalytic cycle. Figure 29 shows a logarithmic plot of the remaining concentration of **M3f** versus time for three cycles; the parallel lines indicate that efficiency is maintained, as similar pseudo-first-order rate constants are obtained.

In a different report, supported **TPP** has been used for the oxidation of organic sulfides, without significant loss of activity.[157] Only when **TPP** is adsorbed onto silica gel does the efficiency decrease, an effect that has been attributed to leaching of the organic catalyst.

In another example,[98] photooxidation of trichlorophenol (**P1o**) is catalyzed by a Pd-phthalocyaninesulfonate (**PC1k**) supported onto a modified bentonite. Figure 30 shows that, although the efficiency decreases slightly with the number of cycles, seven consecutive runs can be carried out with complete elimination of the pollutant. The gradual deactivation of the photocatalyst has been attributed to adsorption of the formed intermediates onto the bentonite surface, together with some decrease in the catalyst concentration because of sampling.

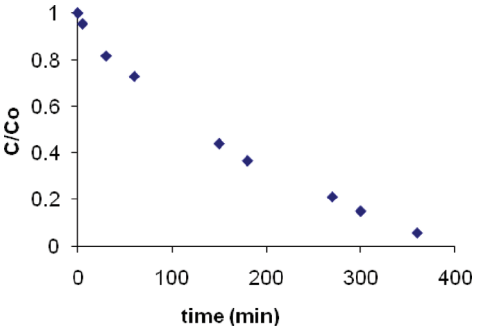

Figure 28. Photodegradation of xylidine **M3f** (100 mg L^{-1}) in aqueous solution, at pH = 2, photocatalyzed by **TPP**, supported onto Y zeolite (1.2 g L^{-1}). Adapted with permission from ref 213. Copyright 2003 Wiley-VCH Verlag GmbH & Co. KGaA.

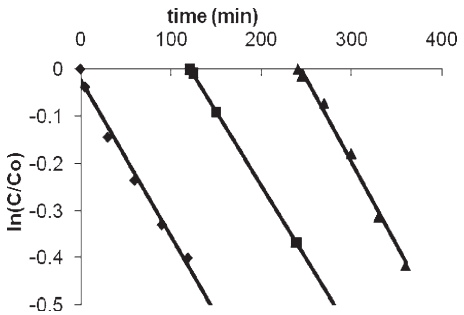

Figure 29. Photocatalytic abatement of **M3f** (C_0 = 100 mg L^{-1}) in aqueous solution, at pH = 2, by **TPP** (C_0 = 1.2 g L^{-1}) on Y zeolite. Repeated cycles with the same batch of catalyst result in similar rate constants. Adapted with permission from ref 213. Copyright 2003 Wiley-VCH Verlag GmbH & Co. KGaA.

A diverging result has been obtained[143] when using **RB** impregnated in a silane gel, deposited onto glass plates, to photooxidize 2-chlorophenol (**P1e**). Figure 31 shows that the percentage of pollutant photodegradation decreases with reuse, to reach stable values after 3−4 cycles.

Overall, these facts seem promising as a proof of the concept; however, for practical applications, determination of the "turnover number" and investigation of the possible poisoning phenomena is a necessary step forward.

5.1.3. Efficiency. The improvements achieved in the synthesis and stabilization of supported organic photocatalysts have prompted their application to remove pollutants as well as the development of further research for optimization of operational variables.[143,160,164,166,171,175,180,196,212,218,230] As an example, abatement of phenol under visible light irradiation (halogen lamp) has been performed in the presence of an aluminum phthalocyanine, **PC1f**.[171] Different operational parameters have been studied, such as the sorption of phenol, the effect of photocatalyst loading, or the possible recycling. In particular, **PC1f** has been compared with Co−Cu containing phthalocyanines. The aluminum-based photocatalyst is more efficient than the copper or cobalt analogues. This is explained by considering that singlet oxygen is the main oxidizing agent; hence, the presence of paramagnetic transition metals, such as Cu or Co,

dx.doi.org/10.1021/cr2000543 |*Chem. Rev.* 2012, 112, 1710–1750

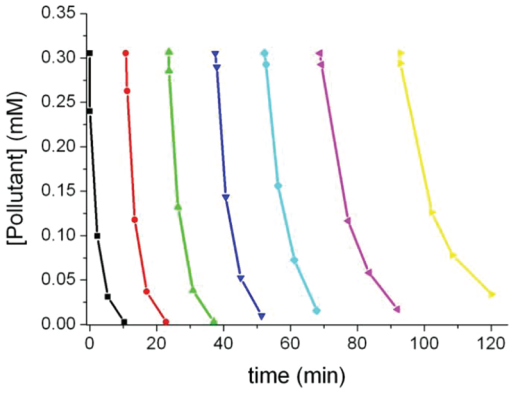

Figure 30. Recycling experiment using **PC1k** (0.05 g L^{-1}) onto a modified bentonite (1.0% w/w) for the phenolic pollutant **P1o** degradation in a mixture of water and dimethylformamide (3:2, v/v) under visible light. The photocatalyst remains stable after seven repeated runs. Adapted with permission from ref 98. Copyright 2005 American Chemical Society.

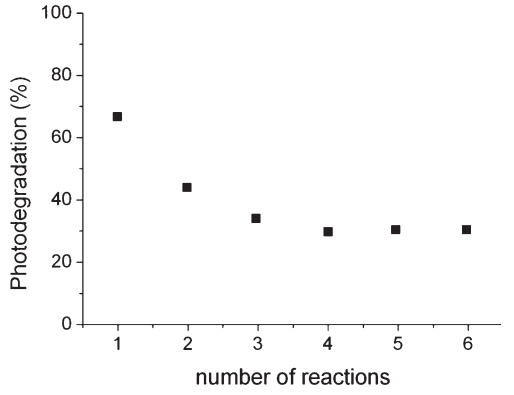

Figure 31. Efficiency of **P1e** ($C_0 = 5 \times 10^{-4}$ M) degradation in phosphoric buffer (pH = 7), after repeated experiments using **RB** impregnated in a silane gel as photocatalyst. Adapted with permission from ref 143. Copyright 2004 Elsevier BV.

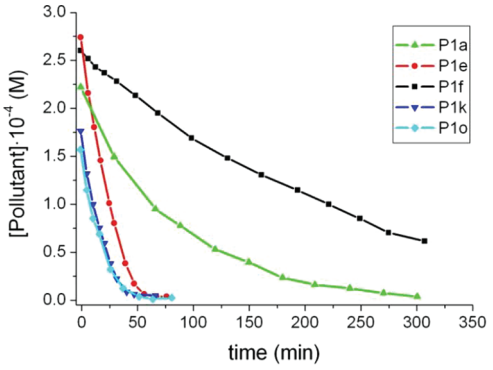

Figure 32. Degradation of a variety of substituted phenols (in aqueous solutions at pH = 12) using phthalocyanine **PC1f** on a modified bentonite as heterogeneus photocatalyst (0.25% w/w). Adapted with permission from ref 171. Copyright 2005 American Chemical Society.

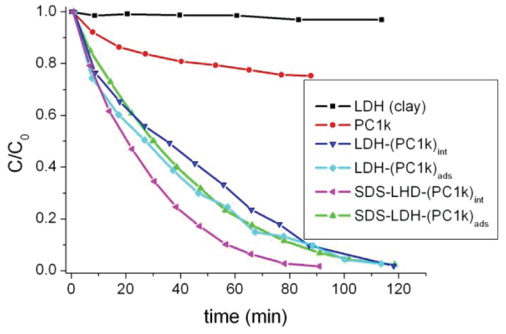

Figure 33. Degradation of chlorophenol **P1o** (3.1×10^{-4} M in water at pH = 6) using homogeneous **PC1k** (8×10^{-3} g L^{-1}) or different heterogeneous photocatalysts based on this phthalocyanine (1 g L^{-1}). Adapted with permission from ref 180. Copyright 2007 American Chemical Society.

results in shorter triplet lifetimes, and therefore triplet quenching with formation of singlet oxygen is less efficient. The effect of the substrate has also been studied. Figure 32 shows photodegradation of phenol (**P1a**), 4-chlorophenol (**P1g**), 4-nitrophenol (**P1j**), 2,4-dichlorophenol (**P1k**), and 2,4,6-trichlorophenol (**P1o**). Because singlet oxygen reacts more efficiently with electron-rich substrates, the reaction is markedly slower in the case of **P1f** bearing a deactivating group.

A specific factor to be taken into account in heterogeneous photocatalysis is the effect of support. Figure 33 shows the photooxidation, under visible light irradiation, of trichlorophenol (**P1o**) catalyzed by a palladium phthalocyanine (**PC1k**) hosted in different related supports.[180] The support itself, a layered double hydroxide (LDH), is inactive, as shown by a blank experiment. Heterogeneized **PC1k** is more efficient than the homogeneous photocatalyst. This is attributed to the aggregation of dissolved **PC1k** molecules, which results in self-quenching of the excited dye and thereby in a loss of efficiency in the formation of singlet oxygen; this phenomenon is reduced by means of heterogeneous catalysis. In addition, adsorption of the pollutant on the support brings the catalyst and the substrate in close proximity, so that singlet oxygen does not need to diffuse far away from where it is produced. Differences among supports are also accounted for in terms of dye aggregation.

The performance of **TPP** and **TPTP** onto Y and β zeolites has also been probed[165,166] using aniline (**M3a**) and phenol (**P1a**) as model compounds. The higher efficiency of **TPTP**-based materials (see, e.g., Figure 34) has been attributed to the increased oxidizing abilitity of **TPTP**.

The photocatalytic activity of different phthalocyanines (**PC1b** and **PC1c**) and **TPP** supported onto SiO_2, TiO_2-SiO_2, and zeolites has been compared using yperite (**S1g**) as pollutant.[160] Data in Figure 35 indicate that Y zeolite-based photocatalyst is very efficient despite the limitation associated with diffusion of the contaminant through the channels; this is attributed to a cooperative effect of the host, adsorbing yperite and favoring the contact between catalyst and substrate.

A comparison between UV and ambient light has also been made in the same work. Under UV irradiation, **PC1b** is more efficient than **PC1c**, while the reverse is true for ambient light; this is explained as the result of the different absorption spectra of the two photocatalysts. The high efficiency of **TPP** hosted in Y zeolites under ambient light is remarkable.

Recently, a more quantitative approach to explain the effect of the support[230] has been provided by calculating the band gap for SiO_2, TiO_2-SiO_2 MCM-41, and Y zeolite loaded with **TPP**, **PC1b**, and **PC1c**. Thus, photooxidation of dipropyl sulfide is achieved with materials showing lower band gap energies.

dx.doi.org/10.1021/cr2000543 |*Chem. Rev.* 2012, 112, 1710–1750

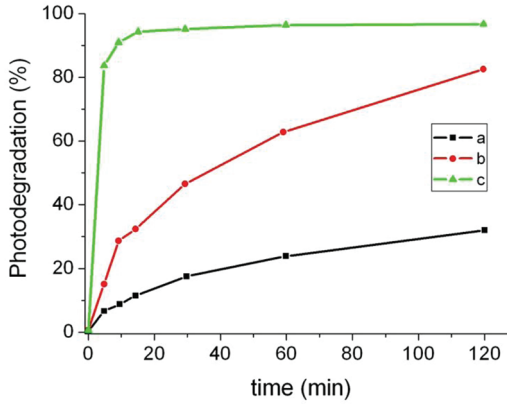

Figure 34. Photodegradation of aniline (**M3a**) in aqueous solutions (40 mg L^{-1}) in the presence of various heterogeneous photocatalysts (1.5 g L^{-1}): (a) **TPP**@Y, (b) **TPTP**@Y, and (c) **TPTP**@β. Adapted from ref 165 by permission of The Royal Society of Chemistry (RSC) for the European Society for Photobiology, the European Photochemistry Association, and the RSC.

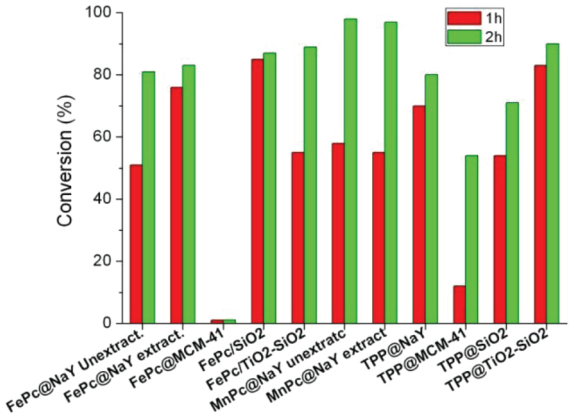

Figure 35. Effect of the support employed with three photocatalysts (**PC1b**, **PC1c**, and **TPP**, 0.34 g L^{-1}) to remove yperite (**S1g**) in dichloromethane solution (170 ppm). Percentages of photoabatement after 1 and 2 h of UV irradiation in an aerated reactor. Adapted with permission from ref 160. Copyright 2008 American Chemical Society.

Because TiO_2 is the most widely used heterogeneous photocatalyst for wastewater treatment, it seems meaningful to compare the performance of heterogeneized organic catalysts with that of TiO_2. An example is provided by the photodegradation of methyl parathion (**PTM**).[164] Figure 36 indicates very efficient photodegradation of **PTM** achieved by TiO_2, faster than by **TPP** supported onto SiO_2 and Y zeolite. In the last case, fast absorption of **PTM** in the zeolite channels is followed by a slower oxidation of this pesticide inside the supercages; this is in agreement with detection of higher amounts of **PTM** when zeolites are submitted to thorough extraction.

Other operational parameters have also been optimized in heterogeneous photocatalysis. They include catalyst concentration (**TPP** hosted in Y zeolite) and initial substrate concentration (xylidine, **M3f**).[212] Higher initial concentrations of **M3f** result in a lower pseudo-first-order constant of pollutant consumption (k). The catalyst amount is important below 1.5 g L^{-1}; beyond this point, addition of extra photocatalyst results in no significant increase of k. This can be easily appreciated in Figure 37, where

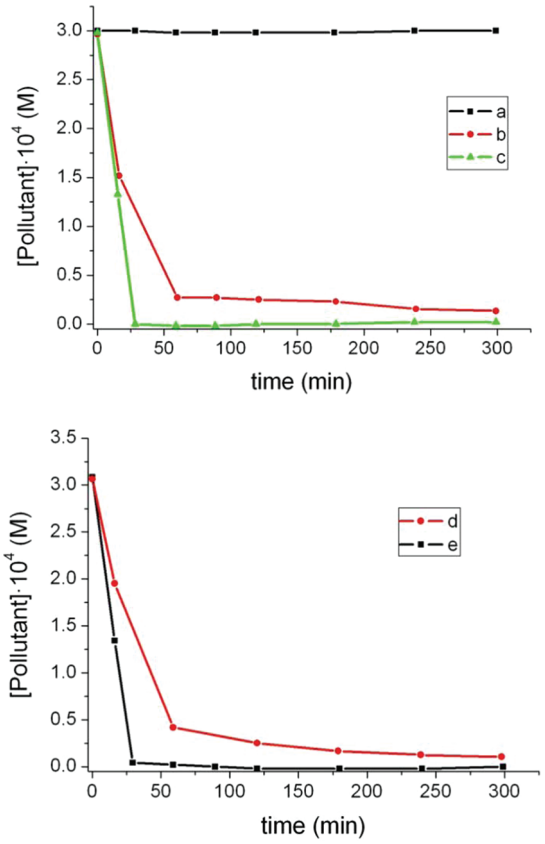

Figure 36. (Top) Concentration of **PTM** versus irradiation time: (a) in the absence of photocatalyst, (b) in the presence of **TPP**−SiO_2 (7.5 g L^{-1}), or (c) in the presence of TiO_2 (2 g L^{-1}) upon direct exposure to sunlight. (Bottom) Concentration of **PTM** versus irradiation time in the presence of **TPP** supported onto Y zeolite (7.5 g L^{-1}) measured in the aqueous phase (d) after exhaustive extraction of the pollutant and (e) during the irradiation. Adapted with permission from ref 164. Copyright 2000 Elsevier BV.

the k values obtained with a xylidine concentration of 100 mg L^{-1} are plotted against catalyst concentration. When the amount of photocatalyst is higher than 1.2−1.6 g L^{-1}, the rate constant reaches a plateau. This is well-known in heterogeneous photocatalysis: once the catalyst amount absorbs all incident photons, a further increase does not lead to a further enhancement of the reaction rate.

5.1.4. Organic Versus Inorganic Photocatalysts. To assess the applicability of organic photocatalysts for the decontamination of real wastewaters, it seems interesting to compare them to inorganic photocatalysts, mainly TiO_2, in terms of their intrinsic properties and/or their reactivity in the photooxidation of pollutants and model compounds. A first issue is the fraction of solar light that can be used to activate the process. In this context, it is widely accepted that titanium dioxide exhibits high efficiency in combination with ultraviolet irradiation. However, a logical step forward would be to take advantage of a broader spectral range by including visible light. Here, organic photocatalysts may provide a complementary tool, as their absorption bands (see Figure 1) may extend to the near-infrared.[218]

By contrast, one of the main drawbacks of organic photocatalysts is that they are less robust than TiO_2. For instance, upon irradiation in aqueous medium, the pyrylium cation (**TPP**) undergoes rapid hydrolytic ring-opening,[218] giving rise to 1,3,5-triphenyl-2-penten-1,5-dione

dx.doi.org/10.1021/cr2000543 |*Chem. Rev.* 2012, 112, 1710–1750

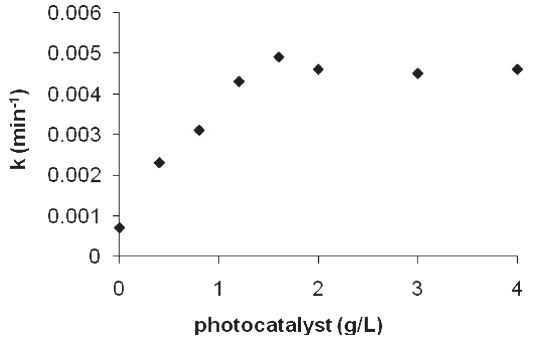

Figure 37. Heterogeneous photocatalysis for the oxidation of **M3f** (100 mg L^{-1} in aqueous media at pH = 3) by **TPP**-containing zeolite: plot of the pseudo-first-order constant k (min^{-1}) versus the amount of heterogeneous catalyst (C_0 = 100 mg L^{-1}). Adapted with permission from ref 212. Copyright 2004 Elsevier BV.

(Scheme 9).[195] Fortunately, this disadvantage can be overcome by adsorption onto inorganic supports.[166] Thus, when **TPP** is encapsulated within zeolites Y or β, it can persist indefinitely, because the geometry of the transition state required for attack by the hydroxyl group does not accommodate within the rigid crystalline framework.[218] This effect is also observed, albeit to a lesser extent, with extra-large-pore MCM-41 or amorphous SiO_2.[166]

In view of these limitations, the activity of organic photocatalysts has been compared to that of TiO_2 mainly when the former are stabilized by incorporation to inorganic supports.[62,63,159,163,165,166,188,196,218] In general, the higher surface area of zeolite-based photocatalysts justifies their higher activity. This is the case of **TPP** or its thia analogue **TPTP** encapsulated within zeolites Y or β, which exhibit higher intrinsic activity than TiO_2 in the photooxidation of thianthrene **S6**[159,166] or *p*-chlorophenoxyacetic acid (**A4a**).[188] This trend is even more remarkable when the effectiveness per photocatalytic site is considered. As an example, **TPP** at β shows a kinetic rate constant 1 order of magnitude higher than that of TiO_2 in the photooxidation of phenol **P1k**.[218] However, in some cases heterogeneous organic photocatalysts are similar to or even less photoactive than P-25 TiO_2. Thus, **TPP** at zeolite Y shows similar photocatalytic efficiency as TiO_2 for the oxidation of methylparathion (**PTM**)[163] whereas TiO_2 is superior for the photodegradation of phenol (**P1a**)[165] or 2,4-dichlorophenol (**P1k**).[218]

Interestingly, the trends observed with the initial activities are not always coincident with those found for the final conversions of a pollutant. Thus, they are parallel for phenols **P1a** or **P1k**[165,218] whereas they converge to similar values when the reactivities of **S6** with P-25 TiO_2 and **TPP** or **TPTP** at either Y or β are compared.[159] This can be associated with a variety of phenomena, such as progressive blocking of the zeolite pores, poisoning, interference of photoproducts, etc. In addition to the overall photocatalytic efficiency, a technical problem from the practical point of view is the poor dispersibility of supported organic photocatalysts, which is worse than that of TiO_2 and has to be improved. Thus, **TPP** on β zeolite displays larger particle size (>0.8 μm) than the nanometric TiO_2 (ca. 300−500 nm), which results in sedimentation of the former.[218]

Mineralization is a widely used endpoint in wastewater treatment. In this connection, the use of TiO_2 generally results in higher TOC removal, compared to organic photocatalysts. This is observed in the photodegradation of **P1k** by TiO_2 or **TPP** at β zeolite.[218] However, when mineralization is not complete, a number of photoproducts with different oxidative states can be formed. Depending on their toxicities, it may be appropriate to combine the photocatalytic step with a subsequent biological treatment to match the desired decontamination levels. In this context, an important aspect that has to be taken into account is the reaction mechanism, because it determines the nature of the subsequent obtained photoproducts. As an example, TiO_2 operates through an electron-transfer mechanism, whereas dicyanoanthracene (**DCA**) generates singlet oxygen as the main reactive species.[62,63] Accordingly, the main photoproduct in the TiO_2-mediated photodegradation of dimethylsulfide **S1a** is dimethyldisulfide whereas photooxidation with **DCA** on silica monolites leads to dimethylsulfoxide and dimethylsulfone.[62]

At the present stage, it is too early to anticipate the potential of organic photocatalysts to compete with TiO_2 for dealing with environmental problems in real life. This would require evaluation of their performance in pilot plants and water treatment facilities, taking also into account factors such as engineering or cost efficiency. However, if the above-mentioned problems (stability, dispersibility, mineralization, etc.) are satisfactorily addressed in future investigations, the prospects for application seem promising.

5.2. Environmental Applicability: Use of Solar Light, Scale-up, Detoxification, and Biodegradability

As indicated in the introduction, the use of sunlight in photocatalysis is an interesting approach, as it might result in an enhanced sustainability of the process.[247] Because the absorption spectra of many organic photocatalysts show important bands in the UVA−visible domain (see Figure 1), their use under real solar irradiation seems to be a logical step forward.

The use of UV−vis emitting lamps[90,97,107,159,163,164,173,188,205,207,222] or commercial solar simulators[67,74,143,185,189,192,193,195,204,205,218] are interesting as their emission spectra closely match the solar light, and they are not subjected to the intrinsically variable conditions of real exposure to sun; hence, they are appropriate to obtain kinetic data, to compare different photocatalysts or to determine the effect of operational parameters (catalyst amount, pH, pollutant concentration...) on the results.

Information is also available on the use of real sunlight for elimination of pollutants. In some cases, very simple experimental set-ups have been used, consisting in flasks or glass vessels left stand in sunny places.[67,74,107,143,164,185,186,188,189,191,193−195,203,204,207,209] A more complex system is based on a plate reactor, able to work in semicontinuous mode (see Figure 38).[143] The flow rate is adjusted to ensure exchange of the total volume (450 mL) every 9 min.

Parallel experiments have been performed using either artificial lamps or real sunlight.[107,164,185,188,189,193,204,207] As an example, Figure 39 shows the results obtained by comparing tungsten lamps with solar irradiation using bisphenol A (**P2a**) as model pollutant and **PC3b** as photocatalyst.[97] As expected, higher lamp potencies result in faster degradation of the pollutant. Although experimental conditions are not the same, and hence comparisons cannot be made straightforward, rather promising results are obtained when real sunlight is employed (complete photodegradation of the pollutant after 40 min).

Recent work has explored the possibilities of solar-based decontamination processes involving organic photocatalysts, which have been scaled-up to gain some insight into the real applicability of these techniques. Plants based on compound parabolic collectors (CPCs) are the most commonly used in solar water treatment (photo-Fenton or photocatalytic titanium

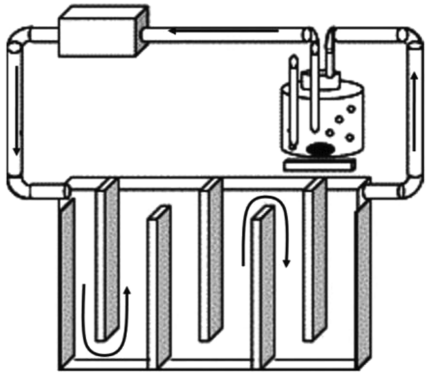

Figure 38. Schematic experimental setup for solar-based experiments consisting of a solar reactor, peristaltic pump, homogeneization/aeration vessel, gas inlet, sampling port, and magnetic stirrer. Adapted with permission from ref 143. Copyright 2004 Elsevier BV.

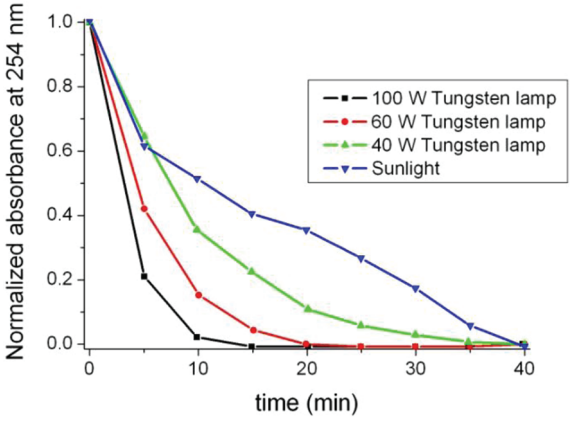

Figure 39. Degradation of bisphenol A (10^{-3} M in aqueous media at pH = 12) (monitored at λ = 254 nm) using **PC3b** as photocatalyst (2×10^{-4} M), employing sunlight or different tungsten lamps. Adapted with permission from ref 97. Copyright 2005 Elsevier BV.

dioxide).[247] This kind of plants consists in an array of pyrex tubes connected in series, through which the effluent flows. Two parabolic mirrors, generally made of aluminum, concentrate solar radiation in the pyrex tube. The setup generally includes a radiometer to measure the instantaneous and accumulated solar irradiation. This configuration allows the use of both, direct and diffuse solar light; additional practical advantages are the relative low price, robustness and simplicity.[30] An example of this type of plant can be seen in Figure 40. However, other plants have been employed with a configuration allowing a concentration of 20.9 suns,[83] which is able to rotate automatically in order to optimize the angle of incidence.

Photodegradation of ferulic acid (**A5d**) photocatalyzed by **AYG** has been scaled-up using a CPC-based pilot plant of 4 L capacity.[74] Figure 41 shows the variation of different parameters monitored along the solar process, namely pollutant concentration and total organic carbon (TOC). The time scale is represented as t_{30W}. This is a convenient form to normalize the intrinsically variable incident radiation during the experiment: the accumulated radiation is calculated, and then converted into time by considering an average UVA irradiance of 30 W/m^2.[248] As an indicator of solution oxidation state carbon oxidation state (COS) is also represented.[249]

Figure 40. Pilot plant for photocatalytic treatment based on CPCs technology.

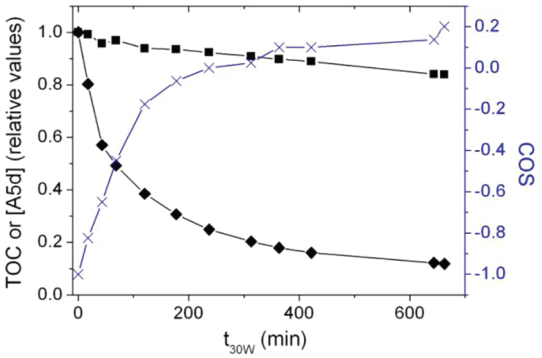

Figure 41. Photodegradation of ferulic acid (**A5d**, 10^{-3} M) catalyzed by **AYG** (10 mg L^{-1}) under solar irradiation in a 4 L CPC-based pilot plant. Left *y*-axis, given in relative units, (♦) ferulic acid concentration and (■) TOC. Right *y*-axis, COS (×). Adapted with permission from ref 74. Copyright 2007 Elsevier BV.

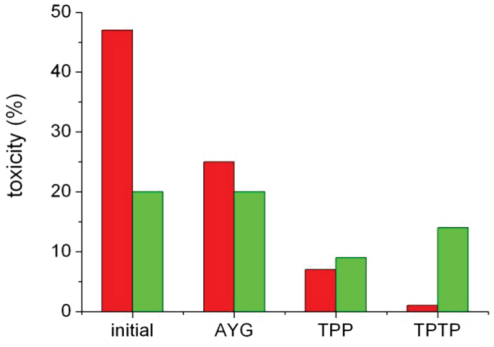

Figure 42. Toxicity measured through inhibition of the respiration of activated sludge for 50 mg L^{-1} aqueous solutions of methidathion (**MTDT**) (blue bars) and carbaryl (**CBR**) (red bars) before and after 3 h of irradiation in a solar simulator, in the presence of three different photocatalysts (**AYG**, **TPP**, and **TPTP**, 10 mg L^{-1}). Adapted from ref 162. Copyright 2009.

Although nearly 80% pollutant degradation is achieved after 5 h of irradiation, mineralization is negligible, which is attributed to formation of organic intermediates more reluctant to photooxidation than the parent compound. Accordingly, COS values are stabilized

Table 5. Types of Studies Performed on the Photooxidation of Different Pollutants with Organic Photocatalysts

	mechanistic evidence	photodegradation	photoproducts	heterogeneous photocatalysts	stability	comparison to other photocatalysts	environmental applicability
TPP	S1b[156]	S1b[156,157]	S1b[156,157]	S1b[157]	S1b[157]	S1b[156,157]	MTDT[162]
	S1c[109]	S1c[109]	S1c[109]	S1f[157,159]	S1f[157]	S1c[109]	PTM[163,164]
	S1f[156]	S1f[107,156,157,159]	S1f[107,156,157,159]	S1g[160]	S1h[157]	S1f[156,157,159]	P1h[185]
	S1i[161]	S1g[160]	S1h[157]	S1h[157]	S1j[157]	S1g[160]	P1k[218]
	S1j[161]	S1h[157]	S1i[161]	S1j[157]	PTM[163,164]	S1h[157]	A2[185]
	S1k[161]	S1i[161]	S1j[157,161]	S2c[159]	P1a[166]	S1i[161]	A3a[186]
	S1l[161]	S1j[157,161]	S1k[161]	S4[159]	P1h[185]	S1j[157,161]	A3c[186]
	S1m[161]	S1k[161]	S1l[161]	S5[159]	P1k[218]	S1k[161]	A3d[186]
	S3[116]	S1l[161]	S1m[161]	S6[159]	A2[185]	S1l[161]	A3e[186]
	S7[116]	S1m[161]	S2c[159]	PTM[163,164]	A5d[195]	S1m[161]	A3f[186]
	MTDT[162]	S2c[159]	S3[116]	P1a[68,165,166]	M3a[166]	S2c[159]	A3g[186]
	PTM[163,164]	S3[116]	S4[159]	P1k[218]	M3f[212,213]	S3[116]	A3h[186]
	P1h[185]	S4[159]	S5[159]	A4a[188]		S4[159]	A4a[188]
	A2[185]	S5[159]	S6[159]	A5a[189]		S5[159]	A5a[189−191]
	A3a[186]	S6[159]	S7[116]	A5b[189]		S6[159]	A5b[189−191,193]
	A3c[186]	S7[116]	MTDT[162]	A5c[189]		S7[116]	A5c[189−192]
	A3d[186]	MTDT[162]	PTM[163,164]	A5d[189,194,195]		MTDT[162]	A5d[67,189−192,194,195]
	A3e[186]	PTM[163,164]	P1b[173]	C1b[196]		PTM[164]	CBR[67,162]
	A3f[186]	P1a[68,165,166]	P1h[173,185]	M3a[165,166]		P1a[68,165,166]	TDM[207]
	A3g[186]	P1b[173]	A2[185]	M3f[212,213]		P1b[173]	
	A3h[186]	P1h[173,185]	A3c[173]	M6[216]		P1h[173]	
	A4a[188]	P1k[218]	A3e[173]			P1k[218]	
	A5a[191]	A2[185]	A4a[188]			A3a[186]	
	A5b[191]	A3a[186]	A5b[173,193]			A3c[173,186]	
	A5c[191,192]	A3c[173,186]	A5c[173]			A3d[186]	
	A5d[191,192]	A3d[186]	C1b[196]			A3e[173,186]	
	C1b[196]	A3e[173,186]	CBR[162]			A3f[186]	
	CBR[162,195]	A3f[186]	TDM[207]			A3g[186]	
	TDM[207]	A3g[186]	M3f[213]			A3h[186]	
	M3f[212,213]	A3h[186]	M6[216]			A4a[188]	
		A4a[188]				A5a[190,191]	
		A5a[189−191]				A5b[173,190,191,193]	
		A5b[173,189−191,193]				A5c[173,190−192]	
		A5c[173,189−192]				A5d[67,190−192,194]	
		A5d[67,189−192,194,195]				C1b[196]	
		C1b[196]				CBR[67,162]	
		CBR[67,162]				TDM[207]	
		TDM[207]				M3a[165,166]	
		M3a[165,166]					
		M3f[212,213]					
		M6[216]					
TPTP	MTDT[162]	S1b[157]	S1b[157]	S1b[157]	S1b[157]	S1b[157]	MTDT[162]
	A5c[192]	S1f[157,159]	S1f[157,159]	S1f[157,159]	S1f[157]	S1f[157,159]	A5c[192]
	A5d[67,192]	S1h[157]	S1h[157]	S1h[157]	S1h[157]	S1h[157]	A5d[67,192]
	CBR[67,162]	S1j[157]	S1j[157]	S1j[157]	S1j[157]	S1j[157]	CBR[67,162]
		S2c[159]	S2c[159]	S2c[159]	P1a[166]	S2c[159]	
		S4[159]	S4[159]	S4[159]	M3a[166]	S4[159]	
		S5[159]	S5[159]	S5[159]		S5[159]	
		S6[159]	S6[159]	S6[159]		S6[159]	
		MTDT[162]	MTDT[162]	P1a[165,166]		MTDT[162]	
		P1a[165,166]	P1a[165]	M3a[165,166]		P1a[165,166]	
		A5c[192]	CBR[162]			A5c[192]	
		A5d[67,192]				A5d[67,192]	

dx.doi.org/10.1021/cr2000543 |*Chem. Rev.* 2012, 112, 1710–1750

Table 5. Continued

	mechanistic evidence	photodegradation	photoproducts	heterogeneous photocatalysts	stability	comparison to other photocatalysts	environmental applicability
TPTP (continued)		CBR[67,162]				CBR[67,162]	
		M3a[165,166]				M3a[165,166]	
BP		P1a[68]		P1a[68]		P1a[68]	
ANT	S1a[106]	S1a[106]	S1a[106]	S1a[106]	S1a[106]	S1a[106]	
	S1c[109]	S1c[109]	S1c[109]	PTE[102]	PTE[102]	S1c[109]	
	S2b[109]	S2b[109]	S2b[109]	P1j[102]		S2b[109]	
	PTE[102]	PTE[102]	PTE[102]				
	P1j[102]	P1j[102]	P1j[102]				
DCA	S1a[106,107]	S1a[63,106,107]	S1a[63,106,107]	S1a[63,106,107]	S1a[63,106]	S1a[63,106,107]	S1c[107]
	S1b[156]	S1b[156]	S1b[156]	S1c[107]	S1c[105,107]	S1b[156]	S1f[107]
	S1c[104,105,107,109]	S1c[104,105,107,109]	S1c[104,105,107,109]	S1f[107]	S1f[107]	S1c[104,105,107,109]	TDM[207]
	S1f[107,156]	S1f[107,156]	S1f[107,156]	S2a[63]	S2a[63]	S1f[107,156]	
	S1h[104]	S1h[104]	S1h[104]			S1h[104]	
	S1i[161]	S1i[161]	S1i[161]			S1i[161]	
	S1j[161]	S1j[161]	S1j[161]			S1j[161]	
	S1k[161]	S1k[161]	S1k[161]			S1k[161]	
	S1l[161]	S1l[161]	S1l[161]			S1l[161]	
	S1m[161]	S1m[161]	S1m[161]			S1m[161]	
	S2b[105]	S2a[63]	S2a[63]			S2a[63]	
	TDM[207]	S2b[105]	S2b[105]			S2b[105]	
		P1b[173]	P1b[173]			P1b[173]	
		P1h[173]	P1h[173]			P1h[173]	
		A3c[173]	A3c[173]			A3c[173]	
		A3e[173]	A3e[173]			A3e[173]	
		A5b[173]	A5b[173]			A5b[173]	
		A5c[173]	A5c[173]			A5c[173]	
		TDM[207]	TDM[207]			TDM[207]	
DCAC	S1c[107]	S1c[107]	S1c[107]	S1c[107]	S1c[107]		S1c[107]
	S1f[107]	S1f[107]	S1f[107]	S1f[107]	S1f[107]		S1f[107]
DMA	H1a[199]	H1a[199]					
	H2a[199]	H2a[199]					
	H2b[199]	H2b[199]					
	H3a[199]	H3a[199]					
	H3b[199]	H3b[199]					
	H5a[199]	H5a[199]					
AQ	S1a[106]	S1a[63,106]	S1a[63,106]	S1a[63,106]	S1a[106]	S1a[63,106]	
	C1a[110]	S1c[109]	S1c[109]	S1c[109]		S1c[109]	
	C1c[110]	S2a[63]	S2a[63]	S2a[63]		S2a[63]	
	M1[110]	C1a[110]	C1a[110]				
		C1c[110]	C1c[110]				
		M1[110]	M1[110]				
PBIa	A5a[83]	A5a[83]	A5a[83]		A5a[83]		A5a[83]
PBIb		A4b[72]					
		H6[72]					
PBIc		P1a[167]				P1a[167]	
RA		A5d[67]				A5d[67]	
NMQ	S1b[156]	S1b[156]	S1b[156]			S1b[156]	
	S1c[104]	S1c[104]	S1c[104]			S1c[104]	
	S1f[156]	S1f[156]	S1f[156]			S1f[156]	
	S1h[104]	S1h[104]	S1h[104]			S1h[104]	
	S3[116]	S3[116]	S3[116]			S3[116]	
	S7[116]	S7[116]	S7[116]			S7[116]	
AYG	A5d[74]	MTDT[162]	MTDT[162]			MTDT[162]	MTDT[162]

dx.doi.org/10.1021/cr2000543 |*Chem. Rev.* 2012, 112, 1710–1750

Table 5. Continued

	mechanistic evidence	photodegradation	photoproducts	heterogeneous photocatalysts	stability	comparison to other photocatalysts	environmental applicability
AYG (continued)		A5d[67,74]	CBR[162]			A5d[67]	A5d[74]
		CBR[162]				CBR[162]	CBR[162]
RB	P1a[168]	S1c[109]	S1c[109]	P1a[169]	P1e[143]	S1c[109]	P1b[173]
	P1d[168]	P1a[167−169]	P1a[167,169]	P1c[124]	P2a[141]	P1a[167]	P1e[143]
	P1e[168]	P1b[173]	P1b[173]	P1e[143,175]		P1b[173]	P1h[173]
	P1f[168]	P1c[124]	P1c[124]	P1m[124]		P1c[124]	P1n[178]
	P1g[168]	P1d[168]	P1e[80]	P3a[124]		P1e[143,167]	A3c[173]
	P1j[168]	P1e[80,143,167,168,175]	P1h[173]			P1f[167]	A3e[173]
	P1k[168]	P1f[167,168]	P1m[124]			P1g[167]	A5b[173]
	P1n[178]	P1g[167,168]	P1n[178]			P1h[173]	M8[129]
	P1o[168]	P1h[173]	P2a[141]			P1m[124]	M9a[129]
	P1p[168]	P1j[168]	P2b[181]			P1n[178]	M9b[129]
	P2a[141]	P1k[168]	P3a[124,182]			P2a[141]	
	P2b[141,181]	P1m[124]	P3b[182]			P2b[141,181]	
	P2c[141]	P1n[178]	A3c[173]			P2c[141]	
	P3a[182]	P1o[168]	A3e[173]			P3a[124,182]	
	P3b[182]	P1p[168]	A5b[173]			P3b[182]	
	H1a[144,198,200]	P2a[141]	H1a[144,198]			A3c[173]	
	H1b[144,198]	P2b[141,181]	TDM[207]			A3e[173]	
	H1c[144,198]	P2c[141]	M7[217]			A5b[173]	
	H1d[144,198]	P3a[124,182]	M8[129]			H1a[144,200]	
	H1e[144,198]	P3b[182]	M9a[129]			H2b[144,200]	
	H1f[144,198]	A3c[173]	M9b[129]			H3a[144]	
	H1g[144,198]	A3e[173]				H3b[144]	
	H1h[144]	A5b[173]				H4[142]	
	H2a[144]	A5c[173]				H5c[144]	
	H2b[144,200]	H1a[144,198−200]				H7a[121]	
	H2c[144]	H1b[144,198]				H7b[121]	
	H3a[144]	H1c[144,198]				H7c[121]	
	H3b[144]	H1d[144,198]				H7d[121]	
	H4[142]	H1e[144,198]				H7e[121]	
	H5a[144,201]	H1f[144,198]				H7f[121]	
	H5b[144,201]	H1g[144,198]				TDM[207]	
	H5c[144,201]	H1h[144]				M2[208]	
	H7a[121]	H2a[144,199]				M7[217]	
	H7b[121]	H2b[144,199,200]				M10a[219]	
	H7c[121]	H2c[144]				M10b[219]	
	H7d[121]	H3a[144,199]					
	H7e[121]	H3b[144,199]					
	H7f[121]	H4[142]					
	M7[217]	H5a[144,199,201]					
	M8[129]	H5b[144,201]					
	M9a[129]	H5c[144,201]					
	M9b[129]	H7a[121]					
	M10a[219]	H7b[121]					
	M10b[219]	H7c[121]					
		H7d[121]					
		H7e[121]					
		H7f[121]					
		TDM[207]					
		M2[208]					
		M7[217]					
		M8[129]					

dx.doi.org/10.1021/cr2000543 |*Chem. Rev.* 2012, 112, 1710–1750

Table 5. Continued

	mechanistic evidence	photodegradation	photoproducts	heterogeneous photocatalysts	stability	comparison to other photocatalysts	environmental applicability
RB (continued)		M9a[129]					
		M9b[129]					
		M10a[219]					
		M10b[219]					
RF	P1a[123]	P1a[123,170]	P2a[141]		P2a[141]	P2a[141]	ATZ[203,204]
	P1d[123]	P1d[123]	P2b[141]		H2b[200]	P2b[141]	ATT[204]
	P1e[176]	P1e[176]	P2c[141]		H4[142]	P2c[141]	AMT[204]
	P1g[123]	P1g[123]	ATZ[203,204]		ATZ[203]	H1a[200]	TNT[209]
	P1i[123]	P1i[123]	ATT[204]		TNT[209]	H2b[200]	M5[214,215]
	P1j[123]	P1j[123]	AMT[204]			H1a[144]	
	P1k[176]	P1k[170,176]	M5[214,215]			H2b[144]	
	P1o[176]	P1o[170,176]				H3a[144]	
	P2a[141]	P1p[170]				H3b[144]	
	P2b[141]	P2a[141]				H4[142]	
	P2c[141]	P2b[141]				H5c[144]	
	A3g[187]	P2c[141]				H7a[121]	
	H1a[144,200]	P3a[170]				H7b[121]	
	H2b[144,200]	A3g[187]				H7c[121]	
	H3a[144]	C2[197]				H7d[121]	
	H3b[144]	H1a[144,200]				H7e[121]	
	H4[142]	H2b[144,200]				H7f[121]	
	H5c[144,202]	H3a[144]				M2[208]	
	H7a[121]	H3b[144]				M7[217]	
	H7b[121]	H4[142]				M10a[219]	
	H7c[121]	H5c[144,202]				M10b[219]	
	H7d[121]	H7a[121]					
	H7e[121]	H7b[121]					
	H7f[121]	H7c[121]					
	M7[217]	H7d[121]					
	M10a[219]	H7e[121]					
	M10b[219]	H7f[121]					
		ATZ[203,204]					
		ATT[204]					
		AMT[204]					
		M2[208]					
		TNT[209]					
		M3a[170]					
		M3b[170]					
		M3c[170]					
		M3d[170]					
		M3e[170]					
		M5[214,215]					
		M7[217]					
		M10a[219]					
		M10b[219]					
MB	S1d[158]	S1d[158]	S1d[158]	S1d[158]		S3[116]	P1n[178]
	S1e[158]	S1e[158]	S1e[158]	S1e[158]		S7[116]	A5b[193]
	S1f[158]	S1f[158]	S1f[158]	S1f[158]		P1a[167]	
	S3[116]	S3[116]	S3[116]	P1c[124]		P1c[124]	
	S7[116]	S7[116]	S7[116]	P1m[124]		P1m[124]	
	P1a[167]	P1a[167]	P1a[167]	P3a[124]		P1n[178]	
	P1c[124]	P1c[124]	P1c[124]			P2b[181]	
	P1n[178]	P1e[143]	P1m[124]			P3a[124,182]	

dx.doi.org/10.1021/cr2000543 |*Chem. Rev.* 2012, 112, 1710–1750

Table 5. Continued

	mechanistic evidence	photodegradation	photoproducts	heterogeneous photocatalysts	stability	comparison to other photocatalysts	environmental applicability
MB (continued)	P2b[181]	P1m[124]	P1n[178]			P3b[182]	
	P3a[124,182]	P1n[178]	P2b[181]			A3a[186]	
	P3b[182]	P2b[181]	P3a[124,182]			A3c[186]	
		P3a[124,182]	P3b[182]			A3d[186]	
		P3b[182]				A3e[186]	
		A1[184]				A3f[186]	
		A3a[186]				A3g[186]	
		A3c[186]				A3h[186]	
		A3d[186]				A5a[191]	
		A3e[186]				A5b[191,193]	
		A3f[186]				A5c[191]	
		A3g[186]				A5d[67,191]	
		A3h[186]				M2[208]	
		A5a[191]					
		A5b[191,193]					
		A5c[191]					
		A5d[67,191]					
		M2[208]					
MG		DDT[211]	DDT[211]				
CH1	P3c[130]	P3c[130]	P3c[130]			P3c[130]	
CH2		P1e[143]		P1e[143]	P1e[143]		P1e[143]
PP1		ATZ[205]	ATZ[205]	ATZ[205]		ATZ[205]	ATZ[205]
PP2a	P3c[130]	P3c[130]	P3c[130]			P3c[130]	
PP2b		NDMA[90]		NDMA[90]	P1g[90]	NDMA[90]	
		DCANa[90]		DCANa[90]	P3d[90]	DCANa[90]	
		P1g[90]		P1g[90]		P1g[90]	
		P3d[90]		P3d[90]		P3d[90]	
		A4b[90]		A4b[90]		A4b[90]	
PP2c	P3c[130]	P3c[130]	P3c[130]			P3c[130]	
PP2d	P3c[130]	P3c[130]	P3c[130]			P3c[130]	
PP2e		P1a[167]	P1a[167]			P1a[167]	
PP2f	P1a[172]	P1a[172]	P1a[172]	P1a[172]	ATZ[206]	P1a[172]	P3c[183]
	P3c[183]	P3c[183]	P3c[183]		AMT[206]	ATZ[206]	
	ATZ[206]	ATZ[206]	ATZ[206]			AMT[206]	
	AMT[206]	AMT[206]	AMT[206]			TNT[210]	
		TNT[210]	TNT[210]				
PP2g		TNT[210]	TNT[210]			TNT[210]	
PP2h		TNT[210]	TNT[210]			TNT[210]	
PP2i	P3c[130]	P3c[130]	P3c[130]			P3c[130]	
PP2j	P1g[88]	P1g[88]	P1g[88]		ATZ[206]	P1g[88]	
	P1l[88]	P1l[88]	P1l[88]		AMT[206]	P1l[88]	
	ATZ[206]	ATZ[206]	ATZ[206]			ATZ[206]	
	AMT[206]	AMT[206]	AMT[206]			AMT[206]	
PP2k	P1g[150]	P1b[174]	P1b[174]		P1g[150]		
		P1g[150]	P1g[150]				
		A5b[174]	A5b[174]				
		A5c[174]	A5c[174]				
PP2l	P1g[88]	P1g[88]	P1g[88]			P1g[88]	
	P1l[88]	P1l[88]	P1l[88]			P1l[88]	
PP2m	P1g[88]	P1g[88]	P1g[88]			P1g[88]	
	P1l[88]	P1l[88]	P1l[88]			P1l[88]	
PP2n		NDMA[90]		NDMA[90]	P1g[90]	NDMA[90]	
		DCANa[90]		DCANa[90]	P3d[90]	DCANa[90]	

dx.doi.org/10.1021/cr2000543 |*Chem. Rev.* 2012, 112, 1710–1750

Table 5. Continued

	mechanistic evidence	photodegradation	photoproducts	heterogeneous photocatalysts	stability	comparison to other photocatalysts	environmental applicability
PP2n (continued)		P1g[90]		P1g[90]		P1g[90]	
		P3d[90]		P3d[90]		P3d[90]	
		A4b[90]		A4b[90]		A4b[90]	
PP3	M4[151]	M4[151]					
PC1a		CN^-[152]		CN^-[152]			
PC1b		S1g[160]	S1g[160]	S1g[160]		S1g[160]	S1g[160]
PC1c		S1g[160]	S1g[160]	S1g[160]		S1g[160]	S1g[160]
PC1d		Na_2S[146]		Na_2S[146]		Na_2S[146]	
		$Na_2S_2O_3$[146]		$Na_2S_2O_3$[146]		$Na_2S_2O_3$[146]	
PC1e	Na_2S[147]	Na_2S[147]				Na_2S[147]	
PC1f	Na_2S[147]	Na_2S[147]	P1a[167,172]	P1a[172]		Na_2S[147]	
	P1a[172]	P1a[167,172]				P1a[167,172]	
		P1e[167]				P1e[167]	
		P1f[167]				P1f[167]	
		P1g[167]				P1g[167]	
PC1g	S1h[153]	S1h[153]	P1a[148,172]	S1h[153]	S1h[153]	S1h[153]	
	S1n[153]	S1n[153]	P1b[148]	S1n[153]	S1n[153]	S1n[153]	
	P1a[148,172]	P1a[148,171,172]	P1g[94,148]	P1a[171,172]	P1a[171]	P1a[148,172]	
	P1b[148]	P1b[148]	P1n[179]	P1g[171]	P1g[171]	P1b[148]	
	P1g[148]	P1g[94,148,171]	P1p[179]	P1j[171]	P1j[171]	P1g[94,148]	
	A3b[153]	P1j[171]		P1k[171]	P1k[171]	A3b[153]	
		P1k[171]		P1o[171]	P1o[171]		
		P1n[179]		A3b[153]	A3b[153]		
		P1o[171]					
		P1p[179]					
		A3b[153]					
PC1h	Na_2S[147]	Na_2S[147]				Na_2S[147]	
		$Na_2S_2O_3$[95]				$Na_2S_2O_3$[95]	
		S1o[95]				S1o[95]	
PC1i		ATZ[205]	ATZ[205]	ATZ[205]		ATZ[205]	ATZ[205]
PC1j		P1a[167]				P1a[167]	
PC1k	S1h[153]	S1h[153]		S1h[153]	S1h[153]	S1h[153]	
	S1n[153]	S1n[153]		S1n[153]	S1n[153]	S1n[153]	
	A3b[153]	P1e[177]		P1o[98,180]	P1o[98,180]	A3b[153]	
		P1g[177]		A3b[153]	A3b[153]		
		P1k[177]					
		P1o[98,177,180]					
		A3b[153]					
PC1l	P1a[148]	Na_2S[147,155]	P1a[148]		P1b[148]	Na_2S[147,155]	
	P1b[148]	$Na_2S_2O_3$[95,155]	P1b[148]		P1j[154]	$Na_2S_2O_3$[95,155]	
	P1g[148]	S1o[95]	P1g[94,148]			S1o[95]	
	P1j[154]	P1a[148,167]	P1j[154]			P1a[148,167]	
		P1b[148]				P1b[148]	
		P1g[94,148]				P1g[94,148]	
		P1j[154]				P1j[154]	
PC1m	Na_2S[146]	Na_2S[146,155]		Na_2S[146]		Na_2S[146,155]	
	$Na_2S_2O_3$[146]	$Na_2S_2O_3$[95,146,155]		$Na_2S_2O_3$[146]		$Na_2S_2O_3$[95,146,155]	
		S1o[95]				S1o[95]	
PC1n		Na_2S[146,155]		Na_2S[146]		Na_2S[146,155]	
		$Na_2S_2O_3$[146,155]				$Na_2S_2O_3$[95,146,155]	
		S1o[95]				S1o[95]	
PC1o		Na_2S[155]	P1g[94]			Na_2S[155]	
		$Na_2S_2O_3$[155]				$Na_2S_2O_3$[155]	

dx.doi.org/10.1021/cr2000543 |*Chem. Rev.* 2012, 112, 1710–1750

Table 5. Continued

	mechanistic evidence	photodegradation	photoproducts	heterogeneous photocatalysts	stability	comparison to other photocatalysts	environmental applicability
PC1o (continued)		P1g[94]				P1g[94]	
PC1p	P1j[154]	Na_2S[155]	P1g[94]		P1g[94]	Na_2S[155]	
		$Na_2S_2O_3$[155]	P1j[154]		P1j[154]	$Na_2S_2O_3$[155]	
		P1g[94]				P1g[94]	
		P1j[154]				P1j[154]	
PC1q		A5d[67]				A5d[67]	
PC2		$Na_2S_2O_3$[95]				$Na_2S_2O_3$[95]	
		S1o[95]				S1o[95]	
PC3a	P2a[97]	Na_2S[155]	P2a[97]			Na_2S[155]	P2a[97]
		$Na_2S_2O_3$[155]				$Na_2S_2O_3$[155]	
		P2a[97]				P2a[97]	
PC3b	P2a[97]	Na_2S[155]	P2a[97]			Na_2S[155]	P2a[97]
		$Na_2S_2O_3$[155]				$Na_2S_2O_3$[155]	
		P2a[97]				P2a[97]	

after 200 min of irradiation, showing that only minor changes in the composition of the dissolved organic fraction occur, as expected for an oxidative process.

Another approach to improve the sustainability and applicability of photocatalytic processes is coupling with a biological treatment.[250] For this purpose, assays to assess the biocompatibility (toxicity/biodegradability) of samples are needed; however, very scarce information is available on the use of bioassays in processes involving organic photocatalysts. *A. branii* alga cultures has been used in toxicity tests, measuring its growth in the presence of treated and untreated samples with respect to a control.[173] Alternatively, respirometric assays of activated sludge have been employed to determine toxicity and short-term biodegradability.[74,162] Inhibition of the respiration of activated sludge is taken as an indicator to monitor the detoxification of solutions of two pesticides, methidathion and carbaryl, when irradiated in the presence of **TPP**, **TPTP**, or **AYG** (see Figure 42).[162] Nearly complete detoxification of the methidathion containing sample is achieved after 3 h in the **TPTP** treatment.

Likewise, *Vibrio fischeri* bacteria are particularly useful for samples showing only moderate toxicity, such as ferulic acid, as this method is more sensitive than those based on activated sludge.[251] Thus, toxicity decreases during solar treatment of ferulic acid catalyzed by **AYG**, from 77% down to 11% at the end of the process.[74] There is also a concomitant increase in the biodegradability of the treated sample, as indicated by the final value (t_{30W} = 420 min) of the short time biological oxygen demand (BOD_{st}), which is ca. 1 order of magnitude higher than the initial measurement.

5.3. Tabular Survey of the Endpoints Addressed with Different Photocatalyst/Pollutant Combinations

A comprehensive review of the different issues that have been dealt with during the studies performed on the oxidation of pollutants and model compounds with a variety of organic photocatalysts is provided in Table 5.

6. SUMMARY AND OUTLOOK

Organic photocatalysts show potential to be used for the photooxidation of pollutants in the decontamination of wastewaters. They exhibit a wide structural diversity and operate through a variety of photochemical mechanisms. On this basis, organic photocatalysts constitute, in principle, an interesting tool for environmental purposes, especially because they can be used in aqueous medium, are activated by sunlight and require the presence of atmospheric oxygen as the only oxidizing reagent. The most important advantage of this approach is probably its versatility, as it is conceivable to design an appropriate photocatalyst for each specific problem, based on mechanistic knowledge. The most important drawback from the practical point of view might be associated with the limited stability of organic photocatalysts under the usual experimental conditions. Nevertheless, this can be circumvented by adsorption onto solid supports, which provides robust materials that can be easily separated from the reaction mixtures and reused in successive catalytic cycles. Among the issues requiring further efforts during the next years, heterogenization will be doubtless one of the most critical; a satisfactory solution of this aspect will make it possible to achieve substantial advancements in the field. After optimization of the procedures, the ultimate challenge will be the use of natural sunlight for the remediation of real wastewaters.

AUTHOR INFORMATION

Corresponding Author

*E-mail: mmiranda@qim.upv.es. Fax: (+34)963879444.

BIOGRAPHIES

M. Luisa Marin was born in Valencia, Spain, in 1968. She did her Ph.D. at the University of Valencia working on the synthesis

of natural products. In 1996 she moved to Imperial College, where she spent two years as postdoctoral Pierre and Marie Curie fellow. When she came back to Spain she moved to the Technical University of Valencia (Spain) and started working in the group of Prof. M. A. Miranda in the field of photochemistry, photophysics, and photobiology, being promoted to Associate Professor in 2004. Her current research interests are (a) molecular mechanisms of photocatalysis, phototoxicity, photoallergy, and photocarcinogenicity; (b) excited states as tools in bioorganic chemistry; and (c) supramolecular photobehavior within biomolecular hosts.

Lucas Santos-Juanes was born in Alcoy in 1978. He followed his engineering studies at the Technical University of Valencia (Spain), where he obtained his Ph.D. degree in 2008, working under the supervision of M. Luisa Marin and Antonio Arques. The main focus of his thesis was the use of organic sensitizers as photocatalysts for water remediation, a work that was awarded with the Ph.D. prize of the Technical University of Valencia. After spending a short research stay at INIFTA (CONICET) in La Plata (Argentina), in 2009 he obtained a postdoctoral position at CIESOL, a joint center of the University of Almeria-CIEMAT, where he is currently engaged in photocatalysis research.

Antonio Arques was born in Alcoy, Spain, in 1972. He studied Chemistry at the University of Alicante and did his Ph.D. at the Technical University of Valencia working on water treatment. Since then, he has been working in the group of Advanced Oxidation Processes of the Technical University of Valencia. In 2008, he was promoted to his current position of Associate Professor in the Department of Textile Engineering. His research is focused on solar photocatalytic processes for the remediation of polluted effluents (textile industry, pesticides, emerging pollutants, etc.).

Ana M. Amat is Professor of Chemistry at the Technical University of Valencia (Spain) and Head of the Advanced Oxidation Processes Group. She studied Pharmacy at the University of Valencia, where she obtained her Ph.D. degree in 1988, working on the photochemistry of carbonyl compounds in strongly acidic media. Since 1989 she works at the Technical University of Valencia, where she has been promoted to her current position as Full Professor in 2010. Her research is currently focused on photocatalysis and solar photodegradation of organic pollutants, eventually coupled with biodegradation processes, with special emphasis on the elucidation of reaction mechanisms.

Miguel A. Miranda is Professor of Organic Chemistry at the Technical University of Valencia (Spain) and Head of the Institute of Chemical Technology. He studied Chemistry at the University of Valencia and obtained his Ph.D. degree at the Autonomous University of Madrid in 1978, working at the Spanish National Research Council (CSIC). He spent postdoctoral periods at the University of Saarland and the University of Würzburg (Germany) and was Associate Professor at the University of Valencia before accepting his present position in 1990. His research interests are mainly focused on photochemistry and photobiology. Dr. Miranda has received the Honda-Fujishima Lectureship Award of the Japanese Photochemistry Association (2007), the Janssen-Cilag Award for Organic Chemistry of the Spanish Royal Society of Chemistry (2008), and the Theodor Förster Memorial Lectureship Award of the German Chemical Society and the Bunsen Society of Physical Chemistry (2010). He is currently the President of the European Society for Photobiology.

ACKNOWLEDGMENT

Financial support from the Spanish Government (CTQ2009-13699, CTQ2009-13459-C05-03/PPQ, RIRRAF RETICS), and the Generalitat Valenciana (Prometeo Program) is gratefully acknowledged. Dedicated to Prof. Avelino Corma on the occasion of his 60th birthday.

REFERENCES

(1) United Nations Educational Science and Cultural Organization, UNESCO; 2006.
(2) Food and Agriculture Organization, FAO; 2007.
(3) Shon, H. K.; Vigneswaran, S.; Snyder, S. A. *Crit. Rev. Environ. Sci. Technol.* **2006**, *36*, 327.
(4) Ren, S. J. *Environ. Int.* **2004**, *30*, 1151.
(5) Comninellis, C.; Kapalka, A.; Malato, S.; Parsons, S. A.; Poulios, L.; Mantzavinos, D. *J. Chem. Technol. Biotechnol.* **2008**, *83*, 769.
(6) Gogate, P. R.; Pandit, A. B. *Adv. Environ. Res.* **2004**, *8*, 501.
(7) Gogate, P. R.; Pandit, A. B. *Adv. Environ. Res.* **2004**, *8*, 553.
(8) Gottschalk, C. L. J. A. S. A. *Ozonation of water and wastewater*; Wiley, VCH: Weinheim, Germany, 2000.
(9) Masten, S. J.; Davies, S. H. R. *Environ. Sci. Technol.* **1994**, *28*, A180.
(10) Imamura, S. *Ind. Eng. Chem. Res.* **1999**, *38*, 1743.
(11) Beltran, F. J.; Gonzalez, M.; Gonzalez, J. F. *Water Res.* **1997**, *31*, 2405.
(12) Chen, G. H. *Sep. Purif. Technol.* **2004**, *38*, 11.
(13) Martinez-Huitle, C. A.; Brillas, E. *Appl. Catal., B* **2009**, *87*, 105.
(14) Legrini, O.; Oliveros, E.; Braun, A. M. *Chem. Rev.* **1993**, *93*, 671.
(15) Openländer, T. *Photochemical purification of water and air. Advanced oxidation processes (AOPs): Principles, Reaction Mechanisms, Reactor Concepts*; Wiley, VCH: Weinheim, Germany, 2003.
(16) Cooper, W. J.; Cramer, C. J.; Martin, N. H.; Mezyk, S. P.; O'Shea, K. E.; von Sonntag, C. *Chem. Rev.* **2009**, *109*, 1302.
(17) Pera-Titus, M.; Garcia-Molina, V.; Banos, M. A.; Gimenez, J.; Esplugas, S. *Appl. Catal., B* **2004**, *47*, 219.
(18) Rajeshwar, K.; Osugi, M. E.; Chanmanee, W.; Chenthamarakshan, C. R.; Zanoni, M. V. B.; Kajitvichyanukul, P.; Krishnan-Ayer, R. *J. Photochem. Photobiol., C* **2008**, *9*, 171.
(19) Chiron, S.; Fernandez-Alba, A.; Rodriguez, A.; Garcia-Calvo, E. *Water Res.* **2000**, *34*, 366.
(20) Gonzalez, M. G.; Oliveros, E.; Worner, M.; Braun, A. M. *J. Photochem. Photobiol., C* **2004**, *5*, 225.
(21) Glaze, W. H.; Kang, J. W.; Chapin, D. H. *Ozone Sci. Eng.* **1987**, *9*, 335.
(22) Braslavsky, S. E. *Pure Appl. Chem.* **2007**, *79*, 293.
(23) Fagnoni, M.; Dondi, D.; Ravelli, D.; Albini, A. *Chem. Rev.* **2007**, *107*, 2725.
(24) Palmisano, G.; Augugliaro, V.; Pagliaro, M.; Palmisano, L. *Chem. Commun.* **2007**, 3425.
(25) Ravelli, D.; Dondi, D.; Fagnoni, M.; Albini, A. *Chem. Soc. Rev.* **2009**, *38*, 1999.
(26) Malato, S.; Fernandez-Ibañez, P.; Maldonado, M. I.; Blanco, J.; Gernjak, W. *Catal. Today* **2009**, *147*, 1.
(27) Blanco-Galvez, J.; Fernandez-Ibañez, P.; Malato-Rodriguez, S. *J. Sol. Energy Eng.* **2007**, *129*, 4.
(28) Malato, S.; Blanco, J.; Alarcon, D. C.; Maldonado, M. I.; Fernandez-Ibañez, P.; Gernjak, W. *Catal. Today* **2007**, *122*, 137.
(29) Malato, S.; Blanco, J.; Vidal, A.; Alarcon, D.; Maldonado, M. I.; Caceres, J.; Gernjak, W. *Sol. Energy* **2003**, *75*, 329.
(30) Malato, S.; Blanco, J.; Vidal, A.; Richter, C. *Appl. Catal., B* **2002**, *37*, 1.
(31) Gaya, U. I.; Abdullah, A. H. *J. Photochem. Photobiol., C* **2008**, *9*, 1.
(32) Hoffmann, M. R.; Martin, S. T.; Choi, W. Y.; Bahnemann, D. W. *Chem. Rev.* **1995**, *95*, 69.
(33) Zhao, J. C.; Chen, C. C.; Ma, W. H. *Top. Catal.* **2005**, *35*, 269.
(34) Fujishima, A.; Honda, K. *Nature* **1972**, *238*, 37.
(35) Carey, J. H.; Lawrence, J.; Tosine, H. M. *Bull. Environ. Contam. Toxicol.* **1976**, *16*, 697.
(36) Han, F.; Kambala, V. S. R.; Srinivasan, M.; Rajarathnam, D.; Naidu, R. *Appl. Catal., A* **2009**, *359*, 25.
(37) Mo, J. H.; Zhang, Y. P.; Xu, Q. J.; Lamson, J. J.; Zhao, R. Y. *Atmos. Environ.* **2009**, *43*, 2229.
(38) Konstantinou, I. K.; Albanis, T. A. *Appl. Catal., B* **2003**, *42*, 319.
(39) Bahnemann, D. *Sol. Energy* **2004**, *77*, 445.
(40) Agrios, A. G.; Pichat, P. *J. Appl. Electrochem.* **2005**, *35*, 655.
(41) Cho, Y. M.; Choi, W. Y.; Lee, C. H.; Hyeon, T.; Lee, H. I. *Environ. Sci. Technol.* **2001**, *35*, 966.
(42) Mopper, K.; Zhou, X. L. *Science* **1990**, *250*, 661.
(43) Miranda, M. A.; Garcia, H. *Chem. Rev.* **1994**, *94*, 1063.
(44) DeRosa, M. C.; Crutchley, R. J. *Coord. Chem. Rev.* **2002**, *233*, 351.
(45) Aoai, T. *J. Synth. Org. Chem. Jpn.* **2008**, *66*, 458.
(46) Lang, K.; Mosinger, J.; Wagnerova, D. M. *Coord. Chem. Rev.* **2004**, *248*, 321.
(47) Plaetzer, K.; Krammer, B.; Berlanda, J.; Berr, F.; Kiesslich, T. *Lasers Med. Sci.* **2009**, *24*, 259.
(48) Yum, J. H.; Chen, P.; Grätzel, M.; Nazeeruddin, M. K. *ChemSusChem* **2008**, *1*, 699.
(49) Fenton, H. J. H. *J. Chem. Soc.* **1894**, 899.
(50) Pignatello, J. J.; Oliveros, E.; MacKay, A. *Crit. Rev. Environ. Sci. Technol.* **2006**, *36*, 1.
(51) Ciesla, P.; Kocot, P.; Mytych, P.; Stasicka, Z. *J. Mol. Catal. A: Chem.* **2004**, *224*, 17.
(52) Xing, C. F.; Xu, Q. L.; Tang, H. W.; Liu, L. B.; Wang, S. *J. Am. Chem. Soc.* **2009**, *131*, 13117.
(53) Kohn, T.; Nelson, K. L. *Environ. Sci. Technol.* **2007**, *41*, 192.
(54) Jemli, M.; Alouini, Z.; Sabbahi, S.; Gueddari, M. *J. Environ. Monit.* **2002**, *4*, 511.
(55) Li, X. Z.; Zhang, M.; Chua, H. *Water Sci. Technol.* **1996**, *33*, 111.
(56) Kuznetsova, N. A.; Makarov, D. A.; Kaliya, O. L.; Vorozhtsov, G. N. *J. Hazard. Mater.* **2007**, *146*, 487.
(57) Bonnett, R.; Krysteva, M. A.; Lalov, I. G.; Artarsky, S. V. *Water Res.* **2006**, *40*, 1269.
(58) Schäfer, M.; Schmitz, C.; Facius, R.; Horneck, G.; Milow, B.; Funken, K. H.; Ortner, J. *Photochem. Photobiol.* **2000**, *71*, 514.
(59) Navntoft, C.; Araujo, P.; Litter, M. I.; Apella, M. C.; Fernandez, D.; Puchulu, M. E.; Hidalgo, M. D. V.; Blesa, M. A. *J. Sol. Energy Eng.* **2007**, *129*, 127.
(60) Street, C. N.; Gibbs, A.; Pedigo, L.; Andersen, D.; Loebel, N. G. *Photochem. Photobiol.* **2009**, *85*, 137.
(61) Ergaieg, K.; Seux, R. *Desalination* **2009**, *246*, 353.
(62) Cantau, C.; Pigot, T.; Brown, R.; Mocho, P.; Maurette, M. T.; Benoit-Marque, E.; Lacombe, S. *Appl. Catal., B* **2006**, *65*, 77.
(63) Cantau, C.; Larribau, S.; Pigot, T.; Simon, M.; Maurette, M. T.; Lacombe, S. *Catal. Today* **2007**, *122*, 27.
(64) Cantau, C.; Pigot, T.; Manoi, N.; Oliveros, E.; Lacombe, S. *ChemPhysChem* **2007**, *8*, 2344.
(65) Saint-Cricq, P.; Pigot, T.; Nicole, L.; Sanchez, C.; Lacombe, S. *Chem. Commun.* **2009**, 5281.
(66) Lacombe, S.; Soumillion, J. P.; El Kadib, A.; Pigot, T.; Blanc, S.; Brown, R.; Oliveros, E.; Cantau, C.; Saint-Cricq, P. *Langmuir* **2009**, *25*, 11168.
(67) Arques, A.; Amat, A. M.; Santos-Juanes, L.; Vercher, R. F.; Marin, M. L.; Miranda, M. A. *Catal. Today* **2007**, *129*, 37.
(68) Alvaro, M.; Carbonell, E.; Domenech, A.; Fornes, V.; Garcia, H.; Narayana, M. *ChemPhysChem* **2003**, *4*, 483.
(69) Oregon, H.; Science, U. http://omlc.ogi.edu/spectra/PhotochemCAD, 2007.
(70) Olea, A. F.; Worrall, D. R.; Wilkinson, F.; Williams, S. L.; Abdel-Shafi, A. A. *Phys. Chem. Chem. Phys.* **2002**, *4*, 161.
(71) Singh-Rachford, T. N.; Islangulov, R. R.; Castellano, F. N. *J. Phys. Chem. A* **2008**, *112*, 3906.
(72) Icli, S.; Demic, S.; Dindar, B.; Doroshenko, A. O.; Timur, C. *J. Photochem. Photobiol., A* **2000**, *136*, 15.

(73) Jiang, Y.; Blanchard, G. J. *J. Phys. Chem.* **1994**, *98*, 9417.
(74) Amat, A. M.; Arques, A.; Galindo, F.; Miranda, M. A.; Santos-Juanes, L.; Vercher, R. F.; Vicente, R. *Appl. Catal., B* **2007**, *73*, 220.
(75) Pierard, F.; Del Guerzo, A.; Kirsch-De Mesmaeker, A.; Demeunynck, M.; Lhomme, J. *Phys. Chem. Chem. Phys.* **2001**, *3*, 2911.
(76) Amat, A. M.; Arques, A.; Miranda, M. A.; Segui, S.; Vercher, R. F. *Desalination* **2007**, *212*, 114.
(77) Lu, C. S.; Mai, F. D.; Wu, C. W.; Wu, R. J.; Chen, C. C. *Dyes Pigm.* **2008**, *76*, 706.
(78) Görner, H. *J. Photochem. Photobiol., B* **2007**, *87*, 73.
(79) Rytwo, G.; Nir, S.; Crespin, M.; Margulies, L. *J. Colloid Interface Sci.* **2000**, *222*, 12.
(80) Miller, J. S. *Water Res.* **2005**, *39*, 412.
(81) Bodaness, R. S. *Biochem. Biophys. Res. Commun.* **1984**, *118*, 191.
(82) Cunderlikova, B.; Gangeskar, L.; Moan, J. *J. Photochem. Photobiol., B* **1999**, *53*, 81.
(83) Dincalp, H.; Icli, S. *Sol. Energy* **2006**, *80*, 332.
(84) Lee, K. S.; Raymond, L. D.; Schoen, B.; Raymond, G. J.; Kett, L.; Moore, R. A.; Johnson, L. M.; Taubner, L.; Speare, J. O.; Onwubiko, H. A.; Baron, G. S.; Caughey, W. S.; Caughey, B. *J. Biol. Chem.* **2007**, *282*, 36525.
(85) Fukushima, M.; Kawasaki, M.; Sawada, A.; Ichikawa, H.; Morimoto, K.; Tatsumi, K.; Tanaka, S. *J. Mol. Catal., A: Chem.* **2002**, *187*, 201.
(86) Mammana, A.; Asakawa, T.; Bitsch-Jensen, K.; Wolfe, A.; Chaturantabut, S.; Otani, Y.; Li, X. X.; Li, Z. M.; Nakanishi, K.; Balaz, M.; Ellestad, G. A.; Berova, N. *Bioorg. Med. Chem.* **2008**, *16*, 6544.
(87) Fukushima, M.; Tatsumi, K. *J. Hazard. Mater.* **2007**, *144*, 222.
(88) Monteiro, C. J. P.; Pereira, M. M.; Azenha, M. E.; Burrows, H. D.; Serpa, C.; Arnaut, L. G.; Tapia, M. J.; Sarakha, M.; Wong-Wah-Chung, P.; Navaratnam, S. *Photochem. Photobiol. Sci.* **2005**, *4*, 617.
(89) Bo Gyu, C.; Soo, Y. K.; Wonwoo, N.; Byeongmoon, J. *Bull. Korean Chem. Soc.* **2005**, *26*, 1819.
(90) Kim, W.; Park, J.; Jo, H. J.; Kim, H. J.; Choi, W. *J. Phys. Chem. C* **2008**, *112*, 491.
(91) Rajaputra, S.; Sagi, G.; Singh, V. P. *Sol. Energy Mater. Sol. Cells* **2009**, *93*, 60.
(92) Menaa, B.; Takahashi, M.; Tokuda, Y.; Yoko, T. *J. Photochem. Photobiol., A* **2008**, *194*, 362.
(93) Hu, M. Q.; Xu, Y. M.; Zhao, J. C. *Langmuir* **2004**, *20*, 6302.
(94) Ozoemena, K.; Kuznetsova, N.; Nyokong, T. *J. Photochem. Photobiol., A* **2001**, *139*, 217.
(95) Iliev, V.; Alexiev, V.; Bilyarska, L. *J. Mol. Catal., A: Chem.* **1999**, *137*, 15.
(96) Baba, A.; Sato, F.; Fukuda, N.; Ushijima, H.; Yase, K. *Nanotechnology* **2009**, 20.
(97) Tai, C.; Jiang, G. B.; Liu, J. F.; Zhou, Q. F.; Liu, J. Y. *J. Photochem. Photobiol., A* **2005**, *172*, 275.
(98) Xiong, Z. G.; Xu, Y. M.; Zhu, L. Z.; Zhao, J. C. *Langmuir* **2005**, *21*, 10602.
(99) Miranda, M. A.; Izquierdo, M. A.; Galindo, F. *J. Org. Chem.* **2002**, *67*, 4138.
(100) Morlet-Savary, F.; Parret, S.; Fouassier, J. P.; Inomata, K.; Matsumoto, T. *J. Chem. Soc., Faraday Trans.* **1998**, *94*, 745.
(101) Akaba, R.; Kamata, M.; Koike, A.; Mogi, K. I.; Kuriyama, Y.; Sakuragi, H. *J. Phys. Org. Chem.* **1997**, *10*, 861.
(102) Nowakowska, M.; Sterzel, M.; Zapotoczny, S.; Kot, E. *Appl. Catal., B* **2005**, *57*, 1.
(103) Murov, S. L.; Carmichael, I.; Hug, G. L. *Handbook of Photochemistry*, 2nd ed.; Marcel Dekker: New York, 1993.
(104) Baciocchi, E.; Giacco, T. D.; Elisei, F.; Gerini, M. F.; Guerra, M.; Lapi, A.; Liberali, P. *J. Am. Chem. Soc.* **2003**, *125*, 16444.
(105) Lacombe, S.; Cardy, H.; Simon, M.; Khoukh, A.; Soumillion, J. P.; Ayadim, M. *Photochem. Photobiol. Sci.* **2002**, *1*, 347.
(106) Latour, V.; Pigot, T.; Mocho, P.; Blanc, S.; Lacombe, S. *Catal. Today* **2005**, *101*, 359.
(107) Soggiu, N.; Cardy, H.; Jiwan, J. L. H.; Leray, I.; Soumillion, J. P.; Lacombe, S. *J. Photochem. Photobiol., A* **1999**, *124*, 1.
(108) Sato, S. I.; Nakamura, T.; Nitobe, S.; Kiba, T.; Hosokawa, K.; Kasajima, T.; Otsuka, I.; Akimoto, S.; Kakuchi, T. *J. Phys. Chem. B* **2006**, *110*, 21444.
(109) Latour, V.; Pigot, T.; Simon, M.; Cardy, H.; Lacombe, S. *Photochem. Photobiol. Sci.* **2005**, *4*, 221.
(110) Galadi, A.; Julliard, M. *Chemosphere* **1996**, *33*, 1.
(111) Itoh, T. *Spectrochim. Acta, Part A* **1986**, *42*, 1083.
(112) Dudko, E. V.; Kalosha, I. I.; Tolkachev, V. A. *J. Appl. Spectrosc.* **2008**, *75*, 80.
(113) Del Giacco, T.; Faltoni, A.; Elisei, F. *Phys. Chem. Chem. Phys.* **2008**, *10*, 200.
(114) Fukuzumi, S.; Fujita, M.; Noura, S.; Ohkubo, K.; Suenobu, T.; Araki, Y.; Ito, O. *J. Phys. Chem. A* **2001**, *105*, 1857.
(115) Yoon, U. C.; Quillen, S. L.; Mariano, P. S.; Swanson, R.; Stavinoha, J. L.; Bay, E. *J. Am. Chem. Soc.* **1983**, *105*, 1204.
(116) Clennan, E. L.; Liao, C. *J. Am. Chem. Soc.* **2008**, *130*, 4057.
(117) Abraham, W.; Glänzel, A.; Stösser, R.; Grummt, U. W.; Köppel, H. *J. Photochem. Photobiol., A* **1990**, *51*, 359.
(118) Fister, J. C.; Harris, J. M.; Rank, D.; Wacholtz, W. *J. Chem. Educ.* **1997**, *74*, 1208.
(119) Goryacheva, I. Y.; Mel'nikov, G. V.; Shtykov, S. N. *J. Anal. Chem.* **2000**, *55*, 874.
(120) Santos-Juanes, L. Ph.D Thesis, *Compuestos Organicos como Fotocatalizadores Solares para la Eliminacion de Contaminantes en Medios Acuosos: Aplicaciones y Estudios Fotofisicos Universidad Politécnica de Valencia*, 2008; p 158.
(121) Escalada, J. P.; Pajares, A.; Gianotti, J.; Massad, W. A.; Bertolotti, S.; Amat-Guerri, F.; Garcia, N. A. *Chemosphere* **2006**, *65*, 237.
(122) Heelis, P. F. *Chem. Soc. Rev.* **1982**, *11*, 15.
(123) Haggi, E.; Bertolotti, S.; Garcia, N. A. *Chemosphere* **2004**, *55*, 1501.
(124) Madhavan, D.; Pitchumani, K. *J. Photochem. Photobiol., A* **2002**, *153*, 205.
(125) Jayaraj, S. E.; Umadevi, M.; Ramakrishnan, V. *J. Inclusion Phenom. Macrocyclic Chem.* **2001**, *40*, 203.
(126) Fujimoto, B. S.; Clendenning, J. B.; Delrow, J. J.; Heath, P. J.; Schurr, M. *J. Phys. Chem.* **1994**, *98*, 6633.
(127) Lambert, C. R.; Kochevar, I. E. *Photochem. Photobiol.* **1997**, *66*, 15.
(128) Neckers, D. C. *J. Photochem. Photobiol., A* **1989**, *47*, 1.
(129) Dell'Arciprete, M. L.; Santos-Juanes, L.; Arques, A.; Vercher, R. F.; Amat, A. M.; Furlong, J. P.; Mártire, D. O.; Gonzalez, M. C. *Catal. Today* **2010**, *151*, 137.
(130) Murtinho, D.; Pineiro, M.; Pereira, M. M.; Gonsalves, A. M. D. R.; Arnaut, L. G.; Miguel, M. D.; Burrows, H. D. *J. Chem. Soc., Perkin Trans. 2* **2000**, 2441.
(131) Lovell, J. F.; Liu, T. W. B.; Chen, J.; Zheng, G. *Chem. Rev.* **2010**, *110*, 2839.
(132) Baskin, J. S.; Yu, H. Z.; Zewail, A. H. *J. Phys. Chem. A* **2002**, *106*, 9837.
(133) Kossanyi, J.; Chahraoui, D. *Int. J. Photoenergy* **2000**, *2*, 9.
(134) Siejak, A.; Wrobel, D.; Siejak, P.; Olejarz, B.; Ion, R. M. *Dyes Pigm.* **2009**, *83*, 281.
(135) Darwent, J. R.; Douglas, P.; Harriman, A.; Porter, G.; Richoux, M. C. *Coord. Chem. Rev.* **1982**, *44*, 83.
(136) Jayanthi, S. S.; Ramamurthy, P. *J. Phys. Chem. A* **1998**, *102*, 511.
(137) Marquis, S.; Ferrer, B.; Alvaro, M.; Garcia, H.; Roth, H. D. *J. Phys. Chem. B* **2006**, *110*, 14956.
(138) Wilkinson, F.; McGarvey, D. J.; Olea, A. F. *J. Am. Chem. Soc.* **1993**, *115*, 12144.
(139) Gutierrez, I.; Bertolotti, S. G.; Biasutti, M. A.; Soltermann, A. T.; Garcia, N. A. *Can. J. Chem.* **1997**, *75*, 423.
(140) Baier, J.; Maisch, T.; Maier, M.; Engel, E.; Landthaler, M.; Bäumler, W. *Biophys. J.* **2006**, *91*, 1452.
(141) Barbieri, Y.; Massad, W. A.; Diaz, D. J.; Sanz, J.; Amat-Guerri, F.; Garcia, N. A. *Chemosphere* **2008**, *73*, 564.
(142) Massad, W.; Criado, S.; Bertolotti, S.; Pajares, A.; Gianotti, J.; Escalada, J. P.; Amat-Guerri, F.; Garcia, N. A. *Chemosphere* **2004**, *57*, 455.

(143) Gryglik, D.; Miller, J. S.; Ledakowicz, S. *Sol. Energy* **2004**, *77*, 615.
(144) Garcia, N. A.; Amat-Guerri, F. *Chemosphere* **2005**, *59*, 1067.
(145) Redmond, R. W.; Gamlin, J. N. *Photochem. Photobiol.* **1999**, *70*, 391.
(146) Iliev, V.; Prahov, L.; Bilyarska, L.; Fischer, H.; Schulz-Ekloff, G.; Wöhrle, D.; Petrov, L. *J. Mol. Catal., A: Chem.* **2000**, *151*, 161.
(147) Spiller, W.; Wöhrle, D.; Schulz-Ekloff, G.; Ford, W. T.; Schneider, G.; Stark, J. *J. Photochem. Photobiol., A* **1996**, *95*, 161.
(148) Lang, K.; Wagnerova, D. M.; Brodilova, J. *J. Photochem. Photobiol., A* **1993**, *72*, 9.
(149) Iliev, V.; Ileva, A. *J. Mol. Catal., A: Chem.* **1995**, *103*, 147.
(150) Silva, E.; Pereira, M. M.; Burrows, H. D.; Azenha, M. E.; Sarakha, M.; Bolte, M. *Photochem. Photobiol. Sci.* **2004**, *3*, 200.
(151) Herath, A. C.; Rajapakse, R. M. G.; Wicramasinghe, A.; Karunaratne, V. *Environ. Sci. Technol.* **2009**, *43*, 176.
(152) Mohamed, R. M.; Mohamed, M. M. *Appl. Catal., A* **2008**, *340*, 16.
(153) Sun, A. H.; Xiong, Z. G.; Xu, Y. M. *J. Hazard. Mater.* **2008**, *152*, 191.
(154) Marais, E.; Klein, R.; Antunes, E.; Nyokong, T. *J. Mol. Catal., A: Chem.* **2007**, *261*, 36.
(155) Iliev, V.; Mihaylova, A. *J. Photochem. Photobiol., A* **2002**, *149*, 23.
(156) Bonesi, S. M.; Manet, I.; Freccero, M.; Fagnoni, M.; Albini, A. *Chem.—Eur. J.* **2006**, *12*, 4844.
(157) Bonesi, S. M.; Carbonell, E.; Garcia, H.; Fagnoni, M.; Albini, A. *Appl. Catal., B* **2008**, *79*, 368.
(158) Zhou, W. H.; Clennan, E. L. *J. Am. Chem. Soc.* **1999**, *121*, 2915.
(159) Alvaro, M.; Carbonell, E.; Garcia, H. *Appl. Catal., B* **2004**, *51*, 195.
(160) Cojocaru, B.; Parvulescu, V. I.; Preda, E.; Iepure, G.; Somoghi, V.; Carbonell, E.; Alvaro, M.; Garcia, H. *Environ. Sci. Technol.* **2008**, *42*, 4908.
(161) Bonesi, S. M.; Fagnoni, M.; Albini, A. *Eur. J. Org. Chem.* **2008**, 2612.
(162) Arques, A.; Amat, A. M.; Santos-Juanes, L.; Vercher, R. F.; Marin, M. L.; Miranda, M. A. *Catal. Today* **2009**, *144*, 106.
(163) Sanjuan, A.; Alvaro, M.; Aguirre, G.; Garcia, H.; Scaiano, J. C. *J. Am. Chem. Soc.* **1998**, *120*, 7351.
(164) Sanjuan, A.; Aguirre, G.; Alvaro, M.; Garcia, H. *Water Res.* **2000**, *34*, 320.
(165) Alvaro, M.; Carbonell, E.; Garcia, H.; Lamaza, C.; Pillai, M. N. *Photochem. Photobiol. Sci.* **2004**, *3*, 189.
(166) Alvaro, M.; Carbonell, E.; Fornes, V.; Garcia, H. *New J. Chem.* **2004**, *28*, 631.
(167) Gerdes, R.; Wöhrle, D.; Spiller, W.; Schneider, G.; Schnurpfeil, G.; Schulz-Ekloff, G. *J. Photochem. Photobiol., A* **1997**, *111*, 65.
(168) Tratnyek, P. G.; Holgne, J. *Environ. Sci. Technol.* **1991**, *25*, 1596.
(169) Nowakowska, M.; Kepczynski, M. *J. Photochem. Photobiol., A* **1998**, *116*, 251.
(170) Larson, R. A.; Ellis, D. D.; Ju, H. L.; Marley, K. A. *Environ. Toxicol. Chem.* **1989**, *8*, 1165.
(171) Xiong, Z. G.; Xu, Y. M.; Zhu, L. Z.; Zhao, J. C. *Environ. Sci. Technol.* **2005**, *39*, 651.
(172) Pepe, E.; Abbas, O.; Rebufa, C.; Simon, M.; Lacombe, S.; Julliard, M. *J. Photochem. Photobiol., A* **2005**, *170*, 143.
(173) Cermola, F.; DellaGreca, N.; Iesce, M. R.; Montella, S.; Pollio, A.; Temussi, F. *Chemosphere* **2004**, *55*, 1035.
(174) Smejkalova, D.; Piccolo, A.; Spiteller, M. *Environ. Sci. Technol.* **2006**, *40*, 6955.
(175) Gryglik, D.; Miller, J. S.; Ledakowicz, S. *J. Hazard. Mater.* **2007**, *146*, 502.
(176) Miskoski, S.; Garcia, N. A. *Toxicol. Environ. Chem.* **1989**, *25*, 33.
(177) Hu, M. Q.; Xu, Y. M.; Xiong, Z. G. *Chem. Lett.* **2004**, *33*, 1092.
(178) Skurlatov, Y. I.; Ernestova, L. S.; Vichutinskaya, E. V.; Samsonov, D. P.; Semenova, I. V.; Rodko, I. Y.; Shvidky, V. O.; Pervunina, R. I.; Kemp, T. K. *J. Photochem. Photobiol., A* **1997**, *107*, 207.
(179) Ozoemena, K.; Kuznetsova, N.; Nyokong, T. *J. Mol. Catal., A: Chem.* **2001**, *176*, 29.
(180) Xiong, Z. G.; Xu, Y. M. *Chem. Mater.* **2007**, *19*, 1452.
(181) Han, S. K.; Bilski, P.; Karriker, B.; Sik, R. H.; Chignell, C. F. *Environ. Sci. Technol.* **2008**, *42*, 166.
(182) Soltermann, A. T.; Luiz, M.; Biasutti, M. A.; Carrascoso, M.; Amat-Guerri, F.; Garcia, N. A. *J. Photochem. Photobiol., A* **1999**, *129*, 25.
(183) Cai, J. H.; Huang, J. W.; Zhao, P.; Zhou, Y. H.; Yu, H. C.; Ji, L. N. *J. Mol. Catal., A: Chem.* **2008**, *292*, 49.
(184) Machado, A. E. H.; Gomes, A. J.; Campos, C. M. F.; Terrones, M. G. H.; Perez, D. S.; Ruggiero, R.; Castellan, A. *J. Photochem. Photobiol., A* **1997**, *110*, 99.
(185) Miranda, M. A.; Marin, M. L.; Amat, A. M.; Arques, A.; Segui, S. *Appl. Catal., B* **2002**, *35*, 167.
(186) Miranda, M. A.; Galindo, F.; Amat, A. M.; Arques, A. *Appl. Catal., B* **2001**, *30*, 437.
(187) Pajares, A.; Bregliani, M.; Montana, M. P.; Criado, S.; Massad, W.; Gianotti, J.; Gutierrez, I.; Garcia, N. A. *J. Photochem. Photobiol., A* **2010**, *209*, 89.
(188) Sanjuan, A.; Aguirre, G.; Alvaro, M.; Garcia, H. *Appl. Catal., B* **1998**, *15*, 247.
(189) Amat, A. M.; Arques, A.; Bossmann, S. H.; Braun, A. M.; Miranda, M. A.; Vercher, R. F. *Catal. Today* **2005**, *101*, 383.
(190) Miranda, M. A.; Amat, A. M.; Arques, A. *Water Sci. Technol.* **2001**, *44*, 325.
(191) Miranda, M. A.; Galindo, F.; Amat, A. M.; Arques, A. *Appl. Catal., B* **2000**, *28*, 127.
(192) Marin, M. L.; Miguel, A.; Santos-Juanes, L.; Arques, A.; Amat, A. M.; Miranda, M. A. *Photochem. Photobiol. Sci.* **2007**, *6*, 848.
(193) Amat, A. M.; Arques, A.; Miranda, M. A. *Appl. Catal., B* **1999**, *23*, 205.
(194) Arques, A.; Amat, A. M.; Santos-Juanes, L.; Vercher, R. F.; Marin, M. L.; Miranda, M. A. *J. Mol. Catal., A: Chem* **2007**, *271*, 221.
(195) Miranda, M. A.; Amat, A. M.; Arques, A. *Catal. Today* **2002**, *76*, 113.
(196) Sanjuan, A.; Aguirre, G.; Alvaro, M.; Garcia, H.; Scaiano, J. C. *Appl. Catal., B* **2000**, *25*, 257.
(197) Chu, W.; Chan, K. H.; Jafvert, C. T.; Chan, Y. S. *Chemosphere* **2007**, *69*, 177.
(198) Amat-Guerri, E.; Pajares, A.; Gianotti, J.; Haggi, E.; Stettler, G.; Bertolotti, S.; Miskoski, S.; Garcia, N. A. *J. Photochem. Photobiol., A* **1999**, *126*, 59.
(199) Pajares, A.; Gianotti, J.; Haggi, E.; Stettler, G.; Amat-Guerri, F.; Criado, S.; Miskoski, S.; Garcia, N. A. *J. Photochem. Photobiol., A* **1998**, *119*, 9.
(200) Pajares, A.; Gianotti, J.; Stettler, G.; Bertolotti, S.; Criado, S.; Posadaz, A.; Amat-Guerri, F.; Garcia, N. A. *J. Photochem. Photobiol., A* **2001**, *139*, 199.
(201) Pajares, A.; Gianotti, J.; Stettler, G.; Haggi, E.; Miskoski, S.; Criado, S.; Amat-Guerri, F.; Garcia, N. A. *J. Photochem. Photobiol., A* **2000**, *135*, 207.
(202) Haggi, E.; Bertolotti, S.; Miskoski, S.; Amat-Guerri, F.; Garcia, N. *Can. J. Chem.* **2002**, *80*, 62.
(203) Cui, H.; Hwang, H. M.; Zeng, K.; Glover, H.; Yu, H. T.; Liu, Y. M. *Chemosphere* **2002**, *47*, 991.
(204) Rejto, M.; Saltzman, S.; Acher, A. J.; Muszkat, L. *J. Agric. Food Chem.* **1983**, *31*, 138.
(205) Hequet, V.; Le Cloirec, P.; Gonzalez, C.; Meunier, B. *Chemosphere* **2000**, *41*, 379.
(206) Rebelo, S. L. H.; Melo, A.; Coimbra, R.; Azenha, M. E.; Pereira, M. M.; Burrows, H. D.; Sarakha, M. *Environ. Chem. Lett.* **2007**, *5*, 29.
(207) Iesce, M. R.; Graziano, M. L.; Cermola, F.; Montella, S.; di Gioia, L.; Stasio, C. *Chemosphere* **2003**, *51*, 163.
(208) Bi, G.; Tian, S. Z.; Feng, Z. G.; Cheng, J. *Chemosphere* **1996**, *32*, 1237.
(209) Cui, H.; Huang, H. M.; Cook, S.; Zeng, K. *Chemosphere* **2001**, *44*, 621.
(210) Harmon, H. J. *Chemosphere* **2006**, *63*, 1094.

(211) Lin, C. S.; Chang, T. C. *Chemosphere* **2007**, *66*, 1003.
(212) Amat, A. M.; Arques, A.; Bossmann, S. H.; Braun, A. M.; Göb, S.; Miranda, M. A.; Oliveros, E. *Chemosphere* **2004**, *57*, 1123.
(213) Amat, A. M.; Arques, A.; Bossmann, S. H.; Braun, A. M.; Göb, S.; Miranda, M. A. *Angew. Chem., Int. Ed.* **2003**, *42*, 1653.
(214) Zhao, X.; Zhang, Y.; Hu, X.; Hwang, H. M. *Bull. Environ. Contam. Toxicol.* **2007**, *79*, 319.
(215) Zhao, X. H.; Hu, X. K.; Hwang, H. M. *Chemosphere* **2006**, *63*, 1116.
(216) Sanjuan, A.; Aguirre, G.; Alvaro, M.; Garcia, H.; Scaiano, J. C.; Chretien, M. N.; Focsaneanu, K. S. *Photochem. Photobiol. Sci.* **2002**, *1*, 955.
(217) Diaz, M.; Luiz, M.; Alegretti, P.; Furlong, J.; Amat-Guerri, F.; Massad, W.; Criado, S.; Garcia, N. A. *J. Photochem. Photobiol., A* **2009**, *202*, 221.
(218) Bayarri, B.; Carbonell, E.; Gimenez, J.; Esplugas, S.; Garcia, H. *Chemosphere* **2008**, *72*, 67.
(219) Escalada, J. P.; Gianotti, J.; Pajares, A.; Massad, W. A.; Amat-Guerri, F.; Garcia, N. A. *J. Agric. Food Chem.* **2008**, *56*, 7355.
(220) Hoffmann, N. *Chem. Rev.* **2008**, *108*, 1052.
(221) Marin, M. L.; Lhiaubet-Vallet, V.; Santos-Juanes, L.; Soler, J.; Gomis, J.; Arques, A.; Amat, A. M.; Miranda, M. A. *Appl. Catal., B* **2011**, *103*, 48.
(222) Kluson, P.; Drobek, M.; Kalaji, A.; Zarubova, S.; Krysa, J.; Rakusan, J. *J. Photochem. Photobiol., A* **2008**, *199*, 267.
(223) Cojocaru, B.; Laferriere, M.; Carbonell, E.; Parvulescu, V.; Garcia, H.; Scaiano, J. C. *Langmuir* **2008**, *24*, 4478.
(224) Snow, A. W. In *The Porphyrin Handbook*; Kadish, K. M. S., Guilard, R., Ed.; Academic Press: San Diego, CA, 2003; Vol. 17, p 129.
(225) Aprile, C.; Martin, R.; Alvaro, M.; Garcia, H.; Scaiano, J. C. *Chem. Mater.* **2009**, *21*, 884.
(226) Aprile, C.; Maretti, L.; Alvaro, M.; Scaiano, J. C.; Garcia, H. *Dalton Trans.* **2008**, 5465.
(227) Corma, A.; Fornes, V.; Garcia, H.; Miranda, M. A.; Sabater, M. J. *J. Am. Chem. Soc.* **1994**, *116*, 9767.
(228) Corma, A.; Garcia, H. *Eur. J. Inorg. Chem.* **2004**, 1143.
(229) Corma, A.; Fornes, V.; Garcia, H.; Miranda, M. A.; Primo, J.; Sabater, M. J. *J. Am. Chem. Soc.* **1994**, *116*, 2276.
(230) Cojocaru, B.; Neatu, S.; Parvulescu, V. I.; Dumbuya, K.; Steinrück, H. P.; Gottfried, J. M.; Aprile, C.; Garcia, H.; Scaiano, J. C. *Phys. Chem. Chem. Phys.* **2009**, *11*, 5569.
(231) Lopez-Periago, A. M.; Fraile, J.; Garcia-Gonzalez, C. A.; Domingo, C. *J. Supercrit. Fluids* **2009**, *50*, 305.
(232) Pere, E.; Cardy, H.; Cairon, O.; Simon, M.; Lacombe, S. *Vib. Spectrosc.* **2001**, *25*, 163.
(233) Lacombe, S.; Cardy, H.; Soggiu, N.; Blanc, S.; Habib-Jiwan, J. L.; Soumillion, J. P. *Microporous Mesoporous Mater.* **2001**, *46*, 311.
(234) Madhavan, D.; Pitchumani, K. *Tetrahedron* **2001**, *57*, 8391.
(235) Pigot, T.; Arbitre, T.; Martinez, H.; Lacombe, S. *Tetrahedron Lett.* **2004**, *45*, 4047.
(236) Pigot, T.; Dupin, J. C.; Martinez, H.; Cantau, C.; Simon, M.; Lacombe, S. *Microporous Mesoporous Mater.* **2005**, *84*, 343.
(237) Nowakowska, M.; Sterzel, M.; Szczubialka, K.; Guillet, J. E. *Macromol. Rapid Commun.* **2002**, *23*, 972.
(238) Nowakowska, M.; Zapotoczny, S.; Sterzel, M.; Kot, E. *Biomacromolecules* **2004**, *5*, 1009.
(239) Nowakowska, M.; Sterzel, M.; Zapotoczny, S. *Photochem. Photobiol.* **2005**, *81*, 1227.
(240) Nowakowska, M.; Sterzel, M.; Szczubialka, K. *J. Polym. Environ.* **2006**, *14*, 59.
(241) Nowakowska, M.; Moczek, L.; Szczubialka, K. *Biomacromolecules* **2008**, *9*, 1631.
(242) Moczek, L.; Nowakowska, M. *Biomacromolecules* **2007**, *8*, 433.
(243) Blossey, E. C.; Neckers, D. C. *J. Am. Chem. Soc.* **1973**, *95*, 5820.
(244) Gerdes, R.; Bartels, O.; Schneider, G.; Wöhrle, D.; Schulz-Ekloff, G. *Polym. Adv. Technol.* **2001**, *12*, 152.
(245) Nowakowska, M.; Kepczynski, M.; Szczubialka, K. *Macromol. Chem. Phys.* **1995**, *196*, 2073.
(246) Corma, A.; Garcia, H. *Chem. Commun.* **2004**, 1443.
(247) Blanco, J.; Malato, S.; Fernandez-Ibañez, P.; Alarcon, D.; Gernjak, W.; Maldonado, M. L. *Renewable Sustainable Energy Rev.* **2009**, *13*, 1437.
(248) Hincapie, M.; Maldonado, M. I.; Oller, I.; Gernjak, W.; Sanchez-Perez, J. A.; Ballesteros, M. M.; Malato, S. *Catal. Today* **2005**, *101*, 203.
(249) Amat, A. M.; Arques, A.; Garcia-Ripoll, A.; Santos-Juanes, L.; Vicente, R.; Oller, I.; Maldonado, M. I.; Malato, S. *Water Res.* **2009**, *43*, 784.
(250) Oller, I.; Malato, S.; Sánchez-Pérez, J. A.; Gernjak, W.; Maldonado, M. I.; Pérez-Estrada, L. A.; Pulgarín, C. *Catal. Today* **2007**, *122*, 150.
(251) Gutierrez, M.; Etxebarria, J.; las Fuentes, L. *Water Res.* **2002**, *36*, 919.